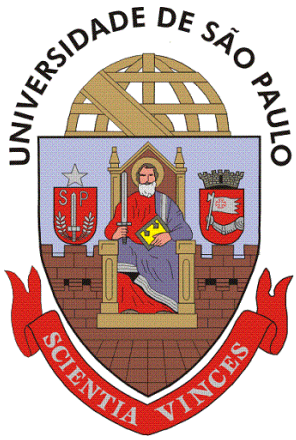

UNIVERSIDADE DE SÃO PAULO

ESCOLA DE ENGENHARIA DE SÃO CARLOS

DEPARTAMENTO DE ENGENHARIA ELÉTRICA E DE COMPUTAÇÃO

PROGRAMA DE PÓS-GRADUAÇÃO EM ENGENHARIA ELÉTRICA

Fluxo de Potência Ótimo com Restrições de Estabilidade

Ana Cecilia Moreno Alamo

São Carlos

2015

ANA CECILIA MORENO ALAMO

Fluxo de Potência Ótimo com Restrições de Estabilidade

Dissertação apresentada à Escola de Engenharia de São Carlos da Universidade de São Paulo, como parte dos requisitos para a obtenção do título de Mestre em Ciências - Programa de Pós-graduação em Engenharia Elétrica.

Área de Concentração: Sistemas Dinâmicos

ORIENTADOR: Prof. Dr. Luís Fernando Costa Alberto

São Carlos

2015

Trata-se da versão corrigida da dissertação. A versão original se encontra disponível na EESC/USP que aloja o Programa de Pós-graduação de Engenheria Elétrica

Ficha catalográfica preparada pela Seção de Tratamento
da Informação do Serviço de Biblioteca – EESC/USP

M843f

Moreno Alamo, Ana Cecilia
Fluxo de potência ótimo com restrições de estabilidade / Ana Cecilia Moreno Alamo; orientador Luís Fernando Costa Alberto. -- São Carlos, 2015.

Dissertação (Mestrado em Engenharia Elétrica e Área de concentração Sistemas Dinâmicos). -- Escola de Engenharia de São Carlos da Universidade de São Paulo, 2015.

1. Computação numérica. 2. Fluxo de potência ótimo. 3. Estabilidade transitória. 4. Sistemas de energia. I. Título.

FOLHA DE JULGAMENTO

Candidata: Engenheira **ANA CECILIA MORENO ALAMO.**

Título da dissertação: "Fluxo de potência ótimo com restrições de estabilidade".

Data da defesa: 06/06/2015

Comissão Julgadora: **Resultado:**

Prof. Associado **Luís Fernando Costa Alberto (Orientador)** Aprovada
(Escola de Engenharia de São Carlos/EESC)

Prof. Titular **Newton Geraldo Bretas** Aprovado
(Escola de Engenharia de São Carlos/EESC)

Prof. Dr. **Daniel Dotta** Aprovada
(Instituto Federal de Santa Catarina/IFSC)

Coordenador do Programa de Pós-Graduação em Engenharia Elétrica:
Prof. Associado **Luis Fernando Costa Alberto**

Presidente da Comissão de Pós-Graduação:
Prof. Associado **Paulo César Lima Segantine**

To my parents: Ana María and Jesús Aurelio

ACKNOWLEDGMENT

I want to thank God, for each day of life. Every time I fell, whenever I felt trapped, God always showed me the way that guided me to the exit. A "thank you" is not enough to show my gratitude. Thank you for guide my way, you made me know that you never leave us alone and you always give us infinite forgiveness.

My deepest gratitude goes to my parents Ana María Alamo Salas and Jesús Aurelio Moreno Miranda; for their love and support; for all sacrifices they made with the target their children have more opportunities they had; for all their concern; for all their prayers; and so on.

My deepest gratitude goes to Prof. Luís Fernando Costa Alberto; for all his patience and lessons; for all his invaluable direction and supervision work, his generous knowledge transmission, for give me the opportunity to develop this work; and so on. This is a great opportunity to thank him for accept me as a researcher and Msc. Candidate, even knowing that my previous background does not belong to this Area. From the first email I sent him, he strongly encouraged me to grow personally and professionally; this demonstration of confidence, motivated me and pushed me forward in academic and personal decisions; and encouraged me in a significant way to take the decision to come to Brazil to follow Post-graduate and Master degree studies.

My gratitude goes to the Prof. Rodrigo Andrade Ramos, Dr. Guilherme Guimarães Lage, for their relevant suggestions; for their generous knowledge transmission, and wise advice; which contributed to the improvement of the contents of this dissertation. My gratitude goes to the Prof. João Bosco Augusto London Jr.; Prof. Rogério Andrade Flauzino; Prof. Eduardo Werley dos Ângelos; Prof. Elmer Pablo Tito Cari; for all their invaluable and generous knowledge transmission; for always have had the better disposition for me, and for all their students.

My gratitude goes to the Prof. Raúl Del Rosario Quinteros; Prof. Rocio Callupe Pérez; Prof. Luis Vilcahuamán; Prof. Javier Sotomayor Soriano; Prof. Bruno Castillón; Prof. José del Carmen Piñeyro Fernández; Prof. Willy Carrera Soria; for always give me their wise and generous advice; their support; confidence; for all their friendship; for their invaluable and generous knowledge transmission; for all their love; for always been there for me, and so on.

I want to give special thanks to my boyfriend Alberto for supporting me, for always give me his heart; his time, for give me strength in many difficult times, for knowing how to wait for me at the other side of each black cloud, for make me see all my own mistakes which let me be a better person, and so on. Without your sincere friendship, I doubt if I could have finished this work.

I want to give special thanks to my family and friends of the "Pontificia Universidad Católica del Perú", "CI Brasil Program", "Universidade Federal do Rio Grande do Sul". I want to thanks for always supported me and give me always their friendship. I will always keep in my heart, many endless experiences and happy times together.

I want to give special thanks to Christian Rivera, Edwin Choque and Rayner Montes; for their support in many situations; for their advice and sincere friendship.

I want to give special thanks to my friends of “Laboratório de Análise Computacional em Sistemas Elétricos de Potência” (LACOSEP): Mariana Guerreiro; Taylon Landgraf; Alexandre Sohn; Breno Bretas; Edson Theodoro; Madeleine Medrano; Julian Zan; Julio Massignan; Adriano Abrantes; Camila Fantin; Leandro Marques; Daniel Siqueira.

Thanks so much to all my friends, to all kind people who make my days happier.

I want to give special thanks the “Coordenação de Aperfeiçoamento de Pessoal de Nivel Superior” (CAPES); for the concession of the scholarship; which allowed me to develop this research.

Resumo

Moreno Alamo, Ana Cecilia (2015). **Fluxo de Potência Ótimo com Restrições de Estabilidade.** Dissertação (Mestrado). - Escola de Engenharia de São Carlos, Universidade de São Paulo, São Carlos, 2015.

Neste trabalho, as restrições de estabilidade transitória são incorporadas ao problema de Fluxo de Potência Ótimo (FPO) por meio da aproximação de equações diferenciais do problema de estabilidade por um conjunto de equações algébricas provenientes de procedimentos de integração numérica. Uma contribuição original desta dissertação é a proposição de um procedimento de otimização multi-passos que minimiza problemas de convergência e acelera o processo computacional. O procedimento de otimização proposto foi testado com sucesso num sistema pequeno de 3 geradores, tendo as potências geradas como variáveis de controle.

Palavras chave-- Computação numérica, Fluxo de Potência Ótimo, Estabilidade transitória, sistemas de energia.

Abstract

Moreno Alamo, Ana Cecilia (2015). ***Stability Constrained Optimal Power Flow.*** Dissertation (Master Thesis) - Escola de Engenharia de São Carlos, Universidade de São Paulo, São Carlos, 2015.

In this work, transient stability constraints are incorporated into the Optimal Power Flow (OPF) problem by approximating differential equations constraints by a set of equivalent algebraic equations originated from numerical integration procedures. A contribution of this dissertation is the proposal of a multi-step optimization procedure, which minimizes convergence problems and speeds up computation. The proposed optimization procedure was successfully tested on a small 3-machine power system, having the generated powers as control variables.

Keywords-- Numerical Computation, Optimal Power Flow, Transient Stability, Power System.

List of Figures

List of Tables

List of Acronyms

BCU	Boundary Controlling UEP
BFGS	Broyden–Fletcher–Goldfarb–Shanno
CUEP	Controlling unstable equilibrium point
EAC	Equal area criterion
ED	Economic Dispatch
EPS	Electrical Power system
GP	General Problem
IPM	Interior point method
KKT	Karush-Kuhn-Tucker
LP	Linear Programming
NP	Nonlinear Programming
ODE	Ordinary differential equation
OPF	Optimal Power Flow
PEBS	Potential Energy Boundary Surface
QP	Quadratic programming
SEP	Stable equilibrium point
SQP	Sequential Quadratic Programming
SCOPF	Stability Constrained Optimal Power Flow
TSCOPF	Transient stability constrained Optimal Power Flow
UEP	Unstable equilibrium point

Contents

Chapter 1

1. Introduction

Blackouts have a pronounced negative impact on the economy and society. However, in a market environment and for economic reasons, power systems are exposed to increasing stress because they are usually operated close to their stability limits. Under these circumstances, blackout risks can increase. To reduce the risk of blackouts, power systems should be operated such that no equipment is overloaded, all bus voltage magnitudes are within appropriate limits, and acceptable steady-state operating conditions can be reached after transient phenomena induced by a plausible contingency (ZÁRATE-MIÑANO, 2012; BALU et al., 1992). Although security is taken into account in the planning and operation stages, security assessment and control procedures are key tasks during real-time operation. In this context, the system operator must respond within a limited time frame, usually from a few minutes to some hours, to ensure security.

Most existing electricity markets are based in economic issues and they do not consider security issues, due to the lack and the insufficient development of tools for secure assessment. For instance, unit commitment, in general, does not consider the AC current network (it considers DC current network), and in consequence does not consider security constraints.

As a result, during real time operation, the operator must assess system security, and implement control actions. Control actions may involve modifications to the market solution by means of variations in generator power outputs (generating unit re-dispatching), modifications in voltage set magnitudes and power flow control devices, and load shedding. Real time-operation of power systems includes three primary tasks: security assessment, contingency filtering, and security control (PAVELLA; ERNST; RUIZ-VEGA, 2000).

Security assessment involves a number of studies in which the state of the network, for all contingencies of a pre-specified set is determined. The method used to select the contingencies that should be included in this set is still a challenging task (KUNDUR et al., 2004). Although diverse criteria can be used, one commonly accepted criterion is to consider all the single outage of any system element, whether or not it is preceded by a single, double or three phase fault. This is known as the N-1 criterion. Contingency filtering identifies contingencies from within a pre-specified set that can lead to system instability. The critical contingencies are those that threaten the integrity of the system. Consequently, the stability of the post-contingency state of the power system is an important characteristic for contingency filtering. Existence of critical contingences requires the implementation of preventive control, to avoid operation in an insecurity state. Security control consists in deciding whether preventive or corrective control actions (or a combination of both) are

convenient against potential stability issues and determining if the corresponding set of control actions improves the global system security level. Security control methodologies shall help the system operator take proper actions.

The problem of design preventive controls to ensure that the system is secure in the context of transient stability is investigated.

1.1 Motivation for this work

The optimal power flow (OPF) - based approach is an appropriate and a well-established mechanism to identify the control actions that are necessary to ensure the aimed security level with a minimum cost. In addition, market participants expect that security controls modify as little as possible the market dispatch solution. To ensure the security controls impact the market solution is necessary to model the power system and the security constraints in detail. As a result, the system engineer, who models such a problem, typically deals with a nonlinear programming problem and advanced stability theories. Studying transient stability under a large disturbance generally requires time-domain simulations. Incorporating transient stability constraints in an OPF model poses the challenge of marrying time-domain simulations and nonlinear programming methodologies. Consequently, the security-targeted re-dispatching step is a complex and not fully solved task (ZÁRATE-MIÑANO; MILANO; CONEJO, 2010).

Optimal Power Flow (OPF) would be the natural choice to treat the problem of preventive or emergency control in tools for the dynamic security analysis of electrical power systems. However, the inclusion of transient stability constraints is a challenging problem. Stability constraints cannot be expressed as equality or inequality constraints, written in terms of known elementary functions. Verification of these constraints requires numerical computation, usually associated to high-cost computational procedures, such as numerical integration of a large set of algebraic-differential equations. Furthermore, the optimization problem is highly non-linear and non-convex, which leads to the existence of multiple solutions and to the non-convergence of the optimization numerical algorithms. This problem is difficult to resolve even for small power systems. The main difficulties of solving this problem include: (1) dealing with the differential equations that represent the dynamic behavior of the system; and (2) the non-suitability of the conventional optimization numerical algorithms in highly non-linear and non-convex scenarios.

Existing works in Optimal Power Flow with transient stability constraints usually represent stability constraints in an approximate way. The sensitivity of the stability margin, measured by an energy function, is one way to approximate stability constraints (CHIANG et al., 2006; WEHENKEL; PAVELLA, 2004; PAVELLA; ERNST; RUIZ-VEGA, 2000; PAI, 1989; CHIANG, 1995; FOUAD; VITTAL, 1991). Some research works in transient stability constrained OPF (TSCOPF) problem

mainly focus on dealing with the differential equations that represent the dynamic behavior of the system. One way is to simplify the TSCOPF problem, as a generation rescheduling based on trajectory sensitivity (NGUYEN; PAI, 2003; SHUBHANGA; KULKARNI, 2004). Trajectory sensitivity concept has been extended to consider multi-contingencies (YUAN; KUBKAWA; SASAKI, 2003); and post-fault steady-state operating limits (LAYDEN; JEYASURYA, 2004). Cai, Chung and Wong, (2008), applied differential evolution, which is an optimization algorithm based in the principles of natural evolution, to solve transient stability constrained OPF problems. This algorithm has the ability to search for the global optimal solution of nonlinear and non-convex problems.

In this work, we follow the ideas of Gan, Thomas and Zimmerman, (2000) and substitute the transient stability constraints by a maximum angle deviation of the synchronous machine rotors. This choice is an approximation based on the fact that a stable system has all their machines synchronized with a bounded angle deviation. The choice of this angle is heuristic but studies towards choosing correct thresholds for this deviation have been already performed (SUAMPUN, 2013). One of the advantages of the representation of stability constraints by means of maximal angular deviation is that these constraints can be written directly as functions of the state variables of the problem. Even so, for the verification of the stability constraints, it is necessary to solve the differential equations that model the stability problem, generating constraints in the form of differential equations for the optimization problem. To resolve this issue, differential equations are approximated by means of numerical integration techniques and converted in a set of algebraic equations, discretized in time. Thus, the OPF problem with transient stability constraints can be solved using conventional optimization techniques; with the cost of a significant increase in the numbers of variables in the optimization problem.

The optimization problem formulated in this way has a high dimension, is nonlinear and non-convex; leading to the existence of multiple solutions and to non-convergence problems of the conventional numerical optimization algorithms. To minimize the aforementioned numerical problems, a procedure of multi-step optimization is proposed in this work. This is a contribution of this work and as far as we know, has not been appeared in the literature.

First, this procedure consists in execute Power Flow solution and step by step integration, then, stability is evaluated. If the stability constraints are violated, the optimization problem is divided into sub-problems. More precisely, the optimization problem is first solved considering a short total simulation time of the transient stability differential equations (for instance: 1s); and the control variables are adjusted by means of an optimization method with the target of bringing all angular deviations below a predetermined value. Then, the maximum simulation time is incremented and the optimization problem is resolved again, using the solution of the previous stage as initial

condition for this stage. This process is repeated until the maximum simulation time reaches the desired value.

The proposed procedure was tested on a 3-generator system, having the generated powers as control variables. The generation cost is minimized subject to transient stability constraints and usual constraints of generation and voltage limits. The results were promising and reveal the proposed procedure is efficient to minimizing convergence problems and speeding up the analysis.

Despite that, the computational effort is still high, suggesting that further work to speed up analysis is still necessary.

1.2 Contributions of this work

1.2.1 General objective

- The general contribution of this dissertation is the development of a Stability-constrained Optimal Power Flow-based control mechanism to mainly solve problems related to security assessment, taking into account transient stability constraints.

1.2.2 Specific contributions

- Investigation of a Transient Stability-Constrained Optimal Power Flow method that considers transient stability constraints using a discrete dynamic model of the power system.

- Investigation of a measure to determine transient stability limit, and incorporation of it into the Stability Constrained Optimal Power Flow.

- Development of a methodology that alleviates the non-convergence problem of TSCOPF. Proposal of a methodology with the target of minimizing convergence problems and speeding up the computational procedure.

1.3 Organization of this work

This document is organized as follows:

Chapter 1 - Introduction

Chapter 1 introduces the preventive control problem in electrical power systems and states the motivation for this dissertation. Subsequently, the main objectives of the dissertation, and then specific objectives are listed. Finally, the organization of the dissertation is presented.

Chapter 2 - Optimal Power Flow (OPF)

Chapter 2 begins with an overview of the Optimal Power Flow (OPF) history. Subsequently, we present the Active set method; which was used to solve the OPF and TSOPF problems.

Chapter 3 - Stability in Electric Power Systems

Chapter 3 presents a review of the state of art of Stability in Electric Power Systems, as well as, important concepts concerned to rotor angle stability, which concerns small-disturbance rotor angle stability and transient rotor angle stability. Then, some concepts about stability and stability region are described, including a description of the theory of characterization of the boundary of stability region. Next, different methodologies for transient stability analysis are presented, including the classic step-by-step methodology and methods based on energy functions.

Chapter 4 - Optimal Power Flow with Transient stability constraints

Chapter 4 begins with a description of issues regarding the formulation of Optimal Power Flow with transient stability constraints, and then a description of two general approaches to resolve these issues are discussed. Next, a description of the procedure of preventive control design that was used in this work to solve the Stability Constrained Optimal Power flow problem is described. Then a procedure of Multi-Step Optimization Approach for Power Flow with Transient Stability Constraints is proposed with the target of minimizing convergence problems and speeding up computation. Finally, results and computational issues are discussed in a 3-machine test system.

Chapter 5 - Comments and final conclusions, contributions and Future research suggested

Chapter 5 provides relevant conclusions of this work, as well as contributions related to the development in this dissertation. Finally, future research work is suggested.

Chapter 2

2. The optimal power flow (OPF)

2.1 History of Optimal Power Flow Problem

In 1962, Carpentier proposed a new formulation for the Economic Dispatch (ED) problem by incorporating the Power Flow problem equations in the set of constraints of the ED problem. Carpentier includes the AC power flow equations, generator active and reactive power constraints, bus voltage magnitude limits constraints, and bus voltage angle difference constraints for buses connected by transmission elements (CAIN; O'NEILL; CASTILLO, 2012).By this way, besides determining the optimal active power dispatch at the minimum operational cost, respecting the limits of each generation unit; Carpentier's formulation considers the power flow in the network and consequently the optimal dispatch respecting limits and capability of the network.

With the target of resolving this problem, Carpentier transformed the ED in an unconstrained problem by using a Lagrangian classic function, and resolved the set of nonlinear equations which resulted from the application of the first order necessary conditions (KKT) of the Lagrangian problem, by means of the use of the Gauss-Seidel method.

Carpentier published the optimality conditions for an OPF, including variable bounds, based on the KKT conditions. This is generally considered the first publication of a fully formulated OPF. The ED Problem solution is determined when the Karush-Kuhn-Tucker (KKT) conditions are satisfied. After the formulation of the ED problem, many other formulations of optimization problems applied to static analysis of Electrical Power System (EPS) and/or proposals for these resolutions were published. After this point, any problem that involves the determination of an EPS optimal state as a function of a determined operational performance is called OPF Problem.

The first proposals to solve OPF problems used gradient techniques known as first order methods. One of the first works, which follows this gradient technique, was the work of Dommel and Tinney (1968), in which an approach which incorporates the gradient descent method to resolve the OPF problem was proposed. This proposed method searches the optimal solution by means of an algorithm of descent steps. In this method, after changes in the control variables, power flow equations are resolved by means of the Newton method. The limits of the dependent variables can be incorporated to the objective function by means of quadratic penalties. Lagrange multipliers are used to associate the Power flow equations to the objective function. For guaranteeing the control

variables keep within their allowed limits, the gradient projection technique is used. This gradient descent method has a first order efficiency in the minimization of the objective function (SOUSA, 2006). The determination of the step size for the adjustment of the control variables is a critical factor for a good performance of this approach: very small steps guarantee the local convergence but this leads to many iterations of the algorithm; very big steps lead to the “zigzagging” phenomena in the proximities of the optimal solution (LAGE, 2013). Slow convergence limited their use.

Sasson, Viloria and Aboytes (1973) applied the penalty method to the OPF problem resolution. The authors proposed a method in which the objective function is penalized with both equality and inequality constraints. The Hessian matrix was used for the first time. This technique has the target of transforming the OPF problem in an unconstrained problem, penalizing all the violated equality and inequality constraints. In this approach, the violated equality and inequality constraints are incorporated to the objective function via quadratic penalties, defining a auxiliary function. This auxiliary function is minimized by means of Newton method. In each iterate of the method, the Hessian matrix of this auxiliary function is calculated, all variables are simultaneously updated and, in case the process does not converge to a feasible solution, the penalty factors are increased. The convergence of this process is reached when all equality and inequality constraints are satisfied. The Hessian matrix of the auxiliary function is sparse, allowing the use of sparsity techniques in the computational algorithms. On the other hand, this Hessian matrix is directly influenced by the penalty parameter, and this Hessian matrix can be ill-conditioned as the penalty parameter grows (LAGE, 2013; SOUZA, 2006).

With the target to overcome some deficiencies of the proposed approach by Dommel and Tinney (1968); Rashed and Kelly (1974) proposed a second order approximation for the OPF problem resolutions by means of the use of the gradient descent method. Equality restrictions represented by power flow equations are incorporated to the Lagrangian function by means of Lagrange multipliers, and the inequality constraints and the dependent variable limits are incorporated to the objective function by means of the use of quadratic penalties. In the updating of the control variables, the variables with violated limits are treated by means of the projection method. The method continues, iteratively, up to a convergence condition as the variation in the objective function, or the absolute value of the adjustment in the control variables become less than a predetermined tolerance (SOUZA, 2006; RASHED; KELLY, 1974; LAGE, 2013).

Sun et al. (1984) proposed a resolution of Optimal Power Flow problem by means of the Newton method. In this approach, the OPF problem is transformed in an unconstrained problem in the following way: The inequality constraints are aggregated to the objective function through Lagrangian multipliers and penalty factors. Thus, the inequality constraints are divided into two

groups: penalty constraints, which are added to the objective function through penalty factors; and active constraints that are grouped with the set of active constraints (power flow equations). This general set of active constraints is incorporated into the objective function by means of the use of Lagrange multipliers (COSTA et al., 2000). According to the authors, efficient and robust solutions can be obtained for problems of any practical size or kind. Solution effort is approximately proportional to network size, and is relatively independent of the number of controls or binding inequalities. Each iterate, minimizes a quadratic approximation of the Lagrangian function (SOUSA, 2006; LAGE, 2013). The key idea is a direct simultaneous solution for all of the unknowns variables of the Lagrangian function, at each iterate. For a given set of binding constraints the process converges to the KKT conditions in a few iterations. The challenge in the development of this algorithm is to efficiently identify "the set of binding constraints" in the solution (SUN et al., 1984).

Interior point methods (IPM) were first introduced by Karmarkar (1984). Clements et al. (1991), was one of the first researches to apply interior points methods to power system analysis. The authors proposed an interior point technique for nonlinear program to resolve the state estimation problem in power systems. Vargas, Quintana and Vanelli (1993) suggested an interior point method to resolve the ED problem. Granville (1994) proposed the use of a primal-dual logarithmic barrier method to the resolution of the optimal reactive dispatch, a particular case of OPF, in which the active controls are fixed. This was the first significant contribution of the IPM applied to OPF problem. In this approach, the optimal reactive dispatch problem is transformed in an unconstrained problem, by the following way: Inequality constraints are transformed in equality constraints by the addition of non-negative slack variables and then, all equality constraints (originals and transformed), are incorporated in the objective function by the use of Lagrange multipliers. Barrier methods transform the constrained problem in an unconstrained problem and insert the constraints in the objective function by means of a barrier parameter that avoids the approximation of a feasible point to the feasible region boundary. Working from the interior of the feasible region, these parameters generate barriers that avoid the variables violating their limits. Then, the approach starts from a feasible point and generates new feasible points. The optimal reactive dispatch solution is found when all constraints are satisfied (KKT conditions) and the barrier parameter tends to zero. The algorithm presents difficulty in the choice of the initial value of the barrier parameter, which is an empiric data of the problem. (SOUZA, 2006; LAGE, 2013; GRANVILLE, 1994)

Computational methods are considered for finding a point satisfying the second-order necessary conditions for a general (possibly non-convex) quadratic program. Quadratic programming (QP) minimizes a quadratic objective function subject to linear constraints on the variables. The difficulty of solving a QP problem depends on the convexity of the quadratic objective function. If the Hessian matrix is positive semi-definite, then the QP problem is convex. In this case, a local solution of the QP is also a global solution. However, when Hessian matrix is indefinite, the QP problem is non-

convex and the problem is Nonlinear Programming-hard even for the calculation of a local minimum (FORSGREN; GILL; MURRAY, 1991; WONG, 2011).

The majority of methods for solving quadratic programs can be categorized into either active-set methods or interior methods. Briefly, active-set methods are iterative methods that solve a sequence of equality-constrained quadratic sub-problems. The goal of the method is to predict the active set, the set of constraints that are satisfied with equality, at the solution of the problem. The conventional active-set method is divided into two phases; the first focuses on feasibility, while the second focuses on optimality. The advantage of active-set methods is that the methods are well-suited for “warm starts”, where a good estimate of the optimal active set is used to start the algorithm. This is particularly useful in applications where a sequence of quadratic programs is solved, for instance, in a sequential quadratic programming method or in an ODE constrained problem with mesh refinements.

Interior-point methods compute iterates that lie in the interior of the feasible region, rather than on the boundary of the feasible region. The method computes and follows a continuous path to the optimal solution. In the simplest case, the path is parameterized by a positive scalar that may be interpreted as a perturbation of the optimality conditions for the problem. This parameter also serves as a regularization parameter of the linear equations that are solved at each iterate. Generally, interior methods require fewer iterates than active-set methods. However, each iterate of interior-point methods is more expensive because the method must solve linear systems involving all the variables of the problem whereas active-set methods solve systems involving some subset of the variables (WONG, 2011).

An advantage of active-set methods is that they are well-suited for "warm starts", where a good estimate of the optimal active set is used to start the algorithm. The active-set algorithm is suitable for indefinite problems (generally associated to nonlinear and non-convex landscapes), making it an ideal QP solver for standalone applications and for use within a sequential quadratic programming method. For these reasons the active-set algorithm is applied in this work.

Matlab's function fmincon with the active set optimization method has been used to implement the Nonlinear programming (NP) problem, which will be presented in the chapter 4.

In the next section, we are going to describe how the active set algorithm works. This algorithm uses sequential quadratic programming (SQP) method, in which a sequence of quadratic sub-problems are solved sequentially, then this SQP method is going to be described.

2.2 Algorithm for Quadratic Programming: Active set optimization method

Optimization is an important tool in decision science and in the analysis of physical systems. To make use of this tool, we must first identify some *objective*, a quantitative measure of the performance of the system under study. The objective depends on certain characteristics of the system, called *variables* or *unknowns*. The goal is to find values of the variables that optimize the objective. Often the variables are restricted, or *constrained*, in some way. The process of identifying objective, variables, and constraints for a given problem is known as *modeling*. Once the model has been formulated, an optimization algorithm can be used to find its solution. After an optimization algorithm has been applied to the model, we must be able to recognize whether it has succeeded in its task of finding a solution.

Optimization techniques are used to find a set of values $x = \{x_1, x_2, ..., x_n\}$, which can in some way be defined as optimal. Optimization is the minimization or maximization of any objective function, $f(x)$, subject to constraints in the form of equality constraints, $G_i(x) = 0, \quad i \in E$; inequality constraints, $G_i(x) \leq 0, \quad i \in I$; and/or parameter bounds, x_l, x_u. A General Problem (GP) description is stated as (NOCEDAL; WRIGHT, 1999):

$$\min_x f(x) \tag{2.1}$$

subject to:

$$G_i(x) = 0, \quad i \in E,$$

$$G_i(x) \leq 0, \quad i \in I$$

where x is a vector of length n, $f(x)$ is the objective function, which returns a scalar value, and the vector function $G_i(x)$ are constraints functions, which return a vector containing the values of the equality and inequality constraints evaluated at x.

An efficient and accurate solution to this problem depends not only on the size of the problem in terms of the number of constraints and variables but also on characteristics of the objective function and constraints. When both the objective function and the constraints are linear functions of the variable x, the problem is known as a Linear Programming (LP) problem. Quadratic Programming (QP) concerns the minimization or maximization of a quadratic objective function that is linearly constrained. For both the LP and QP problems, reliable solution procedures are readily available.

More difficult to solve is the Nonlinear Programming (NP) problem in which the objective function and constraints can be nonlinear functions of the design variables. A solution of the NP problem

generally requires an iterative procedure to establish a direction of search at each major iterate. This is usually achieved by the solution of an LP, a QP, or an unconstrained sub-problem.
In constrained optimization, the general aim is to transform the problem into an easier sub-problem that can then be solved and used as the basis of an iterative process. A characteristic of a large class of early methods is the translation of the constrained problem to a basic unconstrained problem by using a penalty function for constraints that are near or beyond the constraint boundary. In this way the constrained problem is solved using a sequence of parameterized unconstrained optimizations, which in the limit (of the sequence) converge to the constrained problem. These methods are now considered relatively inefficient and have been replaced by methods that have focused on the solution of the Karush-Kuhn-Tucker (KKT) equations. The KKT equations are necessary conditions for optimality of a constrained optimization problem. If the problem is a so-called convex programming problem, that is, $f(x)$ and $G_i(x) = 0, \quad i \in E \cup I$, are convex functions, then the KKT equations are both necessary and sufficient for a global solution point. Referring to a GP (2.1), the Kuhn-Tucker equations can be stated as:

$$\nabla f(x^*) + \sum_{i=1}^{m} \lambda_i \cdot \nabla G_i(x^*) = 0 \tag{2.2}$$

$$\lambda_i \cdot G_i(x^*) = 0, \quad i \in E$$

$$\lambda_i \geq 0, \quad i \in I .$$

in addition to the original constraints in (2.1). The first equation describes a canceling of the gradients between the objective function and the active constraints at the solution point. For the gradients to be canceled, Lagrange multipliers (λ_i, $i \in E \cup I$) are necessary to balance the deviations in magnitude of the objective function and constraint gradients. Because only active constraints are included in this canceling operation, constraints that are not active must not be included in this operation and so are given Lagrange multipliers equal to 0. This is stated implicitly in the last two Kuhn-Tucker equations.

The solution of the KKT equations forms the basis to many nonlinear programming algorithms. These algorithms attempt to compute the Lagrange multipliers directly. Constrained quasi-Newton methods guarantee super-linear convergence by accumulating second-order information regarding the KKT equations using a quasi-Newton updating procedure. These methods are commonly referred to as Sequential Quadratic Programming (SQP) methods; since a QP sub-problem is solved at each major iterate.

2.2.1 Sequential Quadratic Programming (SQP)

SQP is one of the most effective methods for nonlinearly constrained optimization problems. The method generates steps by solving quadratic sub-problems. SQP is appropriate for small and large problems and it is well-suited to solving problems with significant nonlinearities. SQP method can be viewed as a generalization of Newton's method for unconstrained optimization in that it finds a step away from the current point by minimizing a quadratic model of the problem (WISCONSIN INSTITUTE FOR DISCOVERY, 2013). SQP methods are considered the state of the art in nonlinear programming methods. It is an iterative method, which solves a quadratic problem at each iterate (VENKATARAMAN, 2001). Schittkowski (1985) for example, has implemented and tested a version that outperforms every other tested method in terms of efficiency, accuracy, and percentage of successful solutions, over a large number of test problems.

It is based on the calculation of gradient and derivation of the objective function with a generalization of Newton's method for unconstrained optimization problems. At each major iterate, an approximation is made of the Hessian of the Lagrangian function using a quasi-Newton updating method. This is then used to generate a QP sub-problem whose solution is used to form a search direction for a line search procedure. The general method is stated here.

Given the problem description in (2.1) the principal idea is the formulation of a QP sub-problem based on a quadratic approximation of the Lagrangian function.

$$L(x,\lambda) = f(x) + \sum_{i \in E \cup I} \lambda_i \cdot g_i(x) \tag{2.3}$$

Here one simplifies (2.1) by assuming that boundary constraints have been expressed as inequality constraints. You obtain the QP sub-problem by linearization of the nonlinear constraints.

2.2.1.1 Quadratic Programming (QP) Sub-problem

$$\min_{d \in R^n} \quad \frac{1}{2} d^T \nabla^2_{xx} L \quad d + \nabla f(x_k)^T d \tag{2.4}$$

$$\nabla g_i(x_k)^T d + g_i(x_k) = 0, \quad i \in E$$

$$\nabla g_i(x_k)^T d + g_i(x_k) \leq 0, \quad i \in I.$$

This sub-problem can be solved using any QP algorithm. The solution is used to form a new iterate:

$$x_{k+1} = x_k + \alpha_k d_k .$$

The step length parameter α_k is determined by an appropriate line search procedure so that a sufficient decrease in a merit function is obtained. The matrix H_k is a positive definite approximation of the Hessian matrix of the Lagrangian function (2.3). H_k can be updated by any of the quasi-Newton methods, although the Broyden–Fletcher–Goldfarb–Shanno (BFGS) method appears to be the most popular (SHEVADE, 2012).

A nonlinearly constrained problem can often be solved in fewer iterates than an unconstrained problem using SQP. One of the reasons for this is that, because of limits on the feasible area, the optimizer can take decisions regarding directions of search and step length.

2.2.2 SQP Implementation

The SQP implementation consists of three main stages, which are discussed briefly in the following subsections (MATHWORKS, 2008):

1. Updating the Hessian Matrix

At each major iterate a positive definite quasi-Newton approximation of the Hessian of the Lagrangian function, H, is calculated using the BFGS method, where λ_i, $i \in E \cup I$, is an estimate of the Lagrange multipliers (NOCEDAL, WRIGHT, 1999; NAZARETH, 2003).

$$H_{k+1} = H_k + \frac{q_k q_k^T}{q_k^T s_k} - \frac{H_k s_k s_k^T H_k^T}{s_k^T H_k s_k}, \qquad (2.5)$$

Where:

$$s_k = x_{k+1} - x_k$$

$$q_k = \left(\nabla f(x_{k+1}) + \sum_{i=1}^{m} \lambda_i \cdot \nabla g_i(x_{k+1}) \right) - \left(\nabla f(x_k) + \sum_{i=1}^{m} \lambda_i \cdot \nabla g_i(x_k) \right).$$

If the Lagrangian Hessian is positive definite in the region where the minimization takes place, then BFGS quasi-Newton approximations Hk will reflect some of the curvature information of the problem, and the iteration will converge robustly and rapidly, as in the unconstrained BFGS method. If, however, the Lagrangian Hessian contains negative eigenvalues, then the BFGS approach of

approximating it with a positive definite matrix may be problematic. BFGS updating requires that sk and qk satisfy the curvature condition $q_k^T s_k > 0$, even when the iterates are close to the solution.

Powell recommends keeping the Hessian positive definite even though it might be positive indefinite at the solution point. A positive definite Hessian is maintained providing $q_k^T s_k$ is positive at each update and that H is initialized with a positive definite matrix.

When $q_k^T s_k$ is not positive, q_k is modified on an element-by-element basis so that $q_k^T s_k > 0$. The general aim of this modification is to distort the elements of q_k, which contribute to a positive definite update, as little as possible. Therefore, in the initial phase of the modification, the most negative element of $q_k \cdot s_k$ is repeatedly halved. This procedure is continued until $q_k^T s_k$ is greater than or equal to a small negative tolerance. If, after this procedure, $q_k^T s_k$ is still not positive, modify q_k by adding a vector v multiplied by a constant scalar w, that is,

$$q_k = q_k + wv, \tag{2.6}$$

where:

$$v_i = \nabla g_i(x_{k+1}) \cdot g_i(x_{k+1}) - \nabla g_i(x_k) \cdot g_i(x_k)$$

if $(q_k).w < 0$ and $(q_k)_i.(s_k)_i < 0$, $i \in E \cup I$

$v_i = 0$ otherwise,

and increase w systematically until $q_k^T s_k$ becomes positive.

2. Quadratic Programming Solution

At each major iterate of the SQP method, a QP problem of the following form is solved, where Ai refers to the i-th row of the m-by-n matrix A.

$$\min_{d \in R^n} q(d) \quad = \frac{1}{2} d^T H_k d + c^T d, \tag{2.7}$$

$$A_i d = b_i, \qquad i \in E$$

$$A_i d \le b_i, \qquad i \in I.$$

The solution procedure involves two phases. The first phase involves the calculation of a feasible point (if one exists). The second phase involves the generation of an iterative sequence of feasible points that converge to the solution. In this method an active set, $\overline{A}_k$, is maintained that is an estimate of the active constraints (i.e., those that are on the constraint boundaries) at the solution point. Virtually all QP algorithms are active set methods. This point is emphasized because there exist many different methods that are very similar in structure but that are described in widely different terms (WISCONSIN INSTITUTE FOR DISCOVERY, 2013; MATHWORKS, 2008).

$\overline{A}_k$ is updated at each iteration k, and this is used to form a basis for a search direction $\hat{d}_k$. Equality constraints always remain in the active set $\overline{A}_k$. The notation for the variable $\hat{d}_k$ is used here to distinguish it from d_k in the major iterations of the SQP method. The search direction $\hat{d}_k$ is calculated and minimizes the objective function while remaining on any active constraint boundaries. The feasible subspace for $\hat{d}_k$ is formed from a basis Z_k whose columns are orthogonal to the estimate of the active set $\overline{A}_k$ (i.e., $\overline{A}_k Z_k$=0). Thus a search direction, which is formed from a linear summation of any combination of the columns of Z_k, is guaranteed to remain on the boundaries of the active constraints.

The matrix Z_k is formed from the last m – l columns of the QR decomposition of the matrix, where l is the number of active constraints and l < m. That is, Z_k is given by:

$$Z_k = Q[:, l+1:m] \tag{2.8}$$

where $Q^T \overline{A}_k^T = \begin{bmatrix} R \\ 0 \end{bmatrix}$.

Once Z_k is found, a new search direction $\hat{d}_k$ is sought that minimizes $q(d)$ where $\hat{d}_k$ is in the null space of the active constraints. That is, $\hat{d}_k$ is a linear combination of the columns of Z_k: $\hat{d}_k = Z_k p$ for some vector p.

Then if you view the quadratic as a function of p, by substituting for $\hat{d}_k$, one has:

$$q(p) = \frac{1}{2} p^T Z_k^T H Z_k p + c^T Z_k p \tag{2.9}$$

Differentiating this with respect to p yields

$$\nabla q(p) \quad = Z_k^T H Z_k p + Z_k^T c \tag{2.10}$$

∇q(p) is referred to as the projected gradient of the quadratic function because it is the gradient projected in the subspace defined by Z_k. The term $Z_k^T H Z_k$ is called the projected Hessian. Assuming the Hessian matrix H is positive definite (which is the case in this implementation of SQP), then the minimum of the function $q(p)$ in the subspace defined by Z_k occurs when $\nabla q(p) = 0$, which is the solution of the system of linear equations.

$$Z_k^T H Z_k p = -Z_k^T c \tag{2.11}$$

A step is then taken of the form

$$x_{k+1} = x_k + \alpha \hat{d}_k \text{, where } \hat{d}_k = Z_k^T p \tag{2.12}$$

At each iterate, because of the quadratic nature of the objective function, there are only two choices of step length α. A step of unity along $\hat{d}_k$ is the exact step to the minimum of the function restricted to the null space of $\overline{A}_k$. If such a step can be taken, without violation of the constraints, then this is the solution of the QP problem (2.7). Otherwise, the step along $\hat{d}_k$ to the nearest constraint is less than unity and a new constraint is included in the active set at the next iteration. The distance to the constraint boundaries in any direction $\hat{d}_k$ is given by:

$$\alpha = \min_{i \in (E \cup I)} \left\{ \frac{-(A_i x_k - b_i)}{A_i \hat{d}_k} \right\} \tag{2.13}$$

which is defined for constraints not in the active set, and where the direction $\hat{d}_k$ is towards the constraint boundary, i.e., $A_i \hat{d}_k > 0,\ i \in E \cup I$.

When n independent constraints are included in the active set, without location of the minimum, Lagrange multipliers, λ_k, are calculated that satisfy the nonsingular set of linear equations

$$\overline{A}_k^T \lambda_k = c \tag{2.14}$$

If all elements of λ_k are positive, x_k is the optimal solution of the QP problem (2.7). However, if any component of λ_k is negative, and the component does not correspond to an equality constraint, then the corresponding element is deleted from the active set and a new iterate is sought.

3. Initialization

The algorithm requires a feasible point to start. If the current point from the SQP method is not feasible, then you can find a point by solving the linear programming problem

$$\min_{y \in R, x \in R^n} \gamma \quad \text{such that} \tag{2.15}$$

$$A_i x = b_i, \qquad i \in E$$

$$A_i x - \gamma \leq b_i, \qquad i \in I$$

The notation A_i indicates the i-th row of the matrix A. You can find a feasible point (if one exists) to (2.15) by setting x to a value that satisfies the equality constraints. You can determine this value by solving an under or over determined set of linear equations formed from the set of equality constraints. If there is a solution to this problem, then the slack variable γ is set to the maximum inequality constraint at this point.

The search direction $\hat{d}_k$ is initialized with a search direction $\hat{d}_1$ found from solving the set of linear equations

$$H \hat{d}_1 = -g_k \tag{2.16}$$

where g_k is the gradient of the objective function at the current iterate x_k (i.e., $Hx_k + c$). If a feasible solution is not found for the QP problem, the direction of search for the main SQP routine $\hat{d}_k$ is taken as one that minimizes γ.

2.3 Final Remarks

Matlab's function *fmincon* has been used to implement the SCOPF tool in this work. Specifically *fmincon* has been used in the solution of the Nonlinear programming (NP) problem, which will be presented in the chapter 4. This NP problem was resolved using the active set method previously described.

It is important to give a good initial estimate, because the active set method requires starting its searching from a feasible point to find the minimum. If the starting point is far from a feasible starting point, the optimization routine will take many iterates to find a feasible starting point, leading to a unsatisfactory computational performance.

Chapter 3

3. Stability in Power Systems

Stability analysis of power systems is a very challenging problem. Engineers simplify it by dividing stability analysis in types according to the size of perturbation, variable of interest and time-frame of interest. In this work, we will be interested in the problem of transient stability. More precisely, we will incorporate constraints of transient stability into the problem of optimal power flow formulation.

In this chapter, we will introduce concepts about rotor angle stability concerned to both small-disturbance and transient rotor angle stability. A review of the theory of stability and stability region will be presented, including the studies about the characterization of the boundary of stability region. Then a statement of the problem of transient stability in terms of stability region will be given.

3.1 Rotor angle stability

Rotor angle stability is the ability of the synchronous machines of an interconnected Power Electric system to preserve synchronism after a disturbance. This capacity depends on the ability to keep/restore the equilibrium between electromagnetic and mechanical torque of each machine in the system. The instability usually is characterized by a monotonic increase of the rotor angle of some generators, leading them to a lack of synchronism with respect to the other generators.

The time-frame of Rotor angle stability studies is usually between 3 to 5 seconds and can be extended, in the case of large disturbances, to intervals from 10 to 20 seconds after the disturbance (KUNDUR, 1994). For this reason, this stability analysis is classified as a short - time scale.

For a better analysis and understanding; the study of Rotor angle stability is divided in two subcategories, in accordance with disturbance types:

3.1.1 Small-disturbance rotor angle stability

Small-disturbance rotor angle stability is the ability of the synchronous machines of an Electrical Power system in keeping the synchronism after a small disturbance. In this scenario, disturbances are considered small enough to justify the linearization of the system equations.

From the point of view of small disturbances, the electromagnetic torque of a synchronous machine in relationship with the disturbance can be divided in two components:

- *Synchronizing torque*, in phase with the rotor angle deviation.
- *Damping torque*, in phase with the speed variation.

System stability depends on the existence of both components of torque for each synchronous machine. The lack of enough synchronizing torque implies instability with monotonic acceleration of the rotor machines. On the other hand, the lack of enough damping torque; results in oscillatory instability (KUNDUR, 1994).

3.1.2 Transient rotor angle stability

Transient Rotor angle stability is the ability of the synchronous machines of an Electrical Power system in keeping the synchronism after a large disturbance. The dynamics of the system is characterized for large excursions of generator angles and it is strongly influenced by the nonlinear relations between angle and power. In transient stability analysis, the focus is on the transient phenomena that follows a sudden and large disturbance in a power system. Due to the high non-linear dynamic nature of the transient phenomena, static analysis fails and linearization around a system equilibrium point is of no practical use.

Transient Stability is concerned with the ability of a power system to maintain synchronism after a large disturbance, such a fault on a transmission line (KUNDUR et al., 2004). During the fault period, the rotors of the synchronous machines suffer an acceleration or deceleration due to the imbalance between the input mechanical torque and the output electromagnetic torque in the generators. As a consequence, the rotor speed of the machines changes and the kinetic energy stored in the rotating parts of the generators increases or decreases. This causes the angular separation of the machines. If the system cannot absorb the kinetic energy stored during the fault period, synchronism is lost. This kind of instability usually takes the form of aperiodic angular separation of the machines due to lack of synchronizing torque. Transient instability often appears during the first swing of the system transient; thus, the time frame of interest is reduced to one or two seconds after the disturbance. However, in certain systems, transient instability can appear after the first swing because of slow inter-area swing modes (KUNDUR, 1994). This phenomenon is known as multi-swing instability and its study may involve analysis that extends over time periods greater than ten seconds (ZÁRATE-MIÑANO, 2010).

3.2 Stability Region

We are going to start this section, giving some definitions about stability and stability region. Let be an autonomous system $\dot{x} = f(x)$ and x_i be an equilibrium point of this system.

Definition 1: An equilibrium point x_i is stable in the Lyapunov sense, or simply stable; if given an $\varepsilon > 0$ arbitrarily small, there exists a $\delta > 0$, dependent of ε , such that for any initial point x_0 satisfying $|x_0 - x_i| < \delta$, the solution $\phi(t)$ with $\phi(t_0) = x_0$ satisfies $|\phi(t) - x_i| < \varepsilon$ for $t \geq t_0$ (BRETAS; ALBERTO, 2000).

Figure 3.1 shows a geometric representation of the stability definition of an equilibrium point x_i, where the equilibrium point is stable, if and only if, any solution starting in an equilibrium point neighborhood keeps close to the equilibrium point as the time goes by.

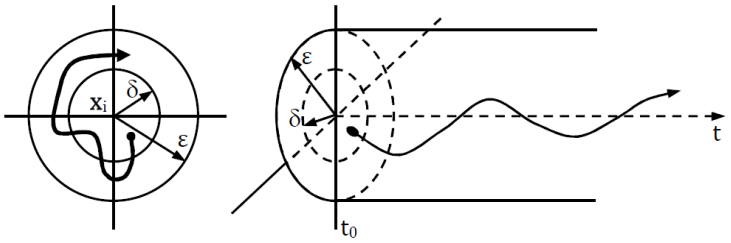

Fig.3.1 Stability definition of an equilibrium point x_i .

Definition 2: An equilibrium point is asymptotically stable, if it is stable and there exists an equilibrium point neighborhood where each solution $\phi(t)$, starting within it, satisfies the following condition: $\lim_{t\to\infty} \phi(t) = x_i$.

Figure 3.2 shows a geometric representation of the previous definition, and illustrates that any solution starting in the equilibrium point neighborhood converges to the equilibrium point x_i as the time goes by (BRETAS; ALBERTO, 2000).

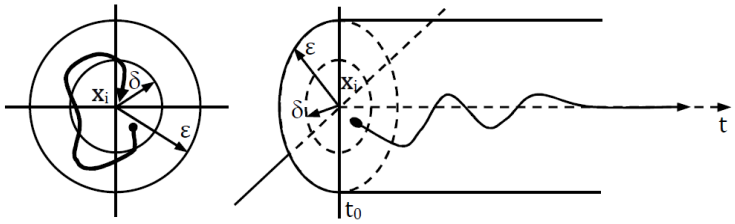

Fig. 3.2 Asymptotic stability definition of an equilibrium point x_i .

Stability does not imply asymptotic stability, even though the inverse is true.

In general, equilibrium in nonlinear systems are not globally asymptotically stable, i.e. only a set of initial conditions produces trajectories that approach to the asymptotically stable equilibrium point as $t \to +\infty$. This set of initial conditions is denominated Stability Region (region of attraction) of an asymptotically stable equilibrium point of the dynamic system.

The stability Region $A(x_s)$ of an asymptotically stable equilibrium point x_s, is defined as the set:

$$A(x_s) = \left\{ x \in R^n : \lim_{t \to \infty} \varphi(x,t) = x_s \right\} \tag{3.1}$$

where $\varphi(t,x)$ denotes the system trajectory that starts in x at the time $t = 0$. In other words, $A(x_s)$ is the set of all initial conditions that produce trajectories that approach to x_s, as time $t \to \infty$. The boundary of the stability region is denoted as $\partial A(x_s)$, and its closure is represented by $\overline{A}(x_s)$. Figure 3.3 shows a geometric representation of a stability region (3.1), where all points $x_{io} \in A(x_s)$ converge to the stable equilibrium point x_s as $t \to +\infty$.

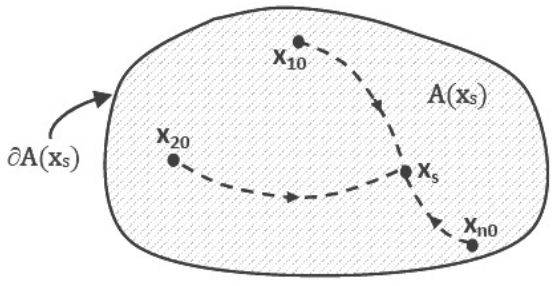

Fig. 3.3 Stability Region of Xs.

3.2.1 Studies to characterize the boundary of stability region

Many investigations were developed in analysis and characterization of the stability region $A(x_s)$ and its boundary $\partial A(x_s)$ (BRETAS; ALBERTO, 2000; CHIANG; WU; VARRAIYA, 1994; CHIANG; WU; VARAIYA, 1987; CHIANG; WU; VARAIYA, 1988; CHENG; MA, 2003). Before studying the characteristics of the stability region boundary of the power systems, it is necessary a brief introduction to the theory of dynamic systems. Consider an autonomous non-linear dynamic system represented by:

$$\dot{x} = f(x) \tag{3.2}$$

where $x \in R^n$ is a vector of system state variables and the vector field is $f : R^n \to R^n$ is a function of class C^1. The point x_i is an equilibrium point of (3.2), if $f(x_i) = 0$. The set formed by the equilibrium points of (3.2) will be denoted by E. The derivative of " f " at x_i is called the Jacobian matrix at x_i and is denoted by $J(x_i)$. The type of the equilibrium point x_i is defined in relation to the numbers of eigenvalues with positive real part of the Jacobian of "f" calculated in x_i. We say that an equilibrium point is hyperbolic if the Jacobian matrix has eigenvalues with non-zero real part (HIRSCH; SMALE, 1974). For a hyperbolic equilibrium point, it is a stable equilibrium point if all eigenvalues of the Jacobian have negative real part, otherwise, it is an unstable equilibrium point (CHIANG; WU; VARAIYA; 1994).

If x_i is a hyperbolic equilibrium point (all the eigenvalues of $J(x_i)$ have non-zero real part), their stable and unstable manifolds are defined respectively by:

$$W^s(x_i) = \{x : \varphi(x,t) \to x_i \qquad as \qquad t \to \infty\} \text{ and}$$

$$W^u(x_i) = \{x : \varphi(x,t) \to x_i \qquad as \qquad t \to -\infty\}$$

It is important to point out that these stable and unstable manifolds of equilibrium points are invariant sets[1]. Two manifolds A and B in R^n, satisfy the transversality condition if they do not intercept each other (i.e. $A \cap B = \phi$), or, if at each point of $x \in (A \cap B)$, the tangent space of A and B generates the tangent space of R^n in x:

[1] A set M is an invariant set if and only if all trajectories of (3.2) starting in M remains within it for all $t \in R$.

$$T_X(A)+T_X(B)=R^n \text{, for any } x\in(A\cap B)$$

Since our objective is to study the stability region boundary of a stable equilibrium point, we need to make the fundamental assumption that a stable equilibrium point exists. Furthermore, we make the following assumptions concerned to the system (3.2) (BRETAS; ALBERTO, 2000).

i) All the equilibrium points on the stability boundary of (3.2) are hyperbolic.

ii) The stable and unstable manifolds $W^s(x_i)$ and $W^u(x_j)$ satisfy the transversally condition for all equilibrium points x_i , x_j .

$W^s(x_i)\cap W^u(x_j)\neq\phi \Rightarrow TW^s(x_i)+TW^u(x_j)=R^n$.

iii) There exists a C^1 function, $V:R^n\rightarrow R$ for (3.2), such that:

1. $\dot{V}(\varphi(x,t))\leq 0$, for all $x\notin E$.
2. The set $\{t\in R,\dot{V}(\varphi(x,t))=0\}$ for $x\notin E$ has a zero measure in R.
3. If $V(\varphi(x,t))$ is bounded for $t\geq 0$, then $\varphi(x,t)$ is bounded for $t\geq 0$.

Based on the previous hypothesis, a series of theorems characterizing the stability region and its boundary were proposed in: Bretas and Alberto, (2000); Chiang; Wu; Varraiya, (1994); Chiang; Wu; Varraiya, (1987); Chiang; Wu; Varraiya, (1988); Cheng; Ma, (2003). In Chiang, Wu and Varraiya (1994), the following two theorems are presented:

Theorem 1: For a dynamic system which satisfies properties i), ii), iii), x_i is an unstable equilibrium point on the stability region boundary $\partial A(x_s)$ of an equilibrium point x_s , if and only if $W^u(x_i)\cap A(x_s)\neq\phi$.

As only trajectories and equilibrium points forms the boundary of the stability region, it becomes necessary to present a second theorem which offers a more accurate characterization of this boundary.

Theorem 2: (Characterization of the stability region). If a dynamic system $\dot{x}=f(x)$ satisfies the properties i), ii) and iii), and x_i , i=1,2,..; are the unstable equilibrium points on the stability region boundary of the asymptotically stable equilibrium point x_s , then:

$$\partial A(x_s) = \bigcup_i W^s(x_i)$$

Every equilibrium point x_i in the stability region boundary is an unstable equilibrium point. This theorem states that the boundary of the stability region is composed of the union of the stable manifolds of all unstable equilibrium points that belong to the stability region boundary. That means the boundary is composed of the union of several sets, where each one is related to a single unstable equilibrium point x_i, i.e. a set of points that converges to x_i. From the uniqueness of solutions, we conclude that these sets have empty intersection (BRETAS; ALBERTO, 2000; CHIANG; WU; VARRAIYA, 1994).

3.2.2 Statement of the problem of transient stability

In this section, we will state the problem of transient stability in terms of the concept of stability region discussed in the previous section. An electrical power system under a disturbance can be described by the following set of differential equations (BRETAS; ALBERTO, 2000):

$$\dot{x}(t) = f^F(x(t)) \qquad 0 < t \leq t_{cl} \qquad x(0) = x_0 \tag{3.3}$$

$$\dot{x}(t) = f(x(t)) \qquad t > t_{cl} \qquad x(t_{cl}) = x^* \tag{3.4}$$

where $x(t) \in R^n$ is a vector of state variables of the system. The system is in an equilibrium state until time t=0, when a fault or a disturbance occurs. During the interval $0 < t \leq t_{cl}$, called fault-on period, the system is governed by the dynamics of the fault-on vector field f^F. Before the fault is removed at time $t = t_{cl}$, multiple switching can occur in the network, each one generating a different f^F. For simplicity, we consider a single f^F, i.e., there is no structural change in the interval $0 < t \leq t_{cl}$. When the fault is removed at $t = t_{cl}$, the system dynamics will be governed by the post-fault vector field $f(x(t))$.

The initial condition $x(t_{cl})$ for the differential equation (3.4) is determined by the fault system solution (3.3) evaluated at the clearing time $t = t_{cl}$. Recognizing that equation (3.4) has an asymptotically stable equilibrium point x_s, it is desired to know if the trajectory $x(t)$ of (3.4), with an initial condition $x(t_{cl})$, will converge to x_s, when $t \to \infty$.

Using the concept of stability region, this problem of stability can be reformulated into the problem of checking if the post-fault initial condition $x(t_{cl})$ is inside the stability region $A(x_s)$. The maximum value of t_{cl} , at which this condition is satisfied, is denominated *critical clearing time* (t_{cr}).

Figure 3.3 illustrates this concept in two dimensions. The fault-on $x^F(t)$ and post-fault $x(t)$ system trajectories, and also the location of key points along the system evolution, such as x_0 , x^* and x_s , are identified in this figure. Where x_0 is the pre-fault equilibrium point, x^* is the intersection of the disturbed trajectory $x^F(t)$, with the boundary of the stability region $A(x_s)$ and x_s is the post-fault asymptotically stable equilibrium point.

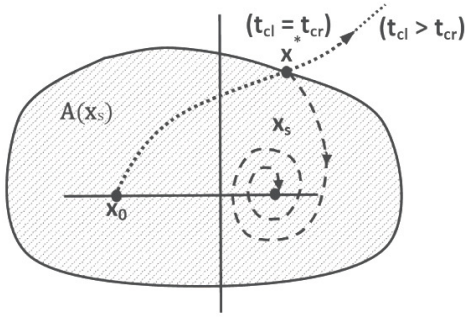

---------- Fault-on trajectory $x^F(t)$

- - - - - - - - Post-fault trajectory $x(t)$

Fig. 3.4 Stability region of x_s .

The determination of the stability region of an asymptotically stable equilibrium point x_s is not trivial, but, once determined, the problem of transient stability analysis, can be resolved following this scheme (BRETAS; ALBERTO, 2000):

i) Determine the stability region $A(x_s)$ of the stable equilibrium point of the post-fault system.

ii) Simulate the fault-on system until its orbit leaves the stability region $A(x_s)$ of the post-fault system.

iii) The time at which the orbit of the fault system leaves the stability region of the post fault system will be the critical clearing time.

Hence, if the fault is removed before the critical clearing time, the post-fault initial condition will be within the stability region and the system will be stable.

3.3 Transient stability analysis

Typically, transient stability analysis is carried out using one of the following techniques:

- Classic methodology (Time-domain simulation)
- Methods based on the energy functions (Direct methods)

These methods are briefly described in the following subsections. Alternatively, other approaches for transient stability analysis based on automatic learning methods have been proposed. Most of these methods are described in (FANG et al., 2007).

3.3.1 Classic methodology

The classic methodology consists of numerically integrating the differential-algebraic equations that model the power system. Typically, implicit numerical integration methods, such as the trapezoidal implicit method, are used to solve transient stability model (SAUER; PAI, 1998; KUNDUR, 1994). The objective of this methodology is to obtain the dynamic response of the generators connected to the system (submitted to a given fault) and determine the critical clearing time for the given fault (BRETAS; ALBERTO, 2000). This approach can be synthesized in the following steps (THEODORO, 2010):

- Modeling of the electrical power system elements and definition of the fault to be analyzed;
- Simulation of the system in the fault configuration until a pre-definite clearing time, (usually this pre-definite time is defined as the delay time of the protection system associated with the equipment submitted to the fault);
- Simulation of the electrical power system in the post-fault configuration until the desired time for the analysis (usually between 0 to 10s. in transient stability analysis);
- Verification of the synchronism between generators connected to the system and stability determination.

In transient stability studies, time-domain simulations are carried out for a maximum simulation period that depends on the complexity of the system model, which is typically set to 3 s (for a simplified model) and up to 15 s (for highly detailed models), (ZÁRATE-MIÑANO, 2010). The time-domain simulations provide the evolution of the system variables over time and the synchronism among generators is usually visually verified. A practice to automatic detect a loss of synchronism is to check whether or not the inter-machine rotor angle deviation lies within a specific range of values during the simulation.

3.3.2 Methods based on the energy functions

Energy functions are used in some recent methods for evaluating stability of system trajectories and to obtain good estimates of stability regions. We consider a general nonlinear autonomous dynamical system:

$$\dot{x}(t) = f(x(t)) \tag{3.5}$$

We say a function, $V : R^n \rightarrow R$, is an energy function type for the system (3.5); if the following three conditions are satisfied:

i. The derivative of the energy function *V(x)* along any system trajectory, *x*(*t*), must be non-positive definite.

ii. If *x*(*t*) is a nontrivial trajectory, the following set: $\left\{t \in R : \dot{V}(x(t)) = 0\right\}$, has a measure zero in R.

iii. If *V*(*x*(*t*)) is bounded for $t \geq 0$, implies that *x*(*t*) trajectory is also bounded for $t \geq 0$.

From the above definition of energy function, it can be inferred that an energy function may not be a Lyapunov function. It is important to point that, a Lyapunov function does not satisfy the conditions of an Energy function definition, and vice versa. In this way, finding an energy function for an Electrical Power system model could be a hard work, with a higher or comparable effort of finding a suitable Lyapunov function for a multi-machine power system. Lyapunov functions used in transient stability studies are functions of the energy type. The best-known is the transient energy function. If the transient energy function is applied to a one machine infinite bus system represented with the classical simplified model, the transient stability estimation is similar to that provided by the equal area criterion. Hence, the equal area criterion can be considered as an application of the Lyapunov theory to a simple power system (CHIANG, 2010).

Equal area criterion: The Equal area criterion (EAC) is a well-known procedure used to study the transient stability of systems that comprise one machine and an infinite bus or two machines. A detailed description can be found in: Bretas and Alberto, (2000). The EAC relies on energy exchange and evaluates transient stability without resolving the post-fault differential equations of the electrical power system. This technique settles that the stability of a one-machine plus infinite bus system or two-machine system, is assured providing that the kinetic energy stored in the system during the fault period (accelerating area) does not exceed the energy that the system can dissipate in the post-fault period (decelerating area).

The determination of the stability region of a general nonlinear dynamical system is not a trivial task. The characterization of the stability region has been theoretically discussed in section 3.2. Under certain conditions, it was shown the boundary of the stability region is constituted by the union of the stable manifolds of all unstable equilibrium points of (3.4), which belong to the boundary. Since the calculation of these manifolds is very difficult and expensive from the computational point of view, usually the interior of stability region of the post-fault system (3.4) is approximated by means of level sets of a given energy function, this means, sets of the form $\{ x : V(x) < V_{cr} \}$(BRETAS, ALBERTO, 2000; SAUER, PAI, 1998). The V_{cr} calculation, called critical energy, is different for each fault and is a difficult task. In the literature there are three main methods used for this task (SAUER; PAI, 1998):

1. Closest Unstable equilibrium point: This methodology uses an unstable equilibrium point (Closest Unstable equilibrium point) which has the lowest value of energy on the boundary; to limit the stability region. The procedure to assess stability via the closest unstable equilibrium point is as follows (BRETAS; ALBERTO, 2000): 1. Calculate all unstable equilibriums x_i , $i = 1,2,....,neq$; in the stability region boundary. 2. Calculate Critical Energy V_{cr}, defined as $V_{cr} = \min V(x_i)$, the minimum of energy of unstable equilibrium points on the stability boundary. 3. Numerically integrate the fault-on system, $x_f(t)$; if $V(x_f(t_{cl}))<V_{cr}$, then the system is stable; where t_{cl} is the clearing time.

2. PEBS Method (Potential Energy Boundary Surface): V_{cr} = maximum value of the potential energy component of $V(x)$ along the fault-on trajectory (3.3). This method was created in order to find a solution for the problem of estimating the attraction area or stability region of a power system without the requirement of calculating unstable equilibrium points. This method has the advantage of providing fast estimates from the computational point of view, for the critical time; but these estimates may not be conservative as the point of maximum potential energy along the fault-on trajectory may not be on the boundary of the stability region (CHIANG; WU; VARRAIYA, 1988).

3. Controlling unstable equilibrium point: $V_{cr} = V(x^u)$, where x^u is a relevant or controlling unstable equilibrium point, that is, an unstable equilibrium point "closest" to the point where the fault-on trajectory (3.3) exits the region of attraction of (3.4). This method is called method of Controlling unstable equilibrium point. The BCU method (Boundary Controlling UEP), (CHIANG; WU; VARRAIYA, 1987) is an efficient technique for calculating this equilibrium point. Determination of t_{cr} is obtained by means of the following steps (SAUER; PAI, 1998): 1.

Calculate x_s , the asymptotically stable equilibrium point of the post-fault system (3.4). 2. Calculate the CUEP x_{co} . 3. Calculate $V_{cr} = V(x_{co})$. 4. if $V(x_f(t_{cl})) < V_{cr}$, then the system is stable; where t_{cl} is the clearing time.

3.4 System Model

In transient stability studies, as in small-signal stability studies, the power system is modeled by a set of differential-algebraic equations (DAE):

$$\begin{bmatrix} \dot{x} \\ 0 \end{bmatrix} = \begin{bmatrix} f(x, y, p) \\ g(x, y, p) \end{bmatrix} \tag{3.6}$$

where $x \in R^{n_x}$ is a vector of state variables (e.g., rotor angle of generators), $y \in R^{n_y}$ is a vector of algebraic variables (e.g., voltages magnitudes at load buses) and $p \in R^{n_p}$ is a vector of control variables (e.g., active power output of generators). Function $f : R^{n_x} \times R^{n_y} \times R^{n_p} \rightarrow R^{n_x}$ is a nonlinear vector function associated with the state variables x that usually represents the system differential equations, such as those associated with the synchronous machine dynamics, control devices, etc.; and vector function $g : R^{n_x} \times R^{n_y} \times R^{n_p} \rightarrow R^{n_y}$ represents the system algebraic equations, including the power flow equations, algebraic equations associated with the synchronous machine model, etc.

In this work, the classical model is used to represent the power system. This model is based on the following assumptions (ANDERSON; FOUAD, 1977):

1. The input mechanical power is constant.
2. Damping is neglected.
3. Synchronous machines are represented by a constant electromotive force behind a transient reactance.
4. The mechanical rotor angle of the synchronous machine coincides with the angle of the electromotive force behind a transient reactance.
5. Loads are represented by constant impedances.

Note that this classical model is a trade of between sufficient accuracy and moderate computational effort. Within the classical model, the transient behavior of synchronous generators is described by the so-called swing equations:

$$\dot{\delta}_i = \omega_i \tag{3.7}$$

$$\dot{\omega} = \frac{1}{M_i}(P_{mi} - P_{ei}) \tag{3.8}$$

where δ_i is the rotor angle, ω_i is the rotor speed, M_i is the inertia coefficient, P_{mi} is the input mechanical power, and P_{ei} is the output electrical power of the i_{th} generator. Since the loads are approximated as constant impedances, the equivalent load admittance at bus n is:

$$Y_{Dn} = \frac{P_{Dn}}{V_n^2} - j\frac{Q_{Dn}}{V_n^2} \tag{3.9}$$

where P_{Dn} is the active power demand, Q_{Dn} is the reactive power demand , V_n is the bus voltage magnitude at bus n. The original network can be reduced into an equivalent network containing only the internal generator nodes (LAYDEN; JEYASURYA, 2004). The admittance matrix of the reduced network is called the reduced admittance matrix and can be used to calculate the electrical power of the generators. Thus, the electrical power P_{ei} in (3.8) can be written as follows:

$$P_{ei} = E_i \sum_{k=1}^{ng} E_k \left(G_{ik}\cos\delta_{ik} + B_{ik} sen\delta_{ik}\right) \tag{3.10}$$

Where E_i is the electromotive force of the corresponding i_{th} generator, G_{ik} and B_{ik} contain the real and imaginary part of the bus admittance matrix, between the busses associated to “i” and “k” generators. For details regarding the modeling of a power system for transient stability analysis purpose see: Sauer and Pai, 1998, and, Bretas and Alberto, 2000.

3.5 Center of inertia

In transient stability studies, it is convenient to express the generator rotor angles with respect to the Center of Inertia (COI) reference. The position of the COI is defined as (BRETAS; ALBERTO, 2002; ZÁRATE-MIÑANO, 2010):

$$\delta_{COI} = \frac{1}{H_T}\sum_{k=1}^{ng} H_k \delta_k \tag{3.11}$$

where:

$$H_T = \sum_{k=1}^{ng} H_k \tag{3.12}$$

The rotor angle of the generator i with respect to the COI is expressed as $\delta_i - \delta_{COI}$. Where “ng”, is the number of generators and H_k is the inertia constant of the k-th generator.

3.6 Transient stability assessment

To illustrate transient stability studies in a multi-machine system, we will consider the following three-generator system given in Bretas and Alberto, (2000). Lines, bars, machine data and the results of a Power flow are presented in Fig. 3.5.

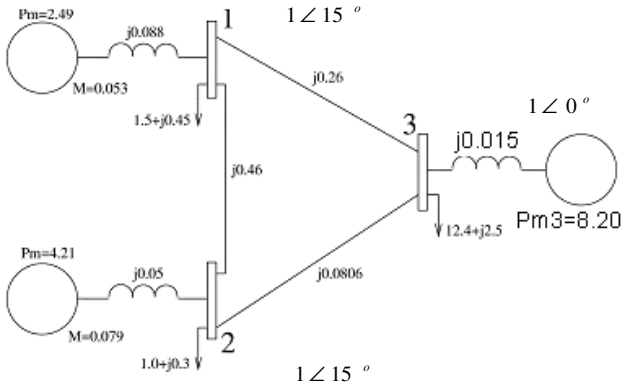

Fig. 3.5 3 machine 3-bus system (BRETAS; ALBERTO, 2000).

A short-circuit happens in the line 1-2, very close to bus 2, so that it was considered that the short-circuit happened at bus 2. The following set of differential equations (3.13) and (3.14), describe the dynamic behavior of the machines. The complete procedure to obtain these equations are described in (BRETAS; ALBERTO, 2000).

Fault-on system

$$0.053\,\dot{\omega}_1 = 2.49 - 1.073^2 \times 0.62 - 2.09\sin(\delta_1 - \delta_3) - 0.485\cos(\delta_1 - \delta_3)$$

$$0.079\dot{\omega}_2 = 4.21$$

$$0.318\dot{\omega}_3 = 8.20 - 1.053^2 \times 8.61 - 2.09\sin(\delta_3 - \delta_1) - 0.485\cos(\delta_3 - \delta_1)$$

$$\dot{\delta}_1 = \omega_1$$

$$\dot{\delta}_2 = \omega_2$$

$$\dot{\delta}_3 = \omega_3 \tag{3.13}$$

Post-fault system

$$0.053\dot{\omega}_1 = 2.49 - 1.073^2 \times 0.82 - 0.28\sin(\delta_1 - \delta_2) - 0.078\cos(\delta_1 - \delta_2) - 2.47\sin(\delta_1 - \delta_3) - 0.63\cos(\delta_1 - \delta_3)$$

$$0.079\dot{\omega}_1 = 4.21 - 1.057^2 \times 0.53 - 0.28\sin(\delta_2 - \delta_1) - 0.078\cos(\delta_2 - \delta_1) - 6.84\sin(\delta_2 - \delta_3) - 1.29\cos(\delta_2 - \delta_3)$$

$$0.318\dot{\omega}_1 = 8.20 - 1.053^2 \times 8.61 - 2.47\sin(\delta_3 - \delta_1) - 0.078\cos(\delta_3 - \delta_1) - 2.47\sin(\delta_3 - \delta_2) - 1.29\cos(\delta_3 - \delta_2)$$

$$\dot{\delta}_1 = \omega_1$$

$$\dot{\delta}_2 = \omega_2$$

$$\dot{\delta}_3 = \omega_3 \tag{3.14}$$

For the purpose of stability studies of this system, it is necessary to resolve the previous differential equations by means of some numerical integration method. In Bretas and Alberto, (2000); the differential equations that describe this power system were resolved using a 4th order Runge-Kutta integration method, and it was found that the critical clearing time is between 0.194 and 0.196s.

In this work, an integration-based method was implemented with MATLAB code. Differential equations were resolved using a trapezoidal integration method with a time step of 0.005s. It was found that the *critical clearing time is between 0.187 and 0.188s.* The swing equations are discretized using the trapezoidal integration method. Thus, generator rotor angles and speeds for a generic time step [n, n+1], are calculated by the following equations:

$$\delta_i^{n+1} - \delta_i^n - \frac{h}{2}(\omega_i^{n+1} + \omega_i^n) = 0;$$

$$\omega_i^{n+1} - \omega_i^n - \frac{h}{2}\frac{1}{M_i}(P_{mi} - P_{ei}^{n+1} + P_{mi} - P_{ei}^n) = 0;$$

where:

$$P_{ei}^n = E_i \sum_{m \in i}^{ng} E_m \left[G_{im}^n \cos(\delta_i^n - \delta_m^n) + B_{im}^n \sin(\delta_i^n - \delta_m^n) \right];$$

$$(n = 1,2,...,nend; i = 1,2,.....,ng);$$

"h" is the integration step length, "n" is the integration step counter, "nend" is the number of integration steps and "ng" is the number of generators. P_{ei} is the Electric Power associated with the generator "i".

When the fault was applied during a time higher than the critical clearing time, the system machines lost their synchronism. In spite of the short-circuit happening at the terminal bus of generator 2, machine 1 loses synchronism with the other system machines. Fig. 3.6(a) and Fig. 3.6(b), illustrate a situation where machines are in synchronism with the others. In this case, the system is considered transiently stable and the clearing time is 0.1 s. Fig. 3.7(a) and Fig. 3.7(b), illustrate a situation where machines lose their synchronism; this means that the system is transiently unstable with a clearing time equal to 0.188 s.

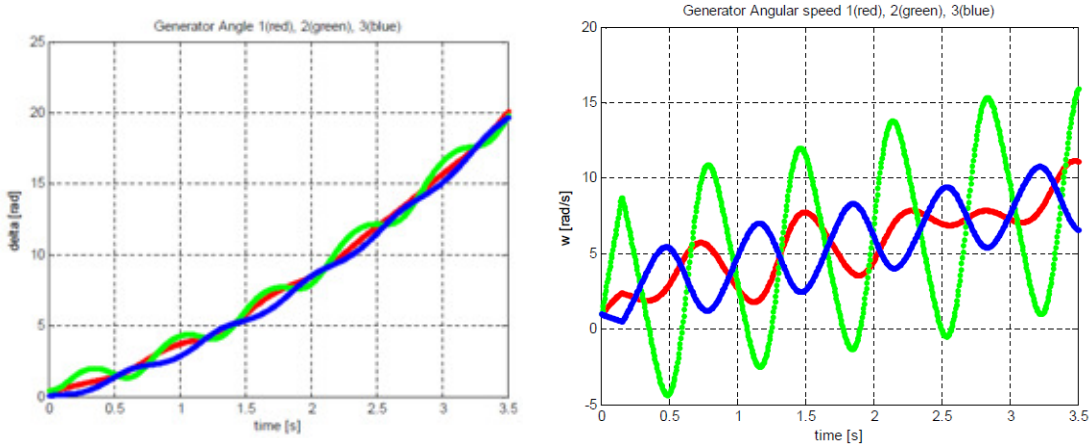

(a) (b)

Fig.3.6. Stable situation with a clearing time of 0.1s. (a) Machines Rotor Angles in synchronism. (b) Machines Rotor Speeds in synchronism

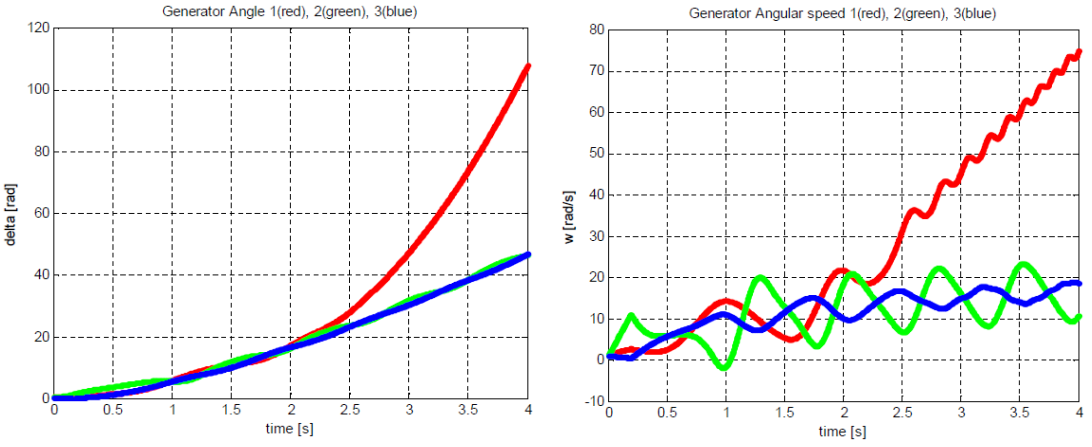

(a) (b)

Fig.3.7 Unstable case with a clearing time of 0.188s. (a) Machines Rotor Angles loss synchronism. (b) Machines Rotor Speeds loss synchronism.

By means of this example, we can see how the machines of the system respond after a disturbance. These are some reasons in which stability is an important constraint in Power System Operation. The objective is to obtain the optimal control actions that should be applied here and now, to ensure the system operate properly if any contingence occurs. The solution of the proposed re-dispatch procedure corresponds to the optimal preventive control actions required to ensure the desired security level.

Chapter 4

4. Optimal Power Flow with Transient Stability Constraints

In this chapter we discuss how to incorporate transient Stability Constraints into the optimal Power Flow Problem.

In chapter 3, we recalled that a power system remains transiently stable if the state $x^f(t_{cl})$, which corresponds to the state of the fault-on trajectory at the clearing time t_{cl}, remains within the stability region $A(x_s)$ of the stable equilibrium point x_s of the post-fault system (BRETAS; ALBERTO, 2000).

$$x^f(t_{cl}) \in A(x_s) \tag{4.1}$$

Thus, the OPF problem with transient stability constraints can be formulated as:

$$\text{Min } f\left(P_{gi}\right) \tag{4.2}$$

where

$$f\left(P_{gi}\right) = \sum_{i=1}^{i=ng} \alpha_i P_{gi}^2$$

Subject to:

$$P_{gi} - P_{li} - P_i(V,\theta) = 0 \tag{4.3}$$

$$Q_{gi} - Q_{li} - Q_i(V,\theta) = 0 \tag{4.4}$$

$$P_{gi}^{\ m} \le P_{gi} \le P_{gi}^{\ M} \tag{4.5}$$

$$E_{gi}^m \le E_{gi} \le E_{gi}^M \tag{4.6}$$

$$x^f(t_{cl}) \in A(x_s), \text{ for each contingency} \tag{4.7}$$

Theoretically this problem is well-posed, however the issue of checking the constraint (4.7) is very challenging, having mainly the following steps:

1. Computing $x^f(t_{cl})$ by solving the fault-on differential equations.
2. Determining the Stability region $A(x_s)$.

Step 1 involves the resolution of the fault-on differential equations for each contingency. The solution of these differential equations changes with the control variables P_{gi}. Since there is no closed analytical form for these solutions as a function of variables P_{gi}, it is difficult to apply conventional existing algorithms for solving this Nonlinear programming (NP) problem because they depend on the knowledge of the derivatives of the constraint functions with respect to the variables of the problem.

Step 2 is very challenging; it has been shown in section 3.2.1 that the stability boundary is formed by the union of the stable manifolds of the unstable equilibrium points on the boundary. Again, there is no closed analytical equation to describe these manifolds as a function of the variables P_{gi}, leading to the same problem previously described related to the application of existing algorithms for the resolution of this nonlinear programming problem.

Existing proposals of Optimal Power Flow with transient stability constraints usually represent stability constraints in an approximate way. Next, it will be discussed two different approaches to formulate the problem of the Optimal Power Flow with Transient Stability Constraints in Power systems. One of them based on direct methods and the other based on time-domain simulation.

4.1 Direct Methods

Directs methods have had a long developmental history spanning six decades, but until recently, many were thought to be impractical for large-scale power systems. Among the direct methods, the classical method of using the concept of closest unstable equilibrium point (UEP) gives a very conservative assessment of stability (CHIANG H.-D; THORP, J.S., 1989). The potential energy boundary surface (PEBS) method is fast but may give inaccurate stability assessments (CHIANG H.-D., WU F. F.; VARAIYA P. P., 1994). The controlling UEP method is the most viable direct method in terms of its accuracy and slightly conservative nature. The success of the controlling UEP method, however, hinges on the ability to compute the controlling UEP (CHANG H.-D.; CHU CH.; CAULEY G., 1995). The BCU (Boundary Controlling UEP) method can reliably compute the controlling UEP (CHIANG H.-D., WU F. F.; VARAIYA P. P., 1994). The combination of the controlling UEP method and the BCU method now emerges as a practical means for solving large-scale transient stability analysis problems. Extensive evaluations of the BCU-based controlling UEP method on large-scale power systems such as a 12,000-bus power system were conducted and promising results were reported in Chiang et al. (2006); and Tada et al. (2005), (CHIANG, 2010).

Direct methods use two steps to solve the stability problem. First, they compute only the relationship between the pre-fault stable equilibrium point (SEP) and the system state at the time of

fault clearing using the step-by-step numerical integration of the fault-on system. In the second step, the direct methods directly determine, without numerical integration of the post-fault system, whether the initial state of the post-fault system lies inside the stability region of a desired stable equilibrium point (SEP). This direct determination of the stability property is based on an energy function (defined for the post-fault system) and on a critical energy (relative to the fault-on trajectory).

If the energy function value of the initial state of the post-fault system is less than the critical energy, then the post-fault trajectory will settle down to the desired post-fault SEP. This is the analytical basis of direct methods. The great challenge in direct methods is determining the critical energy relative to a fault-on trajectory and deriving energy functions for power system stability models (CHIANG, 2010).

Based on this discussion, the stability constraint (4.7) can be replaced by the following constraint: $V\left(x(t_{cl})\right) < V_{cr}$. This constraint is more conservative than (4.7), but it eliminates the necessity of computing the stable manifolds on the boundary of the stability region. Although this constraint is simpler than (4.7), V_{cr} and $x(t_{cl})$ depend on the control variables and there is no closed analytical function describing this dependency on the control variables, leading to difficulties of applying conventional algorithms to solve this NP problem.

Sensitivity analysis could be used to approximately represent this constraint. Wehenkel and Pavella (2004), for example, approximate the stability constraints by means of the sensitivity of the stability margin measured by an energy function. Chiang et al., 2006; also use sensitivities to approximate such constraint.

Future research is required to study how direct methods could be incorporated into the Nonlinear Programming (NP) problem with the target of reducing the computational effort in comparison with the computational effort required by the implemented time-domain based approach.

4.2 Time-domain based approach

Gan, Thomas and Zimmerman, (2000), substitute the transient stability constraints by a maximum angle deviation of the synchronous machine rotors (100 degrees). This choice is based on the fact that a stable system has all the machines synchronized with a bounded angle deviations. The choice of this maximum angle deviation is heuristic. Table 4.1 presents some choices made in the literature.

Table 4.1 - Rotor angle deviation limits for Transient stability analysis used in the literature (ZÁRATE-MIÑANO; MILANO; CONEJO, 2010).

Reference	Rotor angle deviation limit [degrees]
(GAN; THOMAS; ZIMMERMAN, 2000; YUAN; KUBOKAWA; SASAKI, 2003; LAYDEN; JEYARSURYA, 2004)	100
(XIA; CHAN; LIU, 2005)	130
(LUONAN et al., 2001)	144
(NGUYEN; PAI., 2003)	180

The time-domain simulations provide the evolution of the system variables over time, using step-by step numerical integrations to simulate the entire system trajectory. A practice to detect a loss of synchronism is to check whether or not the inter-machine rotor angle deviation lies within a specific range of values during the total simulation (pre-fault and post-fault) for the methods aforementioned. The time-domain approach computes the relationship between the pre-fault stable equilibrium point and the post-fault state, using step-by-step numerical integrations to simulate the entire system trajectory.

4.3 Comparison of Time-Domain and Direct Method based approaches

A comparison between the Time-Domain simulation approach and the Direct Method approach, is presented in Table 4.2.

Table 4.2. A Comparison of these two approaches for transient stability analysis: Time-Domain Approach and Direct Methods (CHIANG, 2010).

Time-domain approach	Direct Methods
Numerical integration methods are required to simulate the fault- on trajectory.	Numerical integration methods are required to simulate the fault-on trajectory.
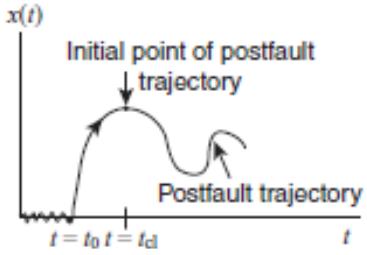 Fig 4.1 Time-frame required to transient stability analysis using time-domain approach (CHIANG, 2010).	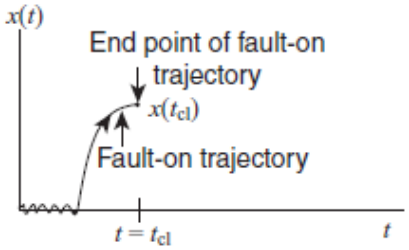 Fig 4.2 Time-frame required to transient stability analysis using direct methods. (CHIANG, 2010).
• Numerical integration methods are used to simulate the post fault trajectory for stability analysis. • If the post-fault trajectory settles down, then the post-fault system is assessed to be stable; otherwise, it is unstable.	• The post-fault trajectory $x(t)$ is not required, while the initial condition $x(t_{cl})$ is required. • The critical energy V_{cr} for the fault-on trajectory is required and the energy function $V(x)$ (for the post-fault system) is required. • Numerical integration of post-fault trajectory is not required. Direct stability assessment of the post-fault trajectory is based on the comparison between the energy after the fault and the associated critical energy. In other words, if $V(x(t_{cl})) < V_{cr}$, then the post-fault trajectory $x(t)$ is stable; otherwise, $x(t)$ may be unstable (CHIANG, 2010).

In this work, transient stability constraints are incorporated into the Optimal Power Flow (OPF) problem by converting differential equations in a set of numerical equivalent algebraic equations Then a procedure of multi-step optimization is proposed in this work to minimize convergence problems and speeding up computation. The proposed procedure was successfully tested on a 3-machine system, having the generated powers as control variables.

As previously mentioned, representation of the dynamics of the system as a set of discrete equations significantly increases the number of variables of the optimization problem. Consequently, computational costs are significantly increased by means of the approach followed in this dissertation. The other way to attack this problem is using direct methods to formulate transient stability constraints. In this case, only the fault-on trajectory will be enough to conclude about stability; which will reduce drastically the computational effort. We are researching how direct methods can be applied to formulate transient stability constraints (4.7), making use of the time-domain simulation to asses transient stability.

We believe direct methods can accelerate the SCOPF solution. Moreover, they might eliminate the heuristic approach of selecting a threshold as an angle constraint (In the approach of Gan; Thomas; Zimmerman, 2000: Center of angle constraint). We believe the existence of two possible ways to achieve this: Use an energy threshold instead of angle threshold or transform the energy threshold into an angle threshold. The issues of this implementation by means of the use of direct methods are under research. But, in both cases, only the fault-on trajectory would be enough to conclude about stability; reducing drastically the computational effort as compared to the approach proposed in Gan, Thomas and Zimmerman, 2000.

4.4 Stability Constrained Optimal Power Flow

One of the advantages of the representation of stability constraints by means of maximal angular deviation is that these constraints can be written directly into the state variables of the problem. Even so, for the verification of the stability constraints, it is necessary to solve the differential equations that model the stability problem, generating constraints in the form of differential equations for the optimization problem. To resolve this issue, differential equations are approximated by means of numerical integration techniques and converted in a set of algebraic equations, discretized in time. Thus, the OPF problem with transient stability constraints can be solved using conventional optimization techniques; with the cost of a significant increase in the numbers of variables of the optimization problem. The optimization problem formulated in this way has a high dimension, is non-linear and non-convex; leading to the existence of multiple solutions and to non-convergence problems of the conventional numerical optimization algorithms.

4.4.1 Stability Constrained Optimal Power Flow formulation

The main objective of incorporating transient stability constraints into the OPF formulation is to develop a tool that helps the operator to take decisions that ensure static and security transient stable operation with respect to a list of potentially harmful contingences. One application is the design of preventive control, whose objective is to prepare the system, while it is in normal operation, so as to make it able to face future (uncertain) events in a satisfactory way (WEHENKEL;

PAVELLA, 2004). One preventive control measure is to achieve a stable power system operating point by rescheduling the mechanical power inputs injected to the generators, while respecting generator limits and static security constraints (line power flows).

Mathematically, we can formulate this problem as a standard Optimal Power Flow problem, as follows:

$$\text{Min}_{P_{gi}} \; f(P_{gi}) \tag{4.8}$$

where

$$f\left(P_{gi}\right) = \sum_{i=1}^{i=ng} \alpha_i P_{gi}^2$$

Subject to:

$$P_{gi} - P_{li} - P_i(V,\theta) = 0 \tag{4.9}$$

$$Q_{gi} - Q_{li} - Q_i(V,\theta) = 0 \tag{4.10}$$

$$P_{gi}^{\,m} \le P_{gi} \le P_{gi}^{\,M} \tag{4.11}$$

$$Q_{gi}^{m} \le Q_{gi} \le Q_{gi}^{M} \tag{4.12}$$

where $i = 1,2,...,ng$, "ng" is the number of generators of the system. Function $f(P_{gi})$ represents the generation cost, α_i is the rate of change or slope between the cost function and the square of the respective output power generation and indicates the sensitivity of the respective variable in the calculation of the cost function. Equations (4.9) are the active power flow equations; the equality constraints (4.10) are the reactive power flow equations; P_{gi} is the vector of generator active power outputs with upper bound P_{gi}^{M} and lower bound P_{gi}^{m} ; Q_{gi} is the vector of generator reactive power outputs with upper bound Q_{gi}^{M} and lower bound Q_{gi}^{m}; P_{li} is the active power demand of the i_{th} bus. $P_i(V,\theta)$ and $Q_i(V,\theta)$ are vectors of active and reactive power injections.

Note: Cost functions usually have the following form: $f(x) = c + bx + a^2 x$. Parameter "c" represents fixed costs. The term bx represents the total cost that increases linearly with "x" and the term $a^2 x$ is negligible if "a" is small and "x" is relatively small and becomes dominant as "x" grows larger. The variable "x" represents the number of some commodity. In this dissertation, terms "c" and "b" assume the value zero, and only the quadratic term $a^2 x$ was considered.

For simplicity we will assume for stability analysis that the loads are modeled by constant impedance and synchronous machine are represented by the classical model. Consequently, we have the following “swing” equation, developed in Chapter 3 (SAUER; PAI, 1998):

$$\dot{\delta}_i = \omega_i \tag{4.13}$$

$$\dot{\omega}_i = \frac{1}{M_i}\left(P_{mi} - P_{ei}\right) \tag{4.14}$$

where:

$$P_{ei} = E_i \sum_{k=1}^{ng} E_k \left(G_{ik}\cos\delta_{ik} + B_{ik} sen\delta_{ik}\right) \tag{4.15}$$

and $i = 1,2,...,ng$; in which “ng” is the number of the generators. “*G”* and *“B*” contain the real and reactive part of the bus admittance matrix and G_{ik} and B_{ik} are the elements of matrices G and B. P_{mi} , is the mechanical power applied to the i_{th} generator; M_i is the inertia constant of the i_{th} generator; ω_i and δ_i , are the rotor speed and the rotor angle of the i_{th} generator. The generators are modeled by the classical model in which the synchronous machine is characterized by a constant voltage E behind a transient reactance X'_{di}.

Observe that we have to establish the equations needed for estimating initial values of rotor angles. To accomplish this, we have to set up the following equations:

$$V_i^2 - E_i V_i \cos\left(\delta^0{}_i - \theta_i\right) + Q_{gi} X`_{di} = 0 \tag{4.16}$$

$$E_i V_i \sin\left(\delta^0{}_i - \theta_i\right) - P_{gi} X`_{di} = 0 \tag{4.17}$$

$$i = 1,2,...,ng$$

where, P_{gi} is the vector of generator’s active power output; Q_{gi} is the vector of generator’s reactive power output. V_i and θ_i are the vectors of bus voltage magnitudes and angles. E_{gi} and X'_{di}, are the constant voltage of the generators and the transient reactance, which are the parameters that represent the i_{th} generator. ng is the number of generators.

To ensure stability, we need to ensure the solution of equations (4.13) and (4.14) for the fault-on and post-fault trajectories, satisfies the following angle deviation restriction for each generator and for each contingency:

$$\overline{\delta}_i(t) = \left\| \delta_i(t) - \frac{\sum_{k=1}^{ng} H_k \delta_k(t)}{\sum_{k=1}^{ng} H_k} \right\| \leq 100^0 \qquad (4.18)$$

$$i = 1, 2, ..., ng$$

where “ng”, is the number of generators; and $\overline{\delta}_i$ is the rotor angle with respect to the center of inertia reference. In (4.18) we use rotor angle to check whether the system is stable.

At first, we remark that there is no general method for measuring the stability region of dynamic system (4.13)-(4.14). Thus, equation (4.18) is an approximation. Secondly, suppose the generators are approximately separated into two groups during the transient duration, then, the well-known equal area principle reveals that the relative rotor angle between the two groups of generators should always be smaller than 180 degrees; otherwise the system is unstable (GAN; THOMAS; ZIMMERMAN, 2000). Finally, nowadays a real-world power system is operated in a way that any generator rotor angle will not be greater than a threshold. If a generator’s rotor angle is larger than such a threshold, the generator will be tripped off-line by out-of-step relay to protect it from being damaged (FOUAD; VITTAL, 1991).

The solution of the Stability Constrained OPF is a set of generator set-points that satisfy equations and inequalities (4.8)–(4.18). This nonlinear programming problem includes both algebraic and differential equation constraints, which is a very challenging problem that has no general method to solve it. In the next section, we will discuss a procedure for solving the Stability Constrained Optimal Power Flow based on a discrete dynamic model that approximates the swing equations of the power system and transforms the problem into a regular nonlinear programming problem with only algebraic constraints.

4.4.2 Outline of the Stability Constrained OPF Formulation

Existing optimization methods cannot handle differential and algebraic equations at the same time. Then, in order to include stability constraints; the alternative which was implemented, consisted in convert the differential-algebraic equations of the Stability Constraints to their numerically equivalent algebraic equations using an appropriate rule. Applying the trapezoidal integration scheme to equations (4.13)-(4.14), for $n = 1,2,...,nend$ and $i = 1,2,.....,ng$, one obtains:

$$\delta_i^{n+1} - \delta_i^n - \frac{h}{2}\left(\omega_i^{n+1} - \omega_i^n\right) = 0 \tag{4.19}$$

$$\omega_i^{n+1} - \omega_i^n - \frac{h}{2M_i}\left(2P_{mi}^{n+1} + P_{ei}^{n+1} + P_{ei}^n\right) = 0 \tag{4.20}$$

where “h” is the integration step length, “n” is the integration step counter, “nend” is the number of integration steps, Pei is the output electrical power (p.u.) of the i-th generator given by (4.15).

The solution of equations (4.19) and (4.20) approximates the solution of the differential equations (4.13) and (4.14) at the discrete times of $t \in [0,.....,t_{final}]$ with $t_{final} = h \times nend$, which corresponds to the desired simulation time. Thus, the stability constraints (4.18) can be simplified into:

$$\left\| \delta_i^n - \frac{\sum_{k=1}^{ng} H_k \delta_k}{\sum_{k=1}^{ng} H_k} \right\| \le 100^o \qquad (n = 1,2...,nend \qquad i = 1,2,...,ng) \tag{4.21}$$

In summary, we obtain the following algebraic nonlinear program (NP) problem:

$$\text{Min}_{P_{gi}} \; f(P_{gi}) \tag{4.22}$$

where

$$f\left(P_{gi}\right) = \sum_{i=1}^{i=ng} \alpha_i P_{gi}^2$$

Subject to:

$$P_{gi} - P_{li} - P_i(V,\theta) = 0 \tag{4.23}$$

$$Q_{gi} - Q_{li} - Q_i(V,\theta) = 0 \tag{4.24}$$

$$P_{gi}^m \le P_{gi} \le P_{gi}^M \tag{4.25}$$

$$Q_{gi}^m \le Q_{gi} \le Q_{gi}^M \tag{4.26}$$

$$V_i^2 - E_i V_i \cos\left(\delta^0{}_i - \theta_i\right) + Q_{gi} X`_{di} = 0 \tag{4.27}$$

$$E_i V_i \sin\left(\delta^0{}_i - \theta_i\right) - P_{gi} X`_{di} = 0 \tag{4.28}$$

$$\delta_i^{n+1} - \delta_i^n - \frac{h}{2}\left(\omega_i^{n+1} - \omega_i^n\right) = 0 \tag{4.29}$$

$$\omega_i^{n+1} - \omega_i^n - \frac{h}{2M_i}\left(2P_{mi}^{n+1} + P_{ei}^{n+1} + P_{ei}^n\right) = 0 \tag{4.30}$$

$$\left\| \delta_i^n - \frac{\sum_{k=1}^{ng} H_k \delta_k}{\sum_{k=1}^{ng} H_k} \right\| \le 100^o \qquad (n = 1, 2..., nend \qquad i = 1, 2, ..., ng) \tag{4.31}$$

where “h” is the integration step length, “n” is the integration step counter, “nend” is the number of integration steps, “ng” is the number of generators.

This standard nonlinear programming problem can be solved using existing numerical methods of optimization. In this work; the active set method described in chapter 2 was employed. Interior point methods were also tested to solve the optimization problem (4.22)-(4.31), but they presented problems of non-convergence for simulation times higher than 200 ms. The main reasons for convergence problems are: Each iterate of the interior-point method is more expensive because the method must solve linear system involving all the variables whereas active-set methods solve systems involving some subsets of variables. As it was previously stated, the number of variables of the NP problem (4.22)-(4.31) is of high dimension, and is increased even more with the increasing of the simulation time. For this reason interior point methods had not a great performance to resolve this NP problem, which requires a high computational performance. Now, we are going to present the overall procedure of the Multi-Step Optimization Approach with Transient Stability Constraints. This is a contribution of this dissertation and as far as we know, has not been appeared in the literature.

4.5 Multi-Step Optimization Approach

One target of this work is to enhance the capabilities of the active-set method with the employment of a Multi-step optimization approach and achieve optimal results in the solution of this non-linear and non-convex optimization problem. To minimize the numerical aforementioned problems, a procedure of multi-step optimization is proposed in this paper. More precisely, the optimization problem is first solved considering a short total simulation time for the transient stability differential equations (for instance: 1s); and the control variables are adjusted by means of the optimization method with the target of bring all angular deviations below a predetermined value. Then, the maximum simulation time is incremented and the optimization problem is resolved again, using the

solution of the previous stage as initial condition for this stage. This process is repeated until the maximum simulation time reaches the desired value. The proposed procedure was tested on a 3-generator system, having the generated powers as control variables. The generation cost is minimized subject to transient stability constraints and to the usual constraints of generation and voltage limits. The results were promising and revealed the proposed procedure is efficient to minimizing convergence problems and speeding up the analysis.

A Multi-Step Optimization Approach for Power Flow with Transient Stability Constraints allows reducing the computational effort by dividing the overall optimization problem into sub-problems.

It is shown that, the proposed algorithm significantly reduces the number of systems and iterations that need to be solved. This is due to the fact that the previous stage optimization results are used as starting points to solve the Stability Constrained Optimal Power Flow (SCOPF) for the next stage, and so on, until the total desired time of analysis is reached.

When this occurs, it is guaranteed that the KKT conditions associated to the previous stage of the multi-step SCOPF are satisfied at the beginning of the iteration process of the subsequent stage (the KKT conditions of this subsequent stage incorporate the KKT conditions associated with the previous stage of the multi-step SCOPF algorithm). This procedure promotes a significant reduction in the number of iterations that need to be run in the next stage of the multi-step SCOPF algorithm.

Simulation results show convergence and provide an indication of the benefits of this multi-step approach. In what follows we explain the procedure displayed in Fig.4.3. For the current operating condition of the system; we start running Power Flow, and step by step integration. With the Power Flow results, which are: bus angles, active power of generators, reactive power of generators, and initial conditions of rotor angles of the generators and constant voltage of the generators, for all generators, can be calculated. We proceed to evaluate if the limits of active and reactive power generator are violated. With the Rotor angles response obtained by means of numerical integration, we can evaluate if the solution respects stability constraints. If the solution does not respect stability constraints, then the Multi-step optimization approach is employed.

We proceed to define the maximal time for transient stability analysis. This Maximal time is composed of intervals of time of the optimization problem. The interval time for the optimization problem is incremented with the value of the maximal time in which the NP problem (4.22)-(4.31) converges to the solution using active set methods. This criteria is used to increase this interval of time until to the maximal time is reached, along the optimization process.

For each stage of the Multi-step optimization approach, the NP problem (4.22)-(4.31) using the Active set method is solved, and the solution is updated until the KKT conditions are satisfied. The

KKT conditions in Fig. 4.3 recalls the Karush-Kuhn-Tucker optimality conditions associated with the Nonlinear Programming (NP) problem (4.22)-(4.31). Once the solution of this NP problem is achieved for the first stage; then, the results of this solution are used as initial conditions to the subsequent stage, and so on, until the last stage. These stages correspond to the interval times that conform the desired maximal time for the transient stability analysis.

In Chapter 2 were mentioned some advantages of Active-set methods. Specially, it was mentioned these methods are well-suited for "warm starts", where a good estimative of the optimal active set is used to start the algorithm. This is particularly useful in applications where a sequence of quadratic programs is solved, for instance, in a SQP method. In quadratic programming, as the solution is not necessarily on one of the edges of the feasible polygon, an estimation of the active set gives us a subset of inequalities to watch while searching the solution, which reduces the complexity of the search (WISCONSIN INSTITUTE FOR DISCOVERY, 2013). On the other hand, if the minimum of the objective function is in the edge of any restriction that belongs to the feasible region of the objective function; the subsequent stage of the multi-step SCOPF algorithm will start its searching from the satisfied restriction which has the minimum of the objective function from the previous stage of the multi-step SCOPF algorithm. These mentioned advantages of the active-set algorithm are efficiently used in this paper for the implementation of the Multi-Step Optimization Approach.

Once all the procedure of the Multi-step approach is finished, results are obtained satisfying the specifications. The output variables are bus angles, active power generators and reactive power generators, initial conditions of rotor angles of the generators, constant voltage of the generators, and the rotor angle trajectories for all generators. Active power of the generators, are the variables which are directly related with the cost function.

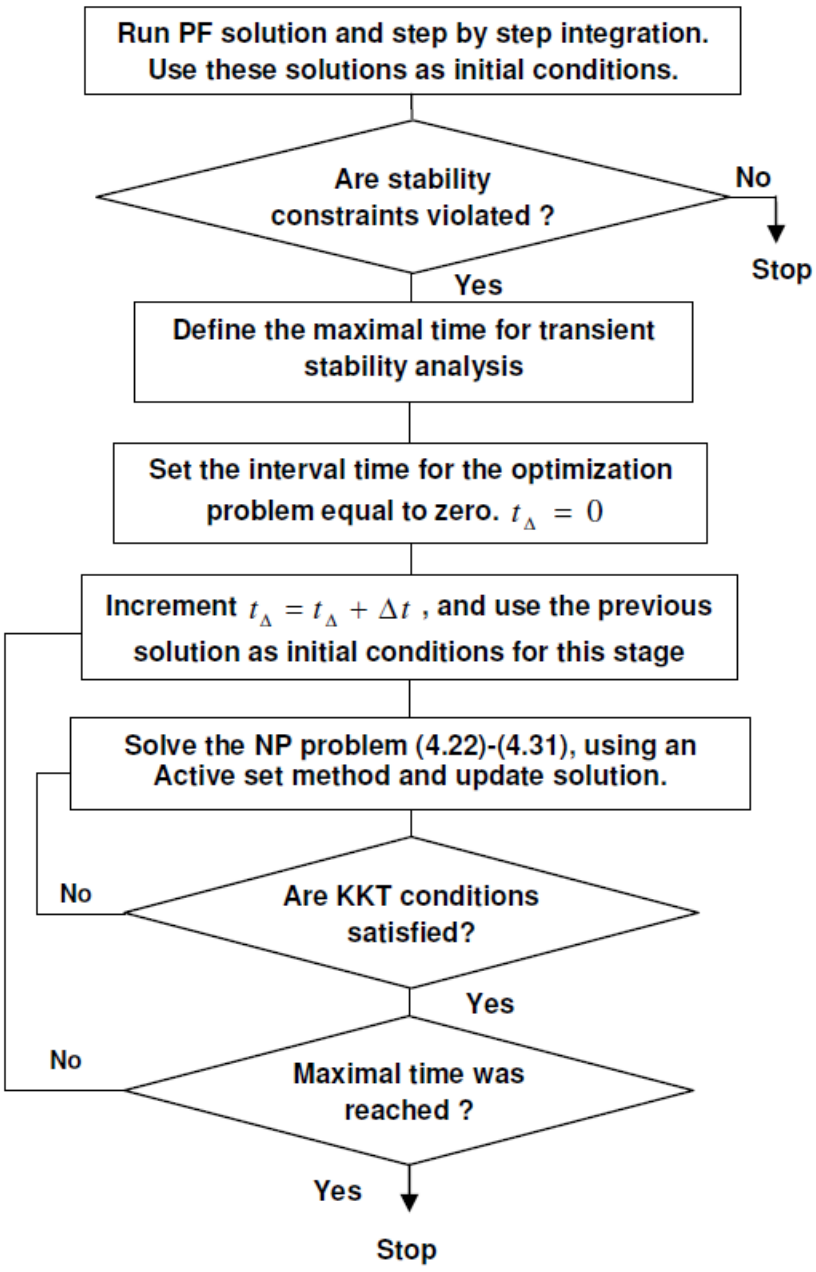

Fig. 4.3 Flowchart of the procedure for the Multi-Step Optimization Approach for Power Flow with Transient Stability Constraints.

4.6 Results

In this section, we present the results of tests made with the proposed Stability Constrained Optimal Power Flow (SCOPF) and Optimal Power Flow (OPF) when applied to a small power system.

4.6.1 Test System

Scenario 1

The proposed multi-step approach to solve the NP problem (4.22)-(4.31) has been tested on the 3-machine 3-bus system represented in Fig. 4.4. A ground fault is applied to bus 2 and the fault is cleared 200ms later, with the removal of line 1–2.

For this scenario 1, $Pm1 = 2.49$ p.u., $Pm2 = 4.21$ p.u., and $Pm3 = 8.2$ p.u.; in Fig. 4.4.

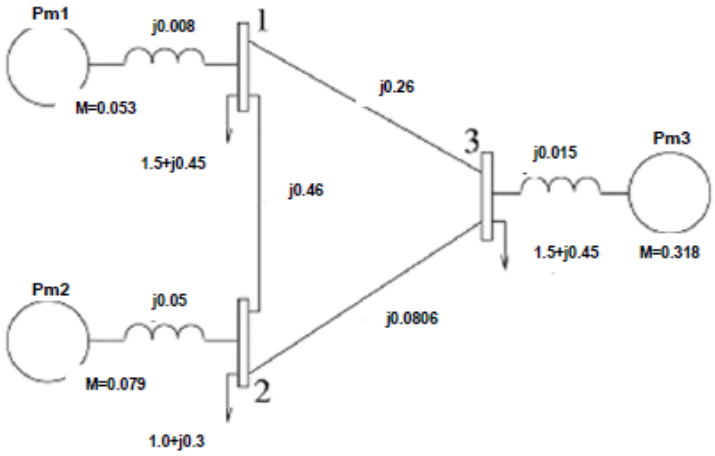

Fig. 4.4 3-machine 3-bus system for the test system.

The limits in the inequality constraints of the active power generation (4.11) and reactive power generation (4.12), for all generators are: $P_{gi}^{m} = 0$ p.u.; $P_{gi}^{M} = 8$ p.u.; $Q_{gi}^{m} = 0$ p.u.; $Q_{gi}^{M} = 4.5$ p.u, respectively. The values of α_i of the generation cost function $f(P_{gi})$ (4.8); are 1 $\$/pu.^2$, for all generators.

Scenario 2

The proposed multi-step approach to solve the NP (4.22)-(4.31) has been tested on the 3-machine 3-bus system represented in Fig. 4.4. A shortage to ground fault is applied to bus 2 and the fault is cleared 232ms. later, with the removal of line 1–2.

For this scenario, $Pm1 = 2.99$ p.u., $Pm2 = 3.71$ p.u., and $Pm3 = 8.2$ p.u.; in Fig. 4.4.

4.6.2 Results for Scenario 1:

In this section we present the results of the application of the Multi-step Approach proposed in section 4.3.2, for scenario 1.

First of all, we have to run Power Flow Solution and step-by-step integration. The Power Flow solution is: $\theta_1 = 15^\circ$, $\theta_2 = 15^\circ$, $P_{g1} = 2.49$ p.u., $P_{g2} = 4.21$ p.u, $P_{g3} = 8.2$ p.u, $Q_{g1} = 0.58$ p.u., $Q_{g2} = 0.72$ p.u., $Q_{g3} = 3.0$ p.u., $\delta_1^0 = 26.8^0$, $\delta_2^0 = 26.5^0$, $\delta_3^0 = 6.71^0$, $E_{G1} = 1.073$ p.u., $E_{G2} = 1.057$ p.u., $E_{G3} = 1.053$ p.u.

It can be seen that the limit of the active power generation of the generator 3 is violated for the upper bound, with the value 8.2 pu. The cost of generation is of $ 91.4.

This Power Flow solution is used to resolve the equivalent algebraic equations of the dynamical swing equations by means of numerical integration for a fault-on time of 200 ms.

The results of this numerical integration are shown in Fig. 4.5, showing that the system is unstable for this contingency. Consequently, stability constraints are violated for the initial state of the system.

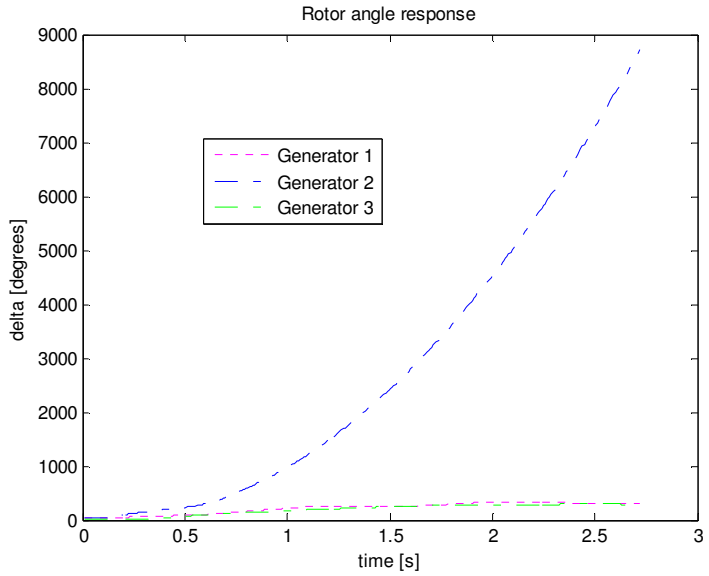

Fig. 4.5 Rotor Angle response of a 3 machine system. Unstable case with a clearing time of 200ms.

The power flow solution and the points obtained for the rotor angles using the trapezoidal integration method were used as starting points to resolve the Stability Constrained Optimal Power Flow (SCOPF) (4.22)-(4.31) and Optimal Power Flow (OPF) (4.8)-(4.18). The maximal time for transient stability analysis is set to be 2.6 s.

The initial interval of time for the optimization problem is set to zero. We increment this interval of time to 1.18 s. We are using the criteria described in section 4.3.2 to set the increments of this interval time, which are established for the interval of time in which the NP problem (4.22)-(4.31) converges to the solution. This criteria is repeated along the optimization process until the desired time on transient stability analysis is achieved.

We proceed to resolve the NP problem (4.22)-(4.31) using the active set method. The solution is updated until the KKT conditions are satisfied (otherwise the increment of this interval of time, has to be reduced).

The results of the first optimization stage using Stability Constrained OPF (4.22)-(4.31) solution are: $\theta_1 = 28.7^\circ$, $\theta_2 = 13.4^\circ$, $P_{g1} = 3{,}92$ p.u., $P_{g2} = 3{,}3$ p.u., $P_{g3} = 7.67$ p.u., $Q_{g1} = 1$ p.u., $Q_{g2} = 0.7$ p.u., $Q_{g3} = 2.73$ p.u., $\delta_1^0 = 46.32^\circ$, $\delta_2^0 = 22.49^\circ$, $\delta_3^0 = 6.31^\circ$, $E_{g1} = 1.142$ p.u., $E_{g2} = 1.045$ p.u., $E_{g3} = 1.047$ p.u.

We also resolve OPF problem (4.8) to (4.18) to compare these two solutions. Results of the first optimization stage using OPF solution are: $\theta_1 = 43.9^\circ$, $\theta_2 = 22.5^\circ$, $P_{g1} = 4.965$ p.u., $P_{g2} = 4.965$ p.u., $P_{g3} = 4{,}968$ p.u., $Q_{g1} = 1.7$ p.u., $Q_{g2} = 1.4$ p.u., $Q_{g3} = 2.82$ p.u., $\delta_1^0 = 64.83^\circ$, $\delta_2^0 = 35.62^\circ$, $\delta_3^0 = 4.09^\circ$, $E_{g1} = 1{,}22$ p.u., $E_{g2} = 1{,}09$ p.u., $E_{g3} = 1{,}044$ p.u.

Fig. 4.6, Fig. 4.8 and Fig. 4.10 respectively, displays the rotor angle of Generator 1, Generator 2 and Generator 3 when the contingency is applied, in two operation points: Optimal Power Flow (OPF) solution and the Stability Constrained OPF (SCOPF) solution. It can be seen that the system does not survive after the contingency at operating point given by OPF solution, but it does at operating point given by SCOPF solution.

Fig. 4.7, Fig. 4.9 and Fig. 4.11 illustrates the Iteration Process of the Stability Constrained OPF (SCOPF) by showing the maximum rotor angle deviation of Generator 1, Generator 2 and Generator 3, respectively, with respect to the inertia center angle. Fig. 4.12 shows the evolution of the cost function in the Iteration Process of the SCOPF while Fig. 4.13 shows the evolution of the cost function for the Iteration Process of the OPF.

Observe that the final cost of the OPF is lower than the final cost of the SCOPF. This was expected because the system is unstable to the contingency with the operating state produced by the OPF. These optimization results; were used as initial variables of a new SCOPF problem with a interval of time for the optimization, incremented to 1.952 s. This procedure allows us to extend the total time in the time domain simulations for the stability analysis.

After applying Stability Constrained Optimal Power Flow (SCOPF) solution and Optimal Power Flow (OPF) solution, we obtain the following results: $\theta_1 = 28.09^\circ$, $\theta_2 = 12.04^\circ$, $P_{g1} = 3{,}912$ p.u., $P_{g2} = 2{,}987$ p.u., $P_{g3} = 7{,}999$ p.u., $Q_{g1} = 0{,}988$ p.u., $Q_{g2} = 0{,}657$ p.u., $Q_{g3} = 2{,}734$ p.u., $\delta_1^0 = 45.6721^\circ$, $\delta_2^0 = 20.2736^\circ$, $\delta_3^0 = 6.5754^\circ$, $E_{g1} = 1{,}140$ p.u., $E_{g2} = 1{,}043$ p.u., $E_{g3} = 1{,}047$ p.u.

Fig. 4.14, Fig. 4.16 and Fig. 4.18 respectively displays the rotor angle of the Generator 1, Generator 2 and Generator 3 when the contingency is applied, in two operation points: Optimal Power Flow (PF) solution and Stability Constrained OPF (SCOPF) solution, for the second optimization stage. It can be seen that the system does not survive after the contingency at operating point given by OPF solution, but it does at operating point given by SCOPF solution.

Fig. 4.15, Fig. 4.17, Fig. 4.19 illustrates the Iteration Process of the stability constrained OPF (SCOPF) by showing the maximum rotor angle deviation of Generator 1, Generator 2 and Generator 3, respectively, with respect to the inertia center angle. Fig. 4.20 shows the evolution of the cost function in the Iteration Process of the SCOPF.

These previous optimization results; were used as initial variables for a new SCOPF problem with a interval of time for the optimization incremented to 2.64 s.

After solving Stability Constrained Optimal Power Flow (SCOPF) and Optimal Power Flow (OPF), we obtain the following results of the third optimization stage using Stability Constrained OPF (SCOPF) solution (4.22)-(4.31): $\theta_1 = 27.9593^\circ$, $\theta_2 = 12.1221^\circ$, $P_{g1} = 3{,}896$ p.u., $P_{g2} = 3{,}012$ p.u., $P_{g3} = 7{,}991$ p.u., $Q_{g1} = 0{,}988$ p.u., $Q_{g2} = 0{,}657$ p.u., $Q_{g3} = 2{,}734$ p.u., $\delta_1^0 = 45.4768^\circ$, $\delta_2^0 = 20.4175^\circ$, $\delta_3^0 = 6.5692^\circ$, $E_{g1} = 1{,}1393$ p.u., $E_{g2} = 1{,}0438$ p.u., $E_{g3} = 1{,}047$ p.u.

Fig. 4.21, Fig. 4.23 and Fig. 4.25 respectively displays the rotor angle of the Generator 1, Generator 2 and Generator 3 when the contingency is applied, in two operation points: Optimal Power Flow (OPF) solution and Stability Constrained OPF (SCOPF) solution, for the last optimization stage.

Fig. 4.22, Fig. 4.24, Fig. 4.26 illustrates the evolution of the maximum rotor angle deviation with respect to the inertia center angle of the Generator 1, Generator 2 and Generator 3, respectively in the iteration Process of the stability constrained OPF (SCOPF). Fig. 4.27 shows the evolution of the cost function along the Iteration Process of SCOPF. It can be concluded from these figures that OPF by itself cannot guarantee a secure operation since the system is unstable to the considered contingency. SCOPF fix this problem at the expense of a larger cost of generation. We have the Output power generation as output variables for all stages of the Multi-step optimization approach. Table 4.3 displays relevant initial conditions of the optimization variables and relevant results after each optimization stage for the OPF and SCOPF.

Table 4.3 Initial conditions and the Optimization variables results: for the first stage, second stage and third stage, respectively.

Initial conditions (PF solution)	**Optimization variables results**			
	1st stage (OPF solution)	**1st stage (SCOPF solution)**	**2nd stage (SCOPF solution)**	**3rd stage (SCOPF solution)**
$P_{g1} = 2.49$	$P_{g1} = 4{,}965$	$P_{g1} = 3{,}92$	$P_{g1} = 3{,}912$	$P_{g1} = 3{,}896$
$P_{g2} = 4.21$	$P_{g2} = 4{,}965$	$P_{g2} = 3{,}3$	$P_{g2} = 2{,}987$	$P_{g2} = 3{,}012$
$P_{g3} = 8.20$	$P_{g3} = 4{,}968$	$P_{g3} = 7.67$	$P_{g3} = 7{,}999$	$P_{g3} = 7{,}991$
$f(P_{gi}) = 91.16$	$f(P_{gi}) = 74$	$f(P_{gi}) = 85.16$	$f(P_{gi}) = 88.23$	$f(P_{gi}) = 86.05$
$\delta_1^{\max} = 165.3^\circ$	$\delta_1^{\max} = 1967^\circ$	$\delta_1^{\max} = 80^\circ$	$\delta_1^{\max} = 90.67^\circ$	$\delta_1^{\max} = 84.19^\circ$
$\delta_2^{\max} = 993.6^\circ$	$\delta_2^{\max} = 1821^\circ$	$\delta_2^{\max} = 68.11^\circ$	$\delta_2^{\max} = 63.5^\circ$	$\delta_2^{\max} = 69.85^\circ$
$\delta_3^{\max} = 219.3^\circ$	$\delta_3^{\max} = 780.3^\circ$	$\delta_3^{\max} = 27.3^\circ$	$\delta_3^{\max} = 29.79^\circ$	$\delta_3^{\max} = 27.95^\circ$

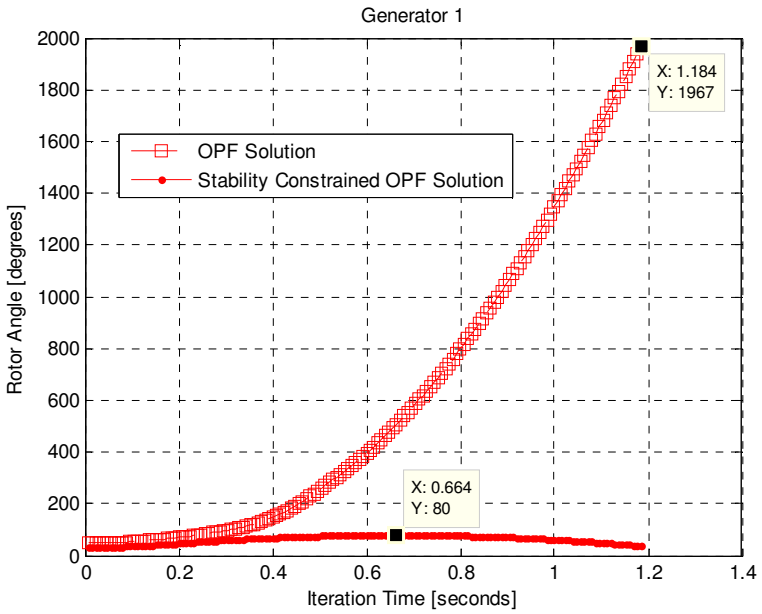

Fig. 4.6 Dynamic Response of the Generator 1 of the 3-machine 3-bus system at two operating points.

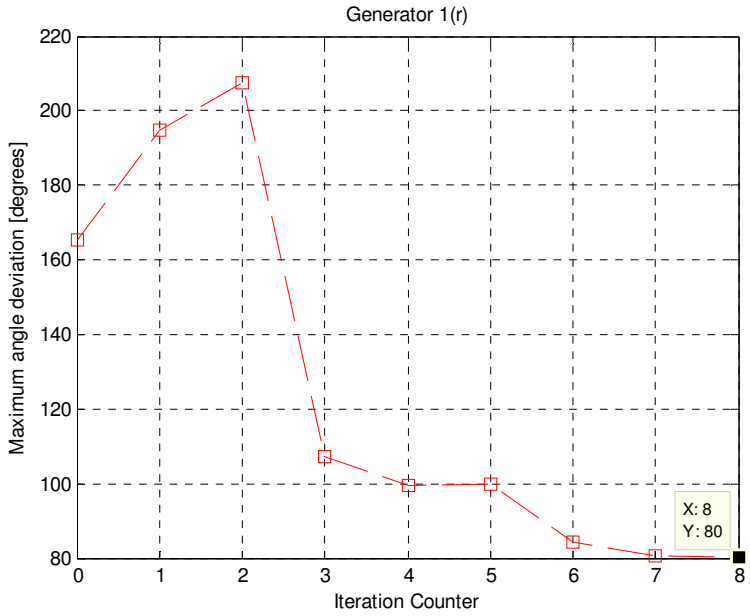

Fig. 4.7 Iteration Process of Stability Constrained OPF. Maximum angle of Generator 1

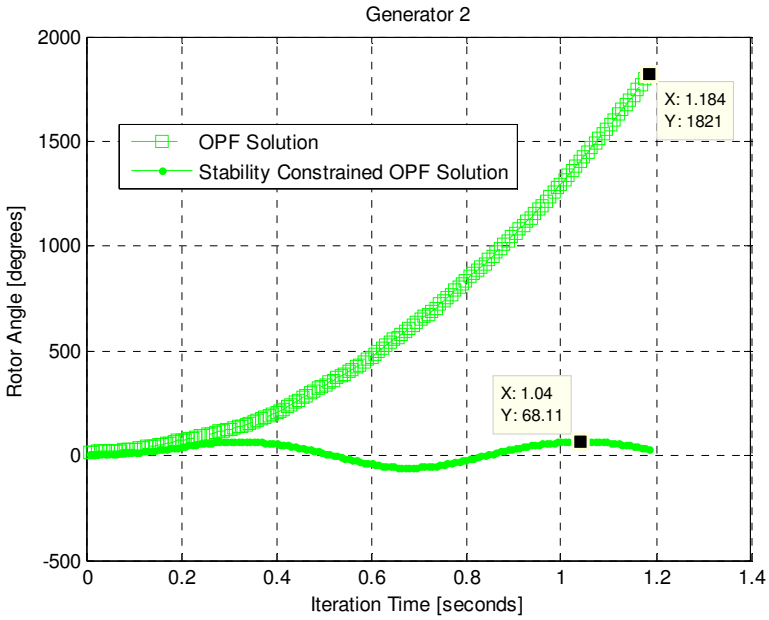

Fig. 4.8 Dynamic Response of the Generator 2 of the 3-machine 3-bus system at two operating points.

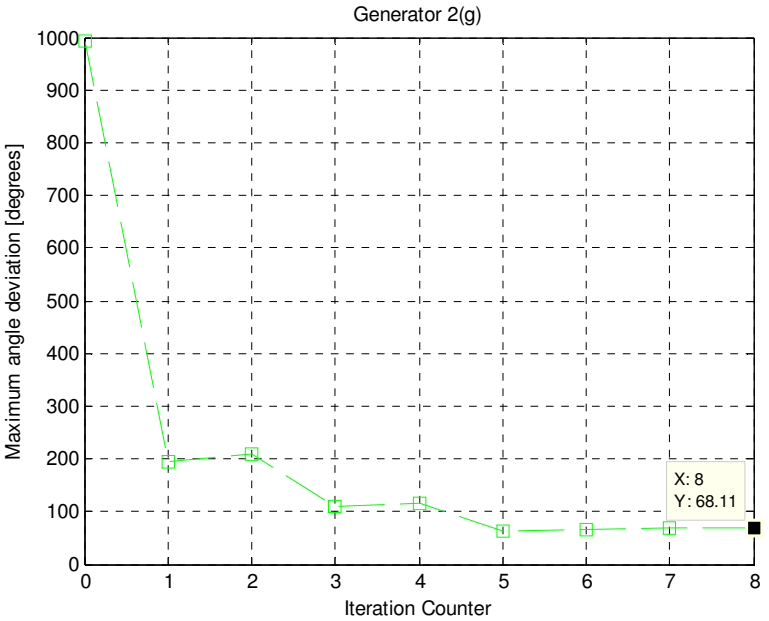

Fig. 4.9 Iteration Process of Stability Constrained OPF. Maximum angle of Generator 2

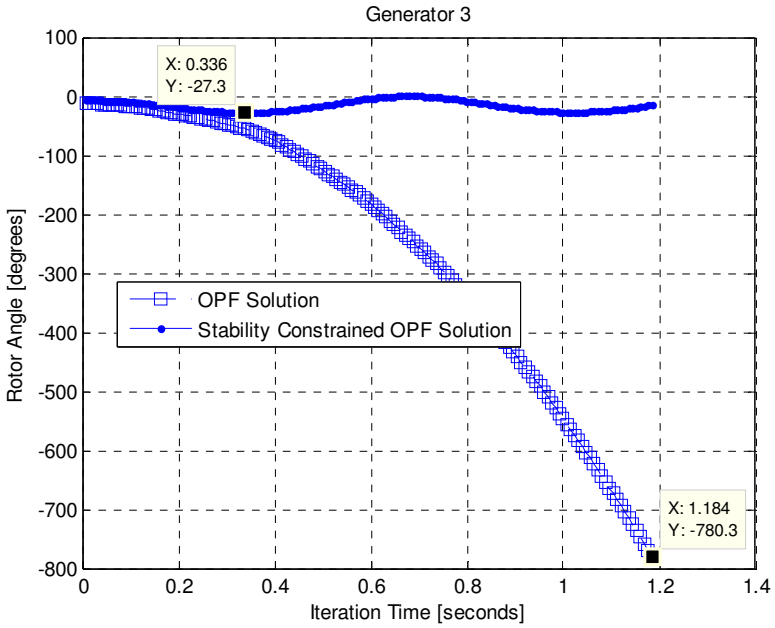

Fig. 4.10 Dynamic Response of the Generator 3 of the 3-machine 3-bus system at two operating points.

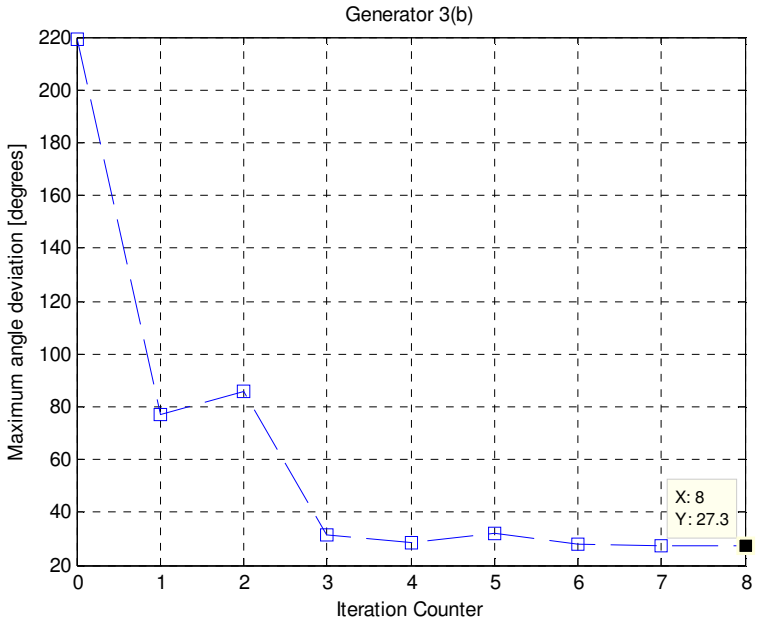

Fig. 4.11 Iteration Process of Stability Constrained OPF. Maximum angle of Generator 3

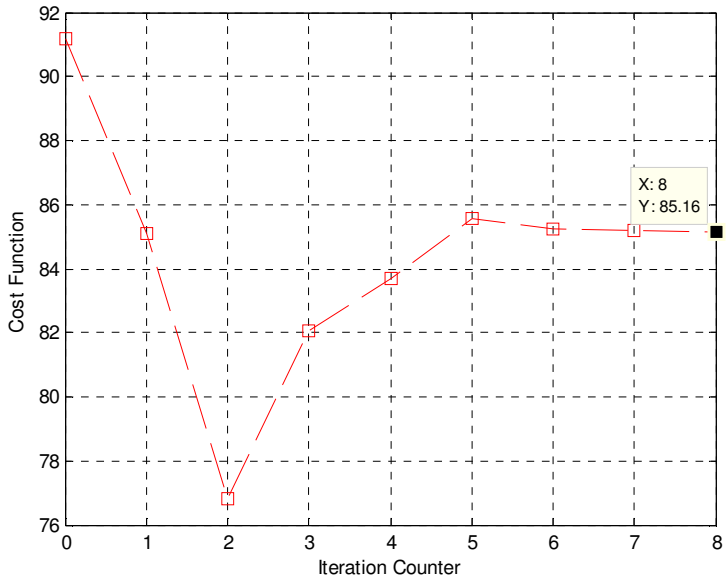

Fig. 4.12 Iteration Process of Stability Constrained OPF. Cost Function.

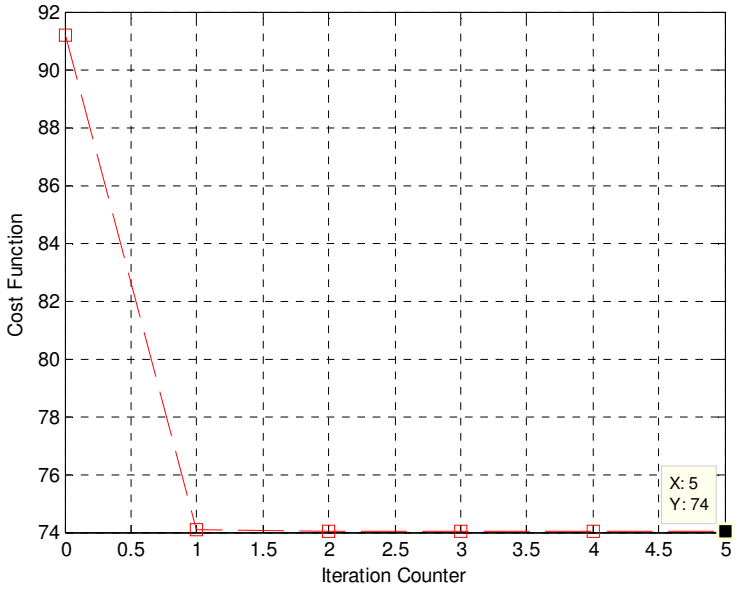

Fig. 4.13 Iteration Process of OPF solution. Cost Function.

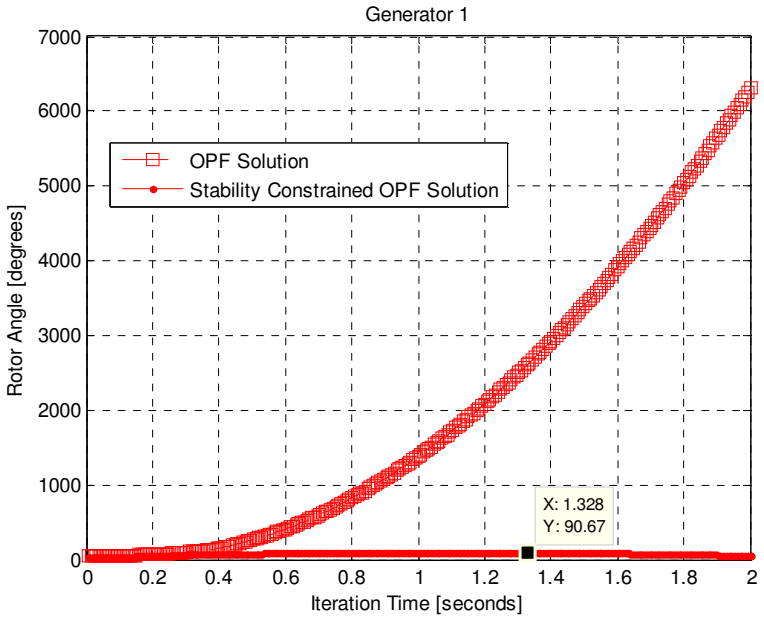

Fig. 4.14 Dynamic Response of the Generator 1 of the 3-machine 3-bus system at two operating points.

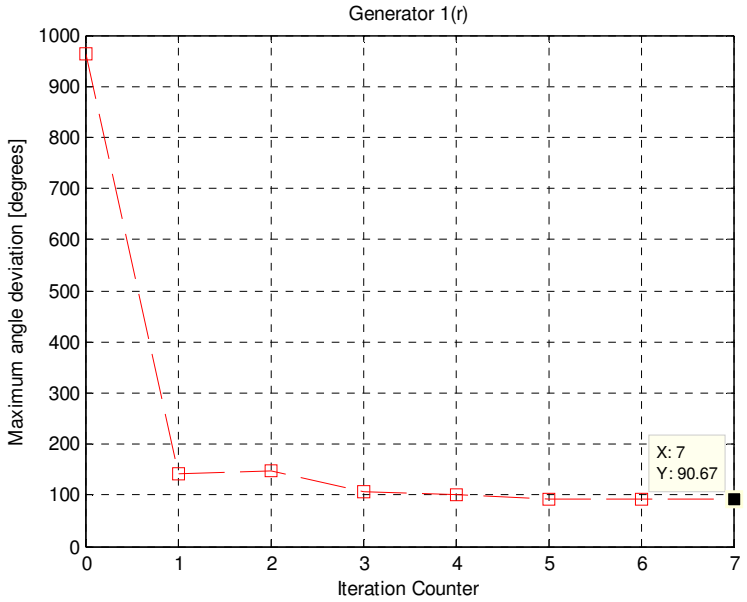

Fig. 4.15 Iteration Process of Stability Constrained OPF. Maximum angle of Generator 1

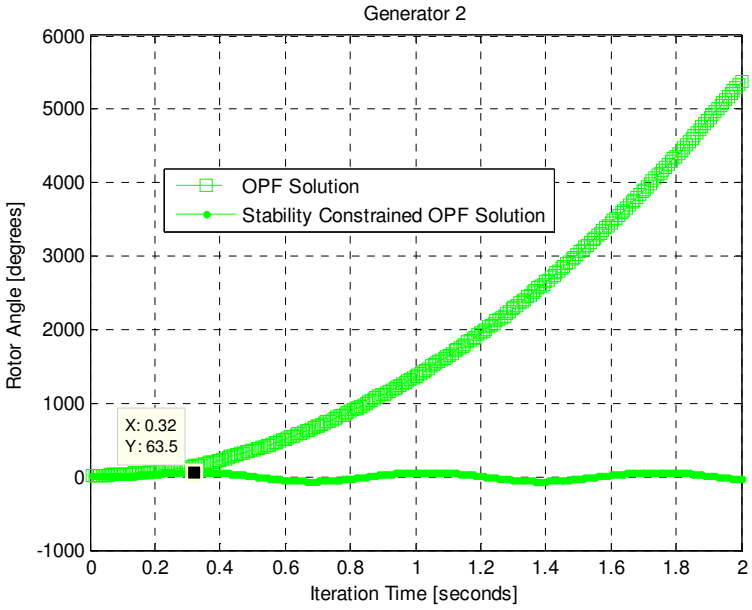

Fig. 4.16 Dynamic Response of the Generator 2 of the 3-machine 3-bus system at two operating points.

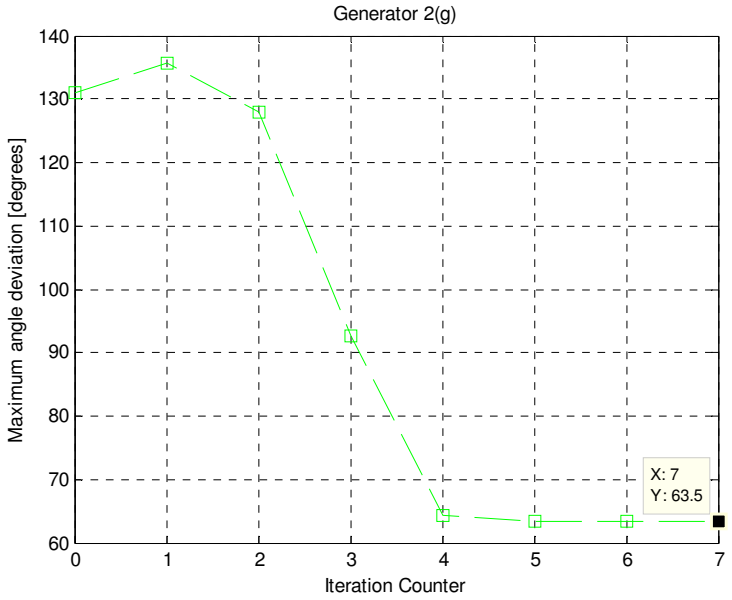

Fig. 4.17 Iteration Process of Stability Constrained OPF. Maximum angle of Generator 2

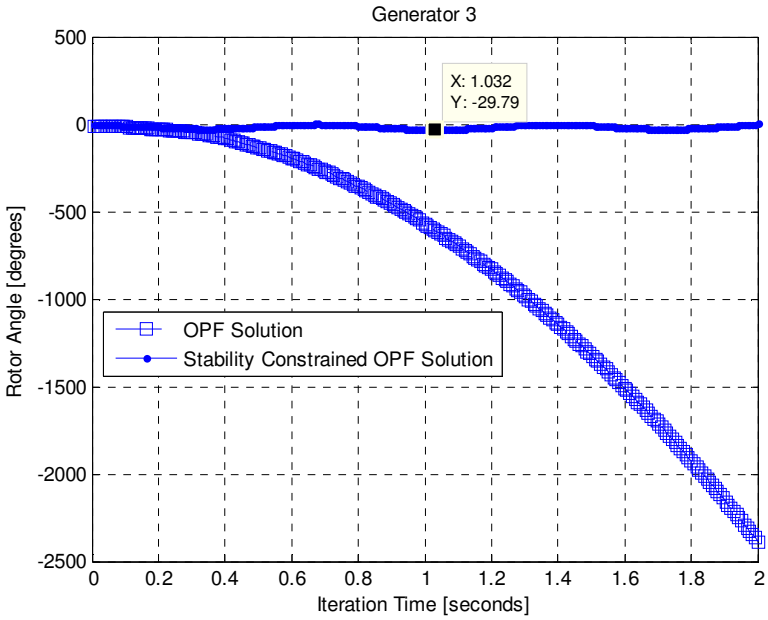

Fig. 4.18 Dynamic Response of the Generator 3 of the 3-machine 3-bus system at two operating points.

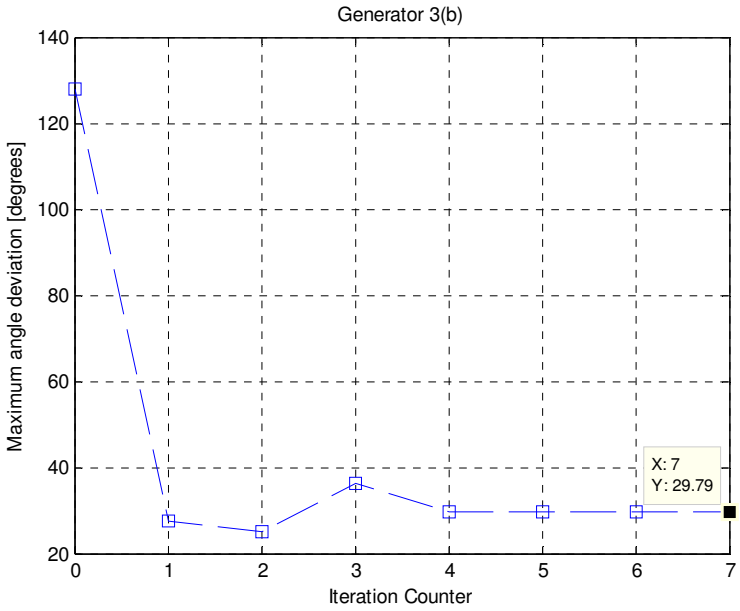

Fig. 4.19 Iteration Process of Stability Constrained OPF. Maximum angle of Generator 3

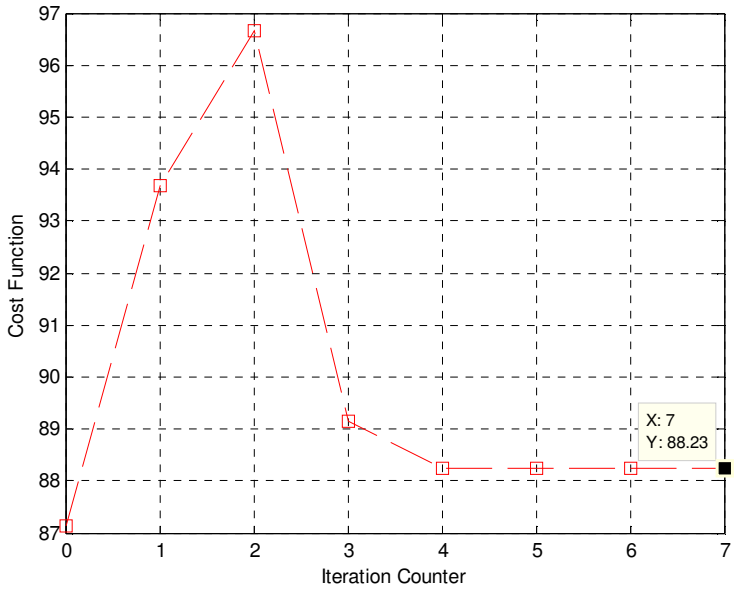

Fig. 4.20 Iteration Process of Stability Constrained OPF. Cost Function.

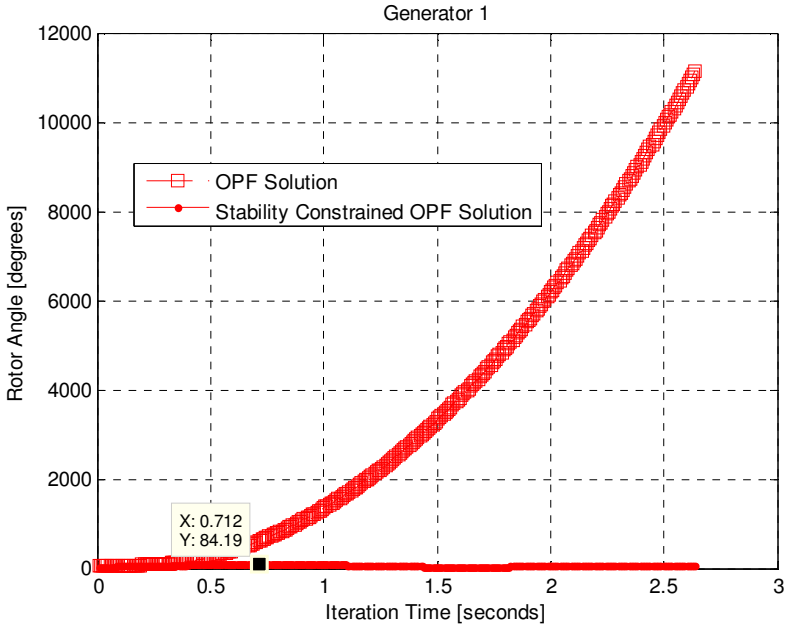

Fig. 4.21 Dynamic Response of the Generator 1 of the 3-machine 3-bus system at two operating points.

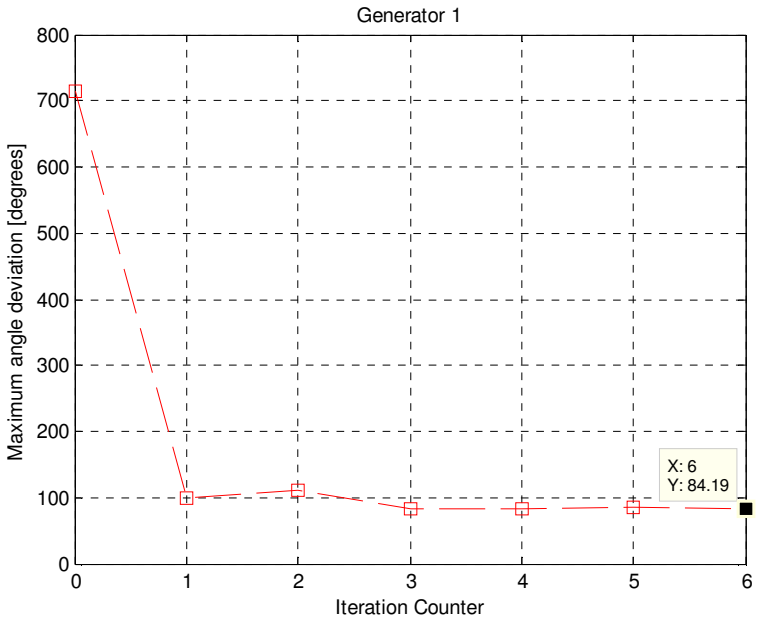

Fig. 4.22 Iteration Process of Stability Constrained OPF. Maximum angle of Generator 1

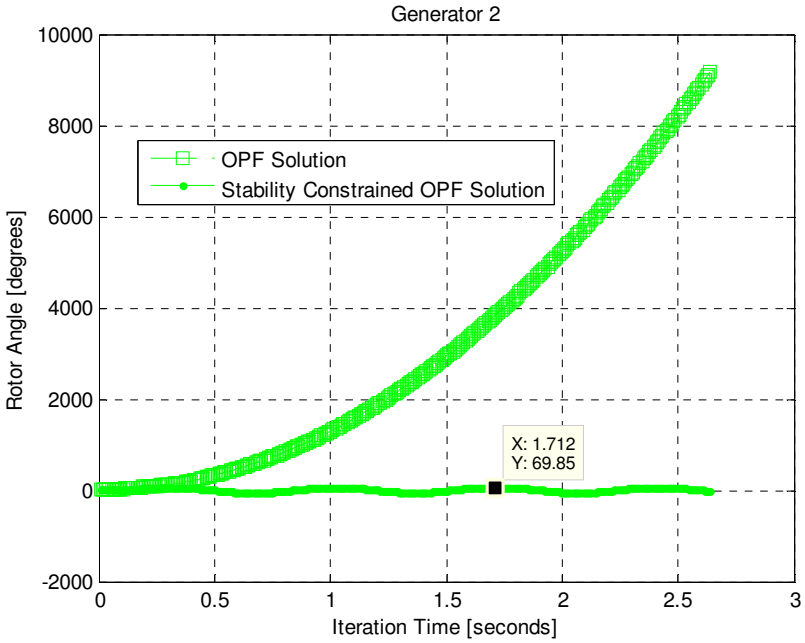

Fig. 4.23 Dynamic Response of the Generator 2 of the 3-machine 3-bus system at two operating points.

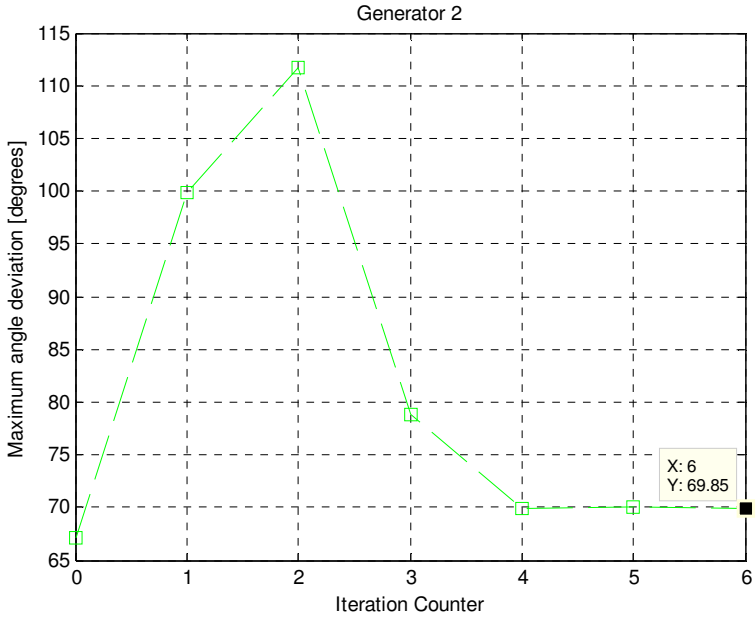

Fig. 4.24 Iteration Process of Stability Constrained OPF. Maximum angle of Generator 2

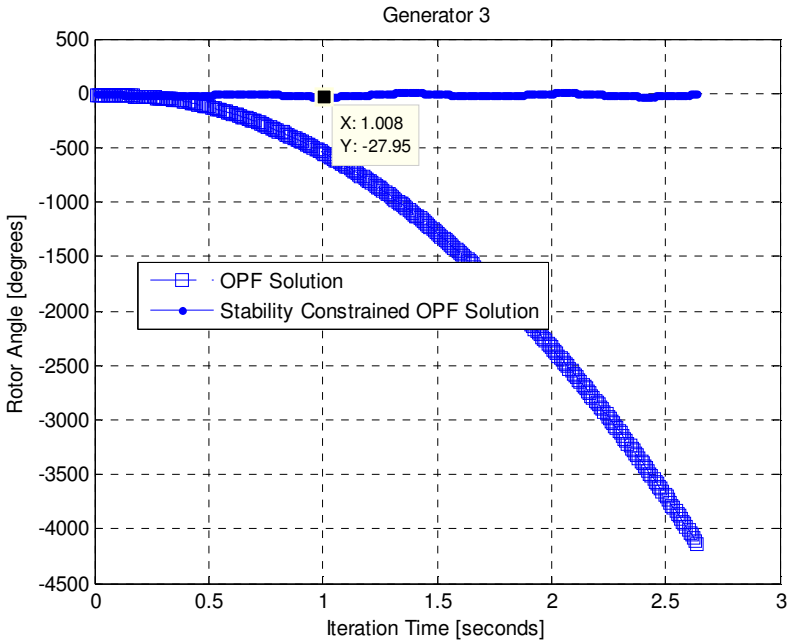

Fig. 4.25 Dynamic Response of the Generator 3 of the 3-machine 3-bus system at two operating points.

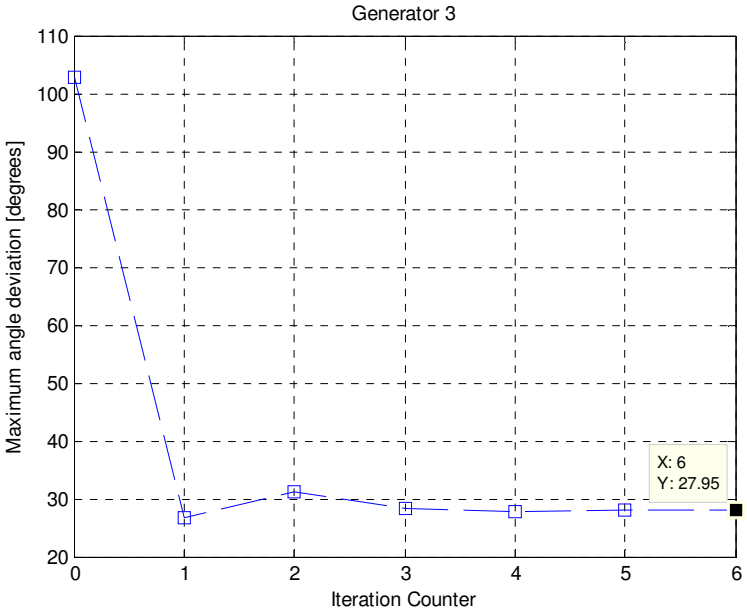

Fig. 4.26 Iteration Process of Stability Constrained OPF. Maximum angle of Generator 3

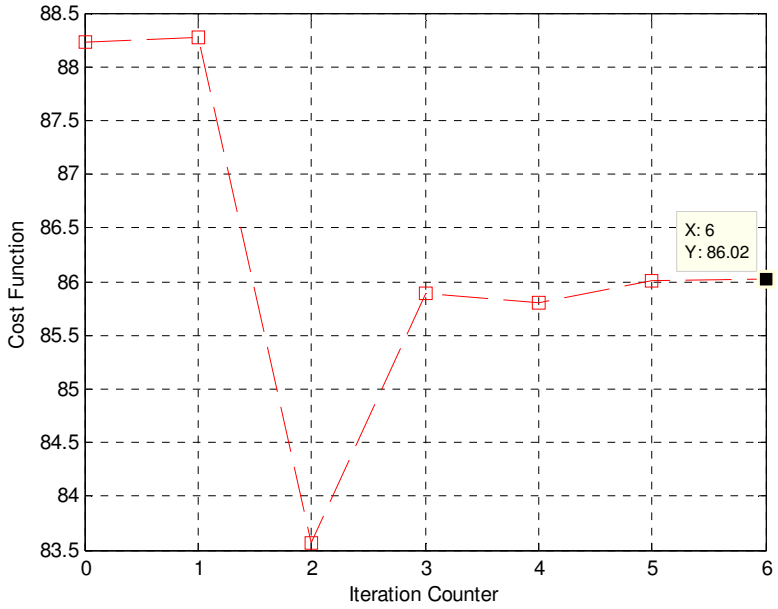

Fig. 4.27 Iteration Process of Stability Constrained OPF. Cost Function.

4.6.3 Results for Scenario 2:

In this section we are going to present the results of the application of the Multi-step Approach proposed in section 4.3.2, for scenario 2.

First of all, we have to run Power Flow Solution and step-by-step integration. The Power Flow solution is: $\theta_1 = 19.34^\circ$, $\theta_2 = 13.64^\circ$, $P_{g1} = 2.99$ p.u., $P_{g2} = 3.71$ p.u, $P_{g3} = 8.2$ p.u, $Q_{g1} = 0.678$ p.u., $Q_{g2} = 0.66$ p.u., $Q_{g3} = 3.01$ p.u., $\delta_1^0 = 33.29^0$, $\delta_2^0 = 23.82^0$, $\delta_3^0 = 6.71^0$, $E_{G1} = 1.092$ p.u. , $E_{G2} = 1.05$ p.u. , $E_{G3} = 1.053$ p.u.

It can be seen that the limit of the active power generation of the generator 3 is violated for the upper bound, with the value 8.2 pu. The cost of generation is of $ 89.94.

This Power Flow solution is used to resolve the equivalent algebraic equations of the dynamical swing equations by means of numerical integration for a fault-on time of 232 ms.

The results of this numerical integration are shown in Fig. 4.28, showing that the system is unstable for this contingency. Consequently, stability constraints are violated for the initial state of the system.

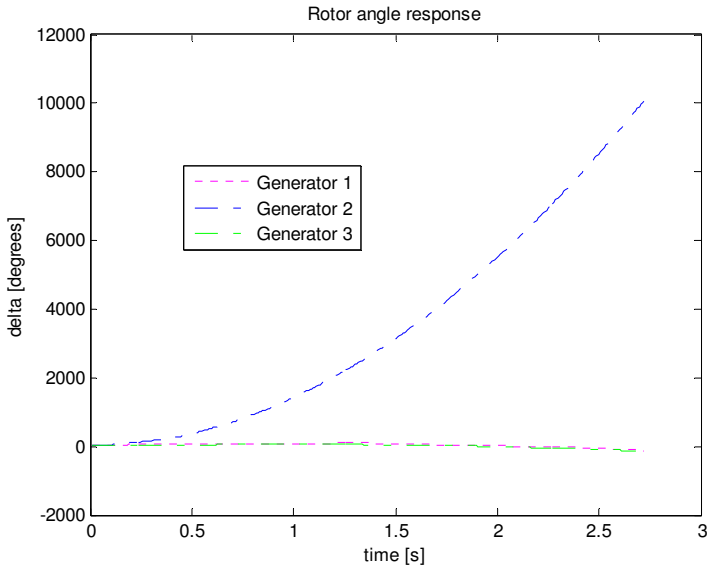

Fig. 4.28 Rotor Angle response of a 3 machine system. Unstable case with a clearing time of 232ms.

The power flow solution and the points obtained for the rotor angles using the trapezoidal integration method were used as starting points to resolve the Stability Constrained Optimal Power Flow (SCOPF) (4.22) and Optimal Power Flow (OPF) (4.8) to (4.18). The maximal time for transient stability analysis is set to be 2.4 s.

The initial interval of time for the optimization problem is set to zero. We increment this interval of time to 1.2 s. We are using the criteria described in section 4.3.2 to set the increments of this interval time, which are established for the interval of time in which the NP problem (4.22) converges to the solution. This criteria is repeated along the optimization process until the desired time on transient stability analysis is achieved.

We proceed to resolve the NP problem (4.22) using the active set method. The solution is updated until the KKT conditions are satisfied (otherwise the increment of this interval of time, has to be reduced).

The results of the first optimization stage using Stability Constrained OPF (4.22) solution are: $\theta_1 = 27.7582^\circ$, $\theta_2 = 12.1923^\circ$, $P_{g1} = 3{,}874$ p.u., $P_{g2} = 3{,}036$ p.u., $P_{g3} = 7{,}988$ p.u., $Q_{g1} = 0{,}972$ p.u., $Q_{g2} = 0{,}659$ p.u., $Q_{g3} = 2{,}718$ p.u., $\delta_1^0 = 45.1956^\circ$, $\delta_2^0 = 20.5546^\circ$, $\delta_3^0 = 6.5676^\circ$, $E_{g1} = 1{,}137$ p.u., $E_{g2} = 1{,}044$ p.u., $E_{g3} = 1{,}047$ p.u.

We also resolve OPF problem (4.8) to (4.18) to compare these two solutions. Results of the first optimization stage using OPF solution are: $\theta_1 = 43.9^\circ$, $\theta_2 = 22.5^\circ$, $P_{g1} = 4{,}96$ p.u.,

$P_{g2} = 4{,}96$ p.u., $P_{g3} = 4{,}97$ p.u., $Q_{g1} = 1{,}67$ p.u., $Q_{g2} = 1{,}4$ p.u., $Q_{g3} = 2{,}81$ p.u., $\delta_1^0 = 64.7^\circ$, $\delta_2^0 = 35.6^\circ$, $\delta_3^0 = 4.09^\circ$, $E_{g1} = 1{,}22$ p.u., $E_{g2} = 1{,}09$ p.u., $E_{g3} = 1{,}044$ p.u.

Fig. 4.29, Fig. 4.31 and Fig. 4.33 respectively, displays the rotor angle of Generator 1, Generator 2 and Generator 3 when the contingency is applied, in two operation points: Optimal Power Flow (OPF) solution and the Stability Constrained OPF (SCOPF) solution. It can be seen that the system does not survive after the contingency at operating point given by OPF solution, but it does at operating point given by SCOPF solution.

Fig. 4.30, Fig. 4.32 and Fig. 4.34 illustrates the Iteration Process of the Stability Constrained OPF (SCOPF) by showing the maximum rotor angle deviation of Generator 1, Generator 2 and Generator 3, respectively, with respect to the inertia center angle. Fig. 4.35 shows the evolution of the cost function in the Iteration Process of SCOPF while Fig. 4.36 shows the evolution of the cost function for the Iteration Process of OPF.

Observe that the final cost of the OPF is lower than the final cost of the SCOPF. This was expected because the system is unstable to the contingency with the operating state produced by the OPF.

These optimization results; were used as initial variables of a new SCOPF problem with a interval of time for the optimization, incremented to 2.08 s. This procedure allows us to extend the total time in the time domain simulations for the stability analysis.

After applying Stability Constrained Optimal Power Flow (SCOPF) solution and Optimal Power Flow (OPF) solution, we obtain the following results: $\theta_1 = 27.596^\circ$, $\theta_2 = 12.1830^\circ$, $P_{g1} = 3{,}85$ p.u., $P_{g2} = 3{,}04$ p.u., $P_{g3} = 7{,}99$ p.u., $Q_{g1} = 0{,}965$ p.u., $Q_{g2} = 0{,}657$ p.u., $Q_{g3} = 2{,}7$ p.u., $\delta_1^0 = 44.9778^\circ$, $\delta_2^0 = 20.5560^\circ$, $\delta_3^0 = 6.5775^\circ$, $E_{g1} = 1{,}136$ p.u., $E_{g2} = 1{,}044$ p.u., $E_{g3} = 1{,}047$ p.u.

Fig. 4.37, Fig. 4.39 and Fig. 4.41 respectively displays the rotor angle of the Generator 1, Generator 2 and Generator 3 when the contingency is applied, in two operation points: Optimal Power Flow (PF) solution and Stability Constrained OPF (SCOPF) solution, for the second optimization stage. It can be seen that the system does not survive after the contingency at operating point given by OPF solution, but it does at operating point given by SCOPF solution.

Fig. 4.38, Fig. 4.40, Fig. 4.42 illustrates the Iteration Process of the stability constrained OPF (SCOPF) by showing the maximum rotor angle deviation of Generator 1, Generator 2 and

Generator 3, respectively, with respect to the inertia center angle. Fig. 4.43 shows the evolution of the cost function in the Iteration Process of the SCOPF.

These previous optimization results; were used as initial variables for a new SCOPF problem with a interval of time for the optimization incremented to 2.4 s.

After solving Stability Constrained Optimal Power Flow (SCOPF) and Optimal Power Flow (OPF), we obtain the following results of the third optimization stage using Stability Constrained OPF (SCOPF) solution (4.22): $\theta_1 = 27.7582^\circ$, $\theta_2 = 12.1923^\circ$, $P_{g1} = 3{,}874$ p.u., $P_{g2} = 3{,}021$ p.u., $P_{g3} = 7{,}988$ p.u., $Q_{g1} = 0{,}958$ p.u., $Q_{g2} = 0{,}657$ p.u., $Q_{g3} = 2{,}7$ p.u., $\delta_1^0 = 45.1956^\circ$, $\delta_2^0 = 20.5546^\circ$, $\delta_3^0 = 6.5676^\circ$, $E_{g1} = 1{,}135$ p.u., $E_{g2} = 1{,}044$ p.u., $E_{g3} = 1{,}047$ p.u.

Fig. 4.44, Fig. 4.46 and Fig. 4.48 respectively displays the rotor angle of the Generator 1, Generator 2 and Generator 3 when the contingency is applied, in two operation points: Optimal Power Flow (OPF) solution and Stability Constrained OPF (SCOPF) solution, for the last optimization stage.

Fig. 4.45, Fig. 4.47, Fig. 4.49 illustrates the evolution of the maximum rotor angle deviation with respect to the inertia center angle of Generator 1, Generator 2 and Generator 3, respectively in the iteration Process of the stability constrained OPF (SCOPF). Fig. 4.50 shows the evolution of the cost function along the Iteration Process of SCOPF.

It can be concluded from these figures that OPF by itself cannot guarantee a secure operation since the system is unstable to the considered contingency. SCOPF fix this problem at the expense of a larger cost of generation. We have the Output power generation as output variables for all stages of the Multi-step optimization approach.

Table 4.4 displays relevant initial conditions of the optimization variables and relevant results after each optimization stage for the OPF and SCOPF.

Table 4.4. Initial Conditions and the Optimization variables results: for the first stage, second stage and third stage, respectively.

Initial conditions (PF solution)	**Optimization variables results**			
	1st stage (OPF solution)	**1st stage (SCOPF solution)**	**2nd stage (SCOPF solution)**	**3rd stage (SCOPF solution)**
$P_{g1} = 2.99$	$P_{g1} = 4{,}97$	$P_{g1} = 3{,}874$	$P_{g1} = 3{,}85$	$P_{g1} = 3{,}874$
$P_{g2} = 3.71$	$P_{g2} = 4{,}95$	$P_{g2} = 3{,}036$	$P_{g2} = 3{,}04$	$P_{g2} = 3{,}021$
$P_{g3} = 8.20$	$P_{g3} = 4{,}96$	$P_{g3} = 7{,}988$	$P_{g3} = 7{,}99$	$P_{g3} = 7{,}988$
$f(P_{gi}) = 89.94$	$f(P_{gi}) = 74$	$f(P_{gi}) = 88.05$	$f(P_{gi}) = 88.14$	$f(P_{gi}) = 88.17$
$\delta_1^{\max} = 164^\circ$	$\delta_1^{\max} = 2122^\circ$	$\delta_1^{\max} = 90.42^\circ$	$\delta_1^{\max} = 99.14^\circ$	$\delta_1^{\max} = 85.1^\circ$
$\delta_2^{\max} = 977^\circ$	$\delta_2^{\max} = 2020^\circ$	$\delta_2^{\max} = 74.32^\circ$	$\delta_2^{\max} = 75.12^\circ$	$\delta_2^{\max} = 72^\circ$
$\delta_3^{\max} = 215.4^\circ$	$\delta_3^{\max} = 855.5^\circ$	$\delta_3^{\max} = 32.36^\circ$	$\delta_3^{\max} = 30.05^\circ$	$\delta_3^{\max} = 28.45^\circ$

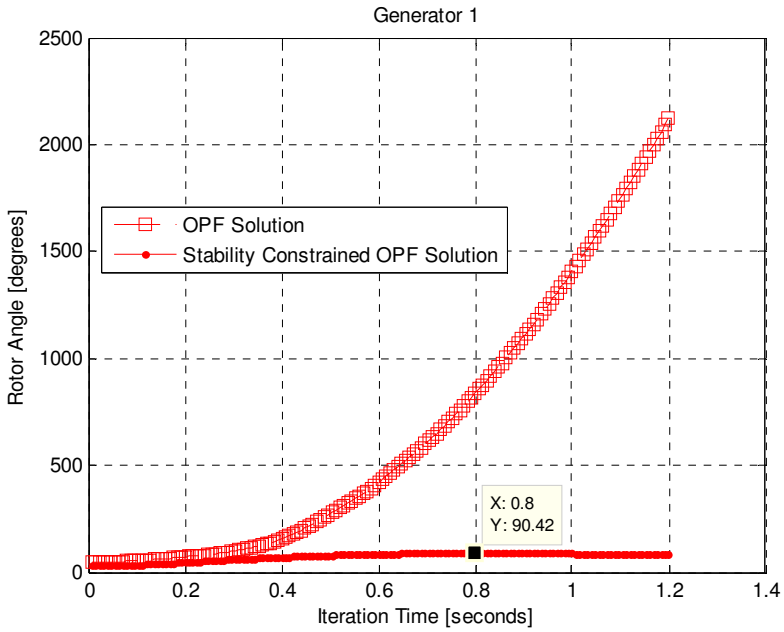

Fig. 4.29 Dynamic Response of the Generator 1 of the 3-machine 3-bus system at two operating points.

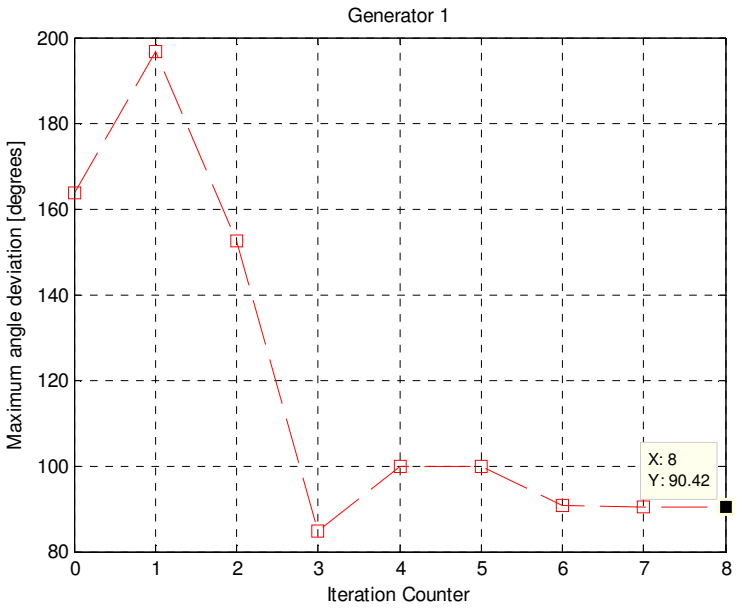

Fig. 4.30 Iteration Process of Stability Constrained OPF. Maximum angle of Generator 1

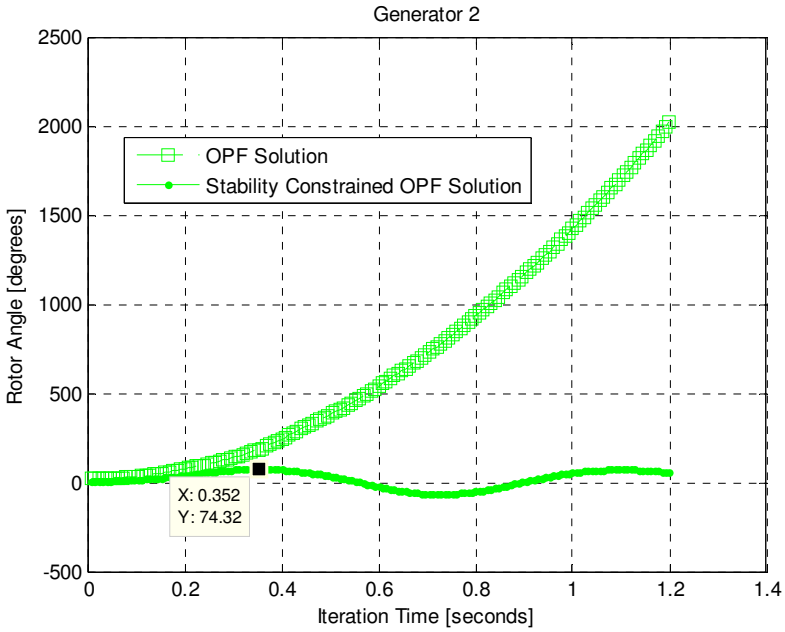

Fig. 4.31 Dynamic Response of the Generator 2 of the 3-machine 3-bus system at two operating points.

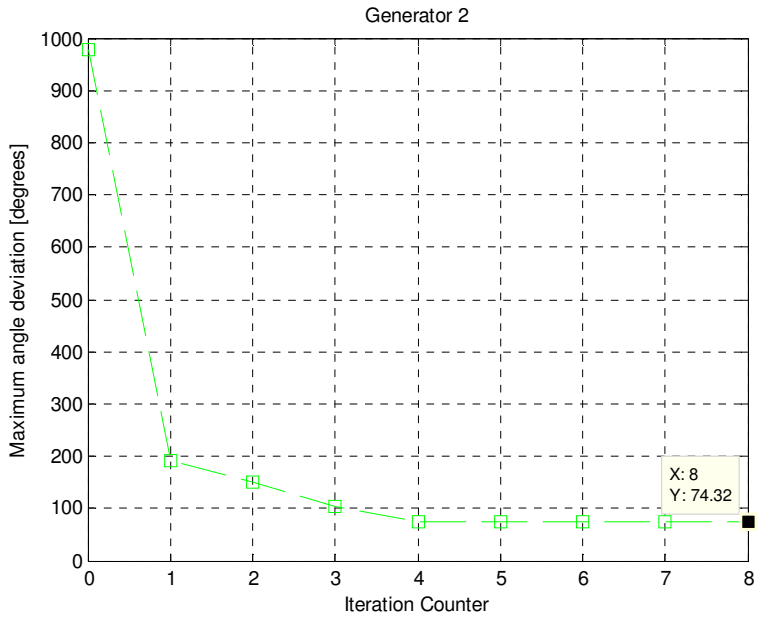

Fig. 4.32 Iteration Process of Stability Constrained OPF. Maximum angle of Generator 2

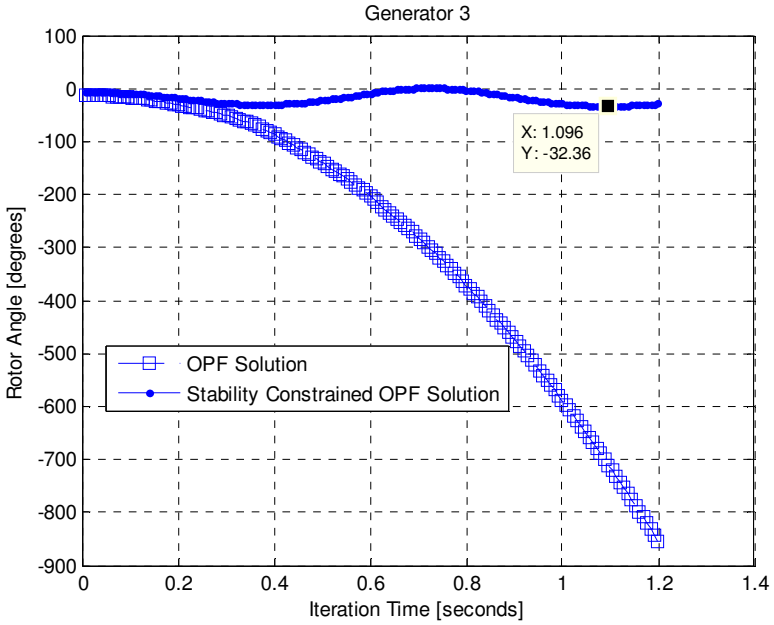

Fig. 4.33 Dynamic Response of the Generator 3 of the 3-machine 3-bus system at two operating points.

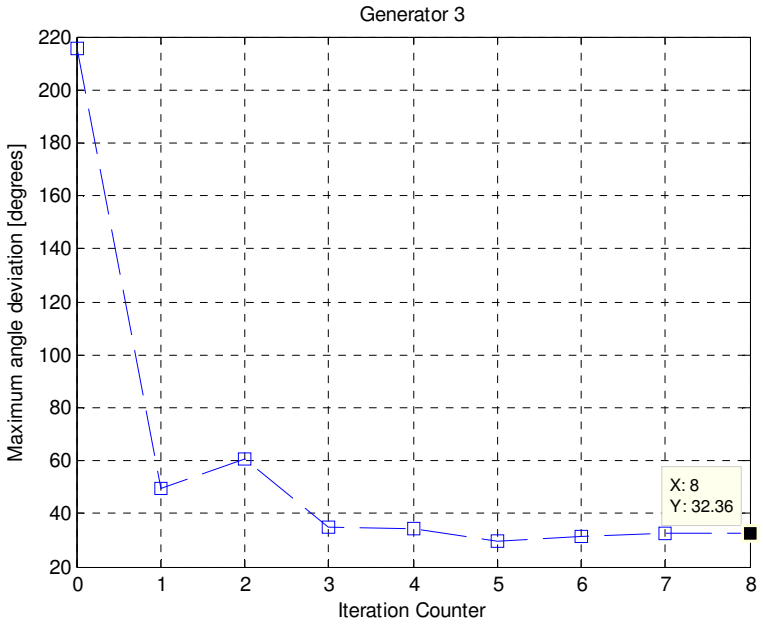

Fig. 4.34 Iteration Process of Stability Constrained OPF. Maximum angle of Generator 3

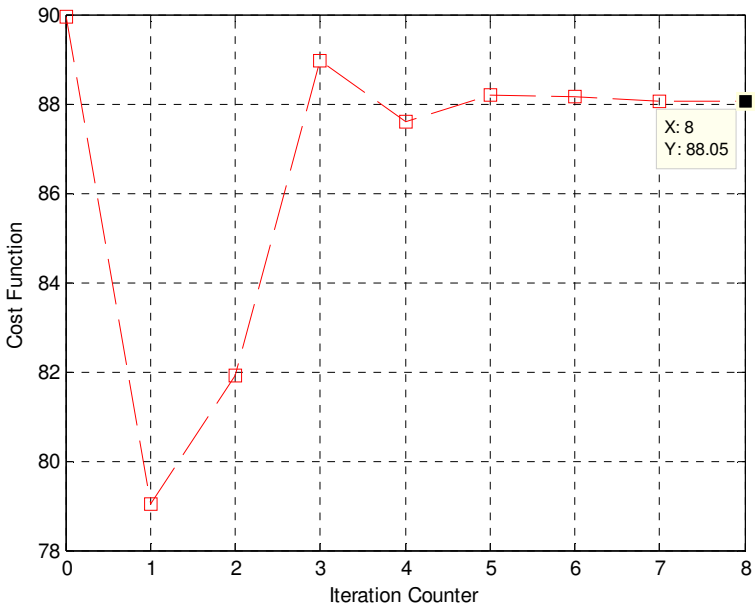

Fig. 4.35 Iteration Process of Stability Constrained SCOPF. Cost Function.

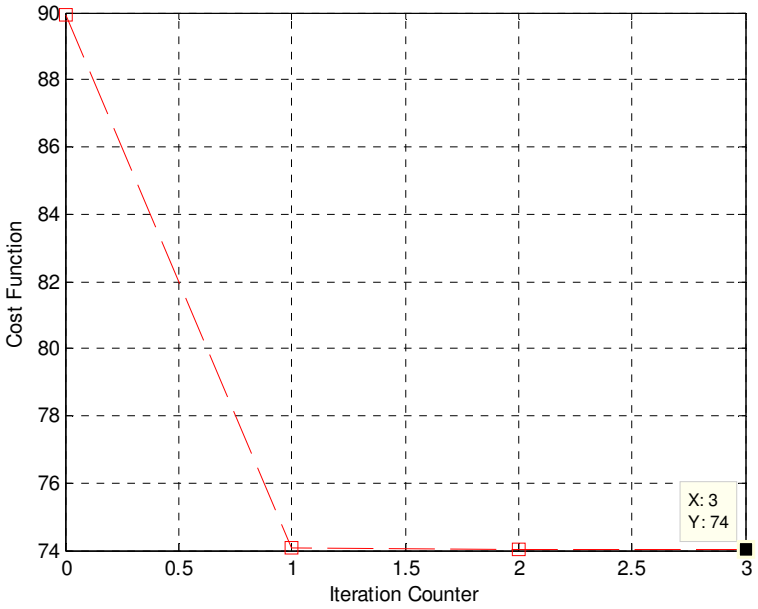

Fig. 4.36 Iteration Process of OPF. Cost Function.

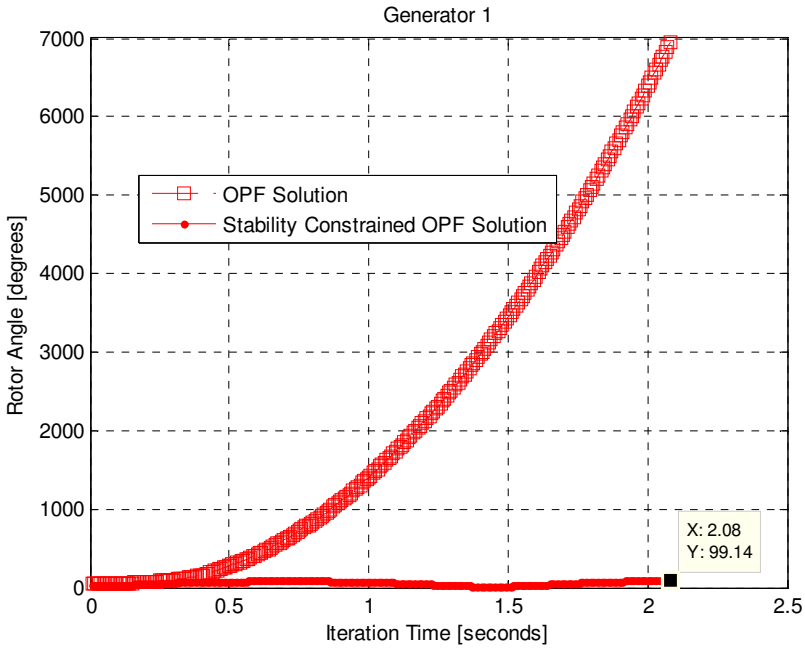

Fig. 4.37 Dynamic Response of the Generator 1 of the 3-machine 3-bus system at two operating points.

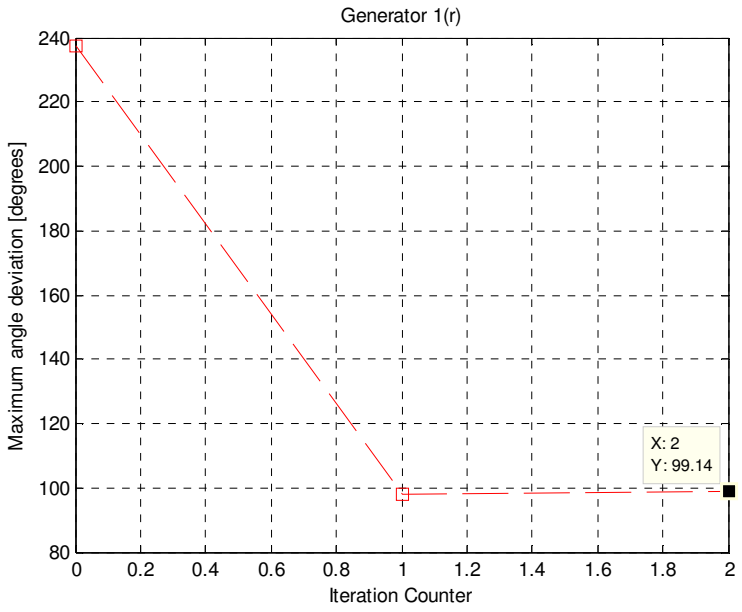

Fig. 4.38 Iteration Process of Stability Constrained OPF. Maximum angle of Generator 1

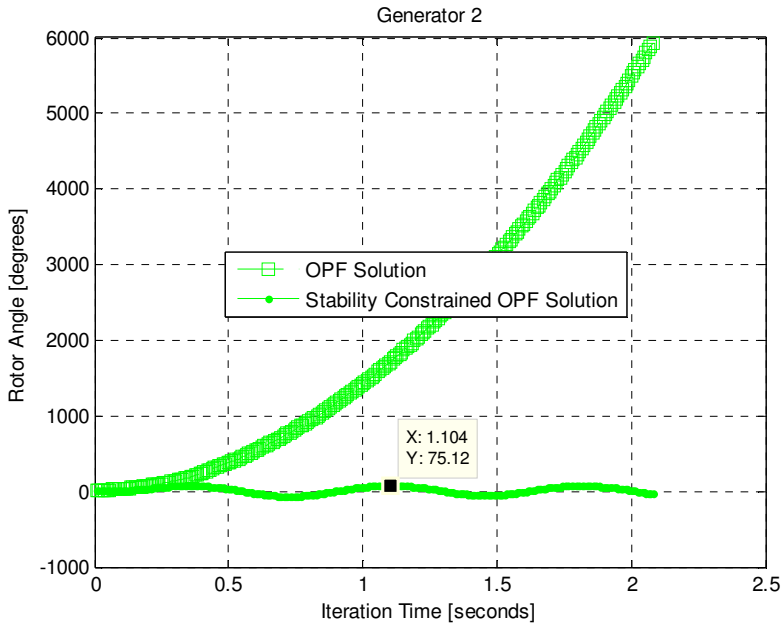

Fig. 4.39 Dynamic Response of the Generator 2 of the 3-machine 3-bus system at two operating points.

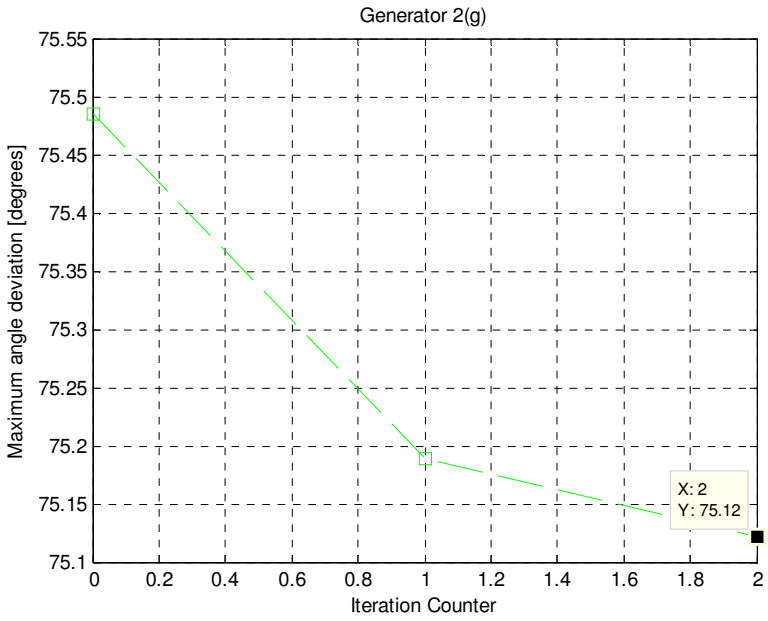

Fig. 4.40 Iteration Process of Stability Constrained OPF. Maximum angle of Generator 2

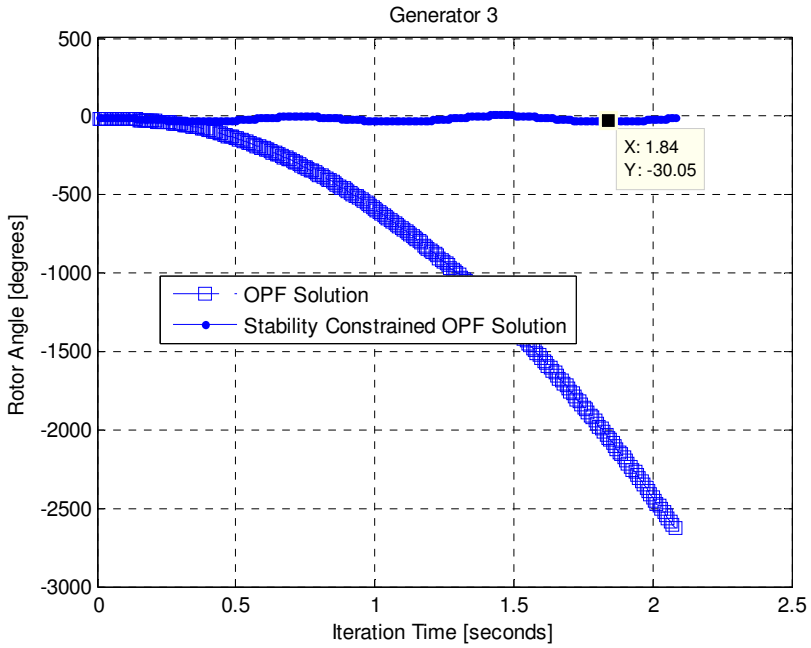

Fig. 4.41 Dynamic Response of the Generator 3 of the 3-machine 3-bus system at two operating points.

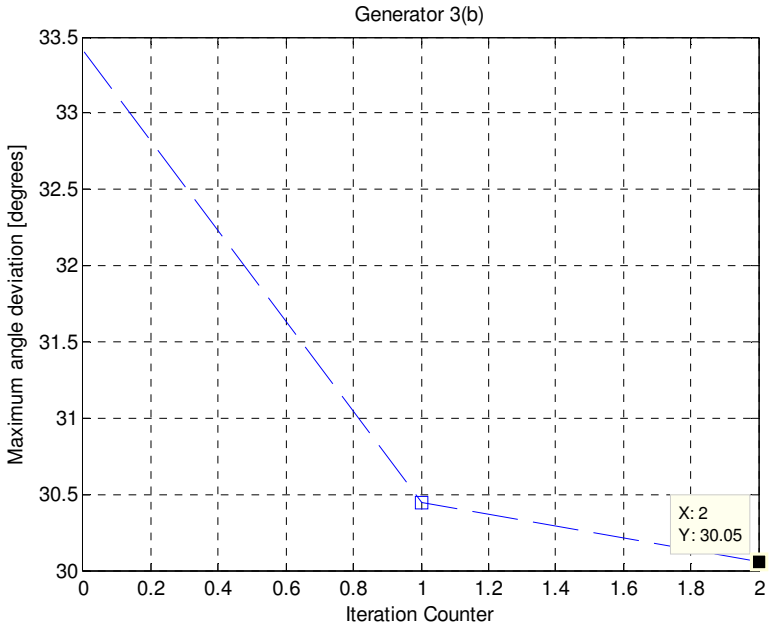

Fig. 4.42 Iteration Process of Stability Constrained OPF. Maximum angle of Generator 3

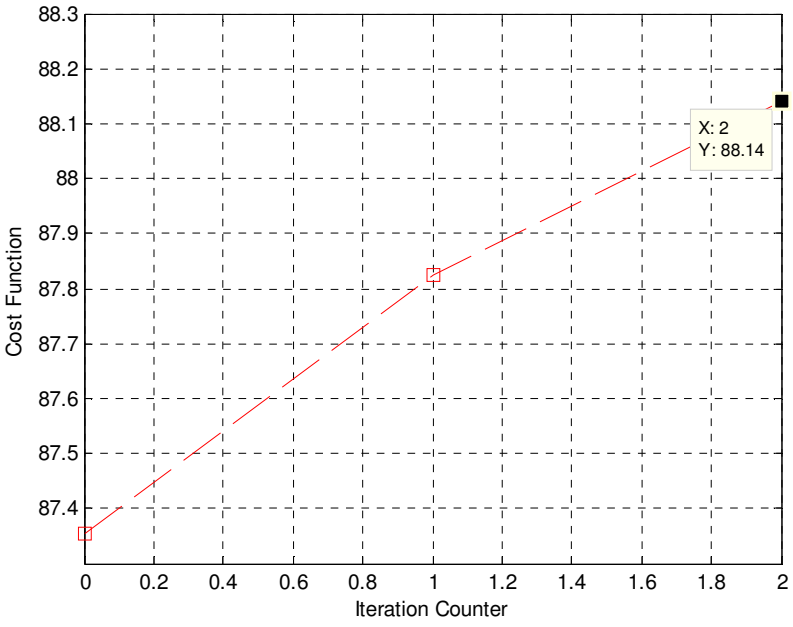

Fig. 4.43 Iteration Process of Stability Constrained OPF. Cost Function.

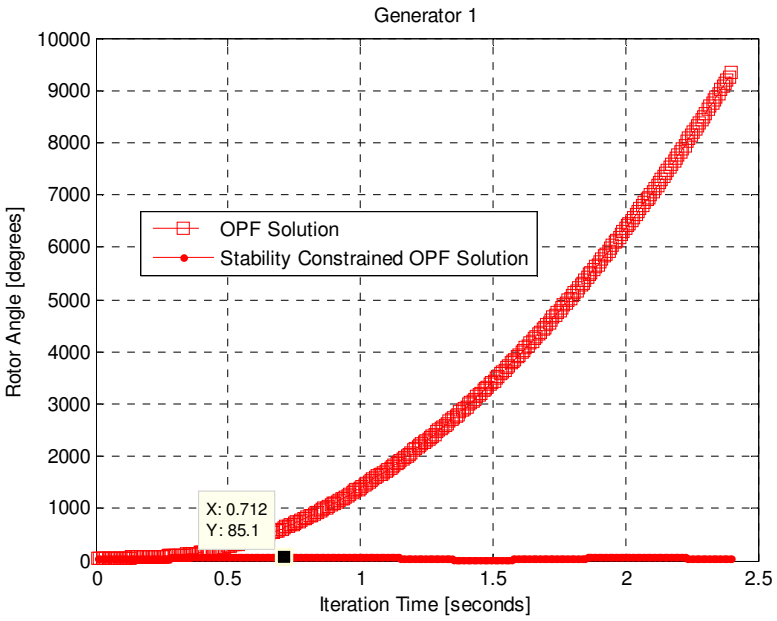

Fig. 4.44 Dynamic Response of the Generator 1 of the 3-machine 3-bus system at two operating points.

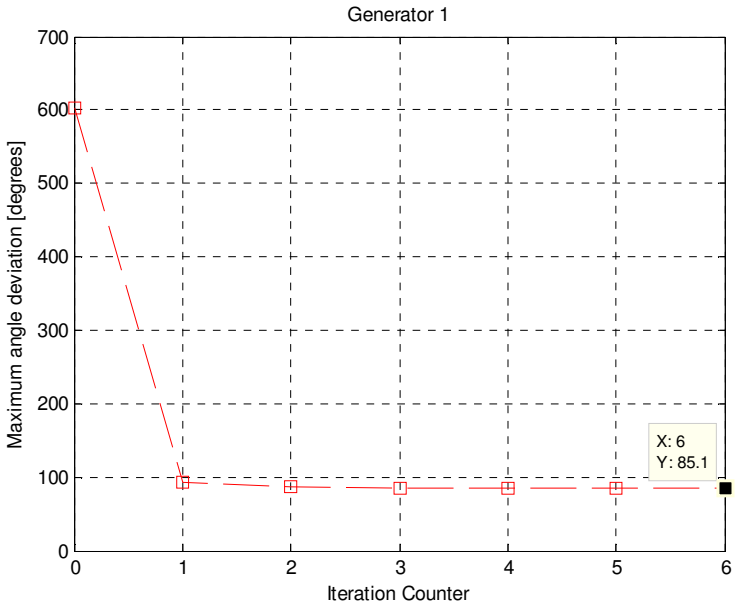

Fig. 4.45 Iteration Process of Stability Constrained OPF. Maximum angle of Generator 1

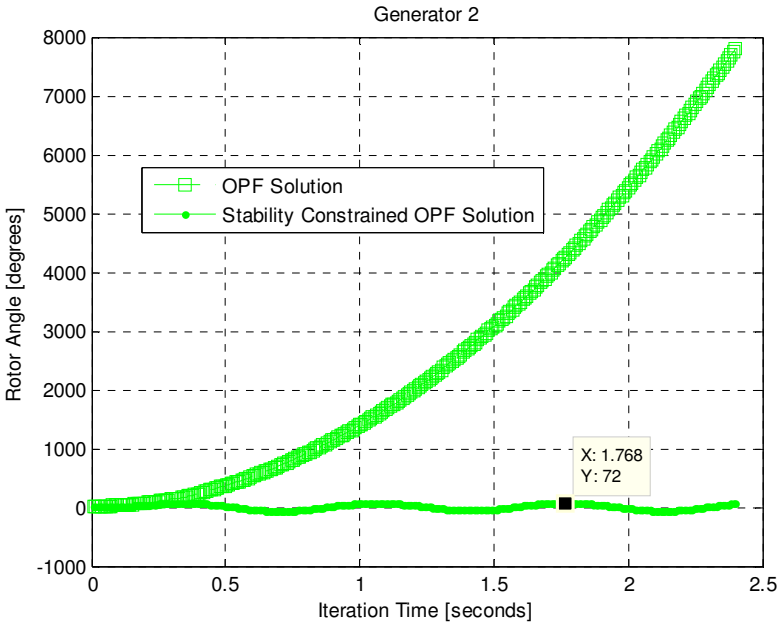

Fig. 4.46 Dynamic Response of the Generator 2 of the 3-machine 3-bus system at two operating points.

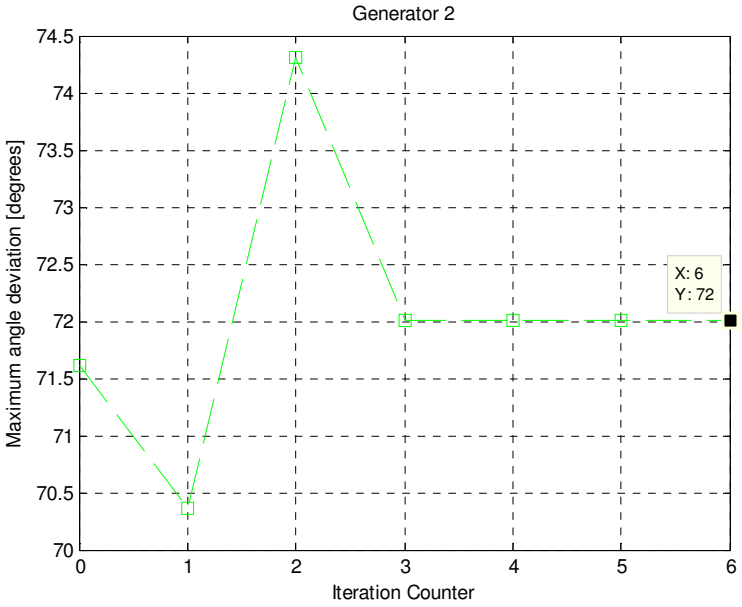

Fig. 4.47 Iteration Process of Stability Constrained OPF. Maximum angle of Generator 2

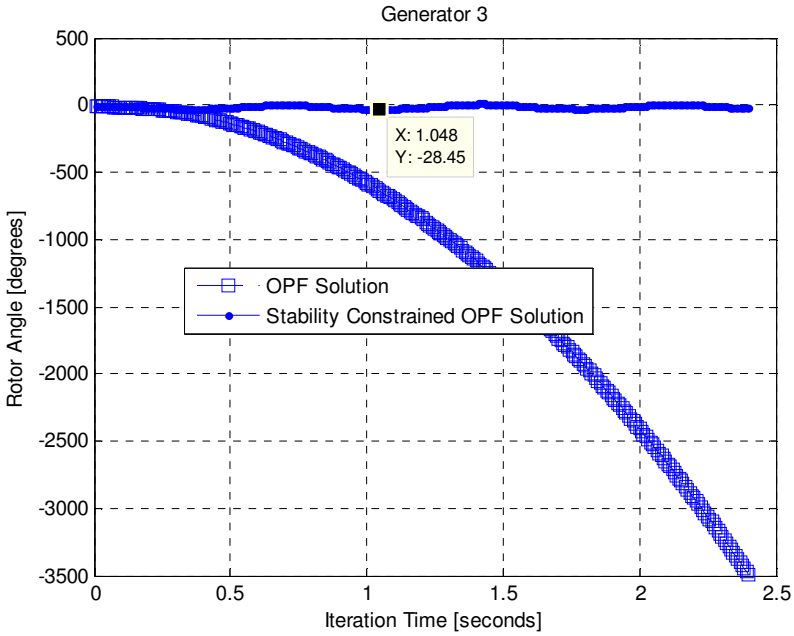

Fig. 4.48 Dynamic Response of the Generator 3 of the 3-machine 3-bus system at two operating points.

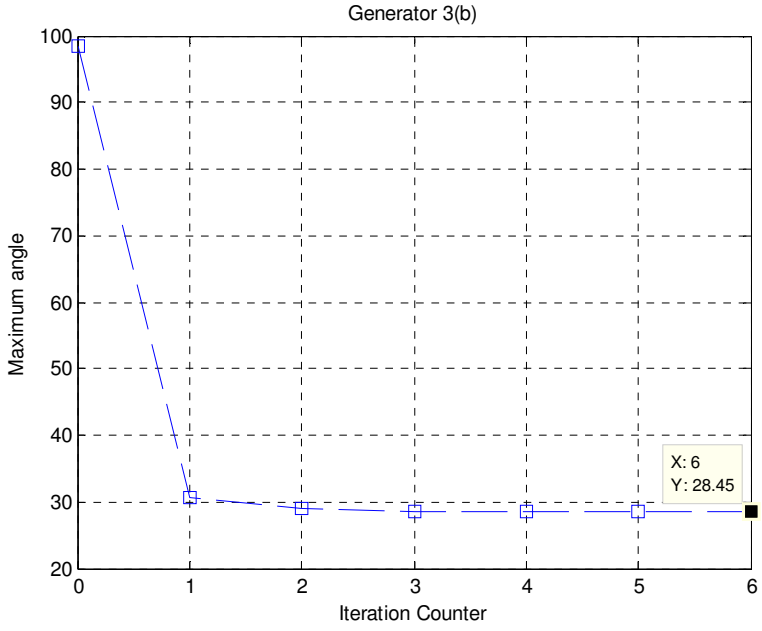

Fig. 4.49 Iteration Process of Stability Constrained OPF. Maximum angle of the Generator 3

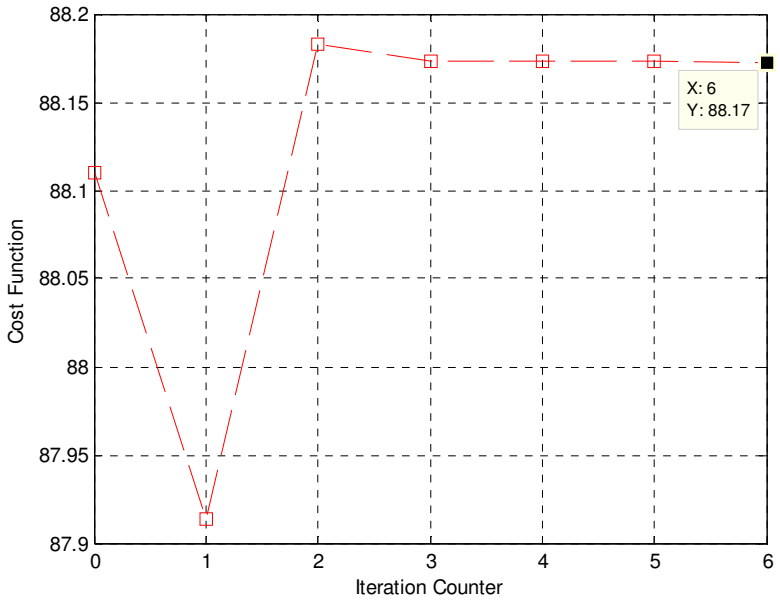

Fig. 4.50 Iteration Process of Stability Constrained OPF. Cost Function.

4.6.4 Results with the use of interior point method

4.6.4.1 Results for Scenario 1

In this section we present the results of the application of the Interior point method for the first stage of the Multi-step optimization approach for the scenario 1 described in section 4.6.1.

The Power Flow solution of scenario 1 presented in section 4.6.2 is used to resolve the equivalent algebraic equations of the dynamical swing equations by means of numerical integration for a fault-on time of 200 ms. The results of this numerical integration are shown in Fig. 4.5, showing that the system is unstable for this contingency. Consequently, stability constraints are violated for the initial state of the system.

The power flow solution and the points obtained for the rotor angles using the trapezoidal integration method were used as starting points to resolve the Stability Constrained Optimal Power Flow (SCOPF) (4.22)-(4.31) and Optimal Power Flow (OPF) (4.8)-(4.18).

The initial interval time for the optimization problem is set to zero. We increment this interval of time to 0.832 s for the resolution of the SCOPF and OPF problem using Interior point method. The solution is updated until the KKT conditions are satisfied.

The results for the Stability Constrained OPF (4.22)-(4.31) solution are: $\theta_1 = 29.8^\circ$, $\theta_2 = 15.6^\circ$, $P_{g1} = 3{,}95$ p.u., $P_{g2} = 3{,}8$ p.u., $P_{g3} = 7.14$ p.u., $Q_{g1} = 1$ p.u., $Q_{g2} = 0.8$ p.u., $Q_{g3} = 2.6$ p.u., $\delta_1^0 = 47.6^\circ$, $\delta_2^0 = 25.99^\circ$, $\delta_3^0 = 5.88^\circ$, $E_{g1} = 1.14$ p.u., $E_{g2} = 1.05$ p.u., $E_{g3} = 1.04$ p.u.

We also resolve OPF problem (4.8) to (4.18) to compare these two solutions. Results for the OPF solution are: $\theta_1 = 44.0^\circ$, $\theta_2 = 22.5^\circ$, $P_{g1} = 4.96$ p.u., $P_{g2} = 4.96$ p.u., $P_{g3} = 4{,}96$ p.u., $Q_{g1} = 1.7$ p.u., $Q_{g2} = 1.4$ p.u., $Q_{g3} = 2.81$ p.u., $\delta_1^0 = 64.84^\circ$, $\delta_2^0 = 35.63^\circ$, $\delta_3^0 = 4.09^\circ$, $E_{g1} = 1{,}22$ p.u., $E_{g2} = 1{,}09$ p.u., $E_{g3} = 1{,}04$ p.u.

Fig. 4.51, Fig. 4.53 and Fig. 4.55 respectively display the rotor angle of Generator 1, Generator 2 and Generator 3 when the contingency is applied, in two operation points: Optimal Power Flow (OPF) solution and the Stability Constrained OPF (SCOPF) solution. It can be seen that the system does not survive after the contingency at operating point given by OPF solution, but it does at operating point given by SCOPF solution.

Fig. 4.52, Fig. 4.54 and Fig. 4.56 illustrate the Iteration Process of the Stability Constrained OPF (SCOPF) by showing the maximum rotor angle deviation of Generator 1, Generator 2 and Generator 3, respectively, with respect to the inertia center angle. Fig. 4.57 shows the evolution of the cost function in the Iteration Process of the SCOPF while Fig. 4.58 shows the evolution of the cost function for the Iteration Process of the OPF. Observe that the final cost of the OPF is lower than the final cost of the SCOPF. This was expected because the system is unstable to the contingency with the operating state produced by the OPF.

These results are obtained applying Interior point method. Convergence for times higher than 0.832s was not achieved.

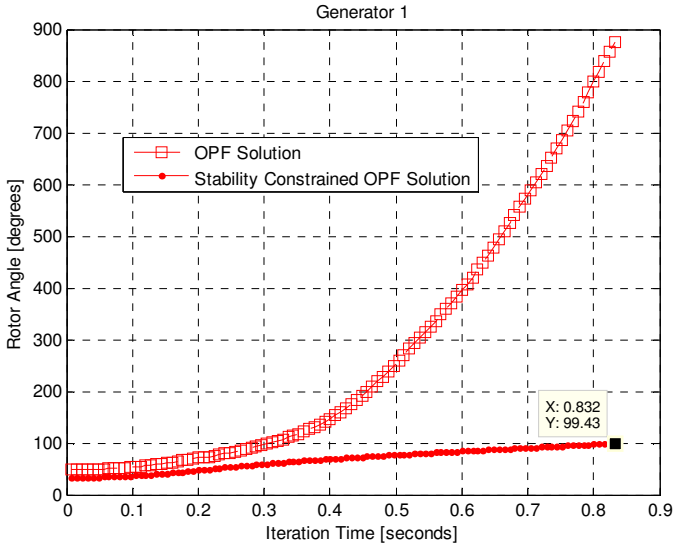

Fig. 4.51 Dynamic Response of the Generator 1 of the 3-machine 3-bus system at two operating points.

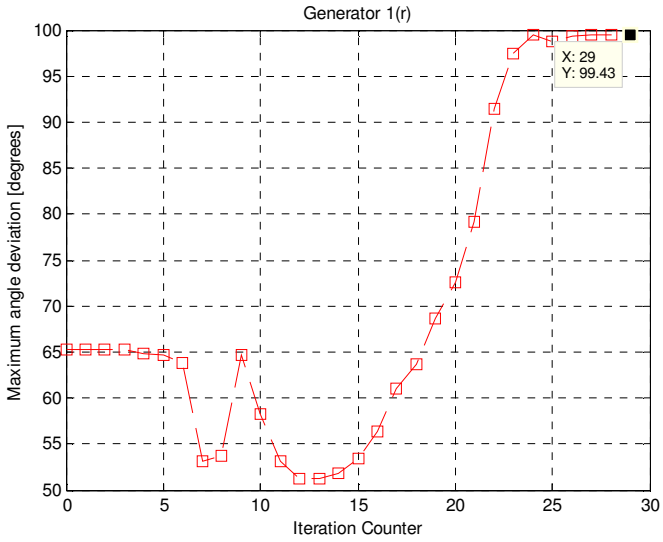

Fig. 4.52 Iteration Process of Stability Constrained OPF. Maximum angle of Generator 1

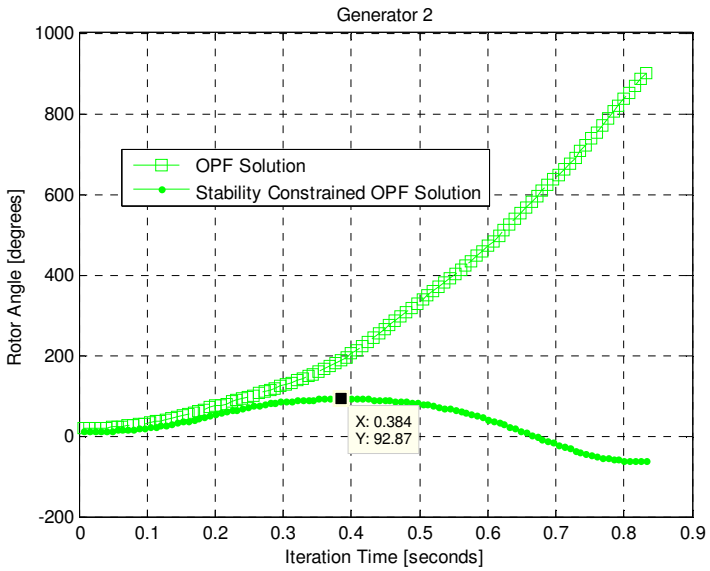

Fig. 4.53 Dynamic Response of the Generator 2 of the 3-machine 3-bus system at two operating points.

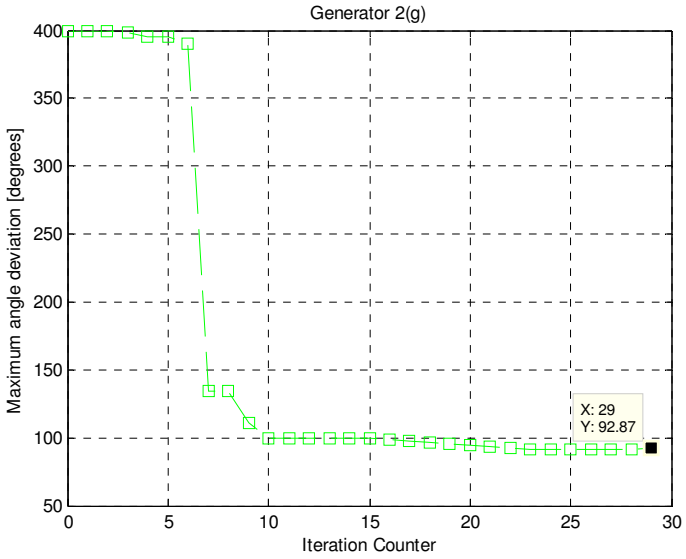

Fig. 4.54 Iteration Process of Stability Constrained OPF. Maximum angle of Generator 2

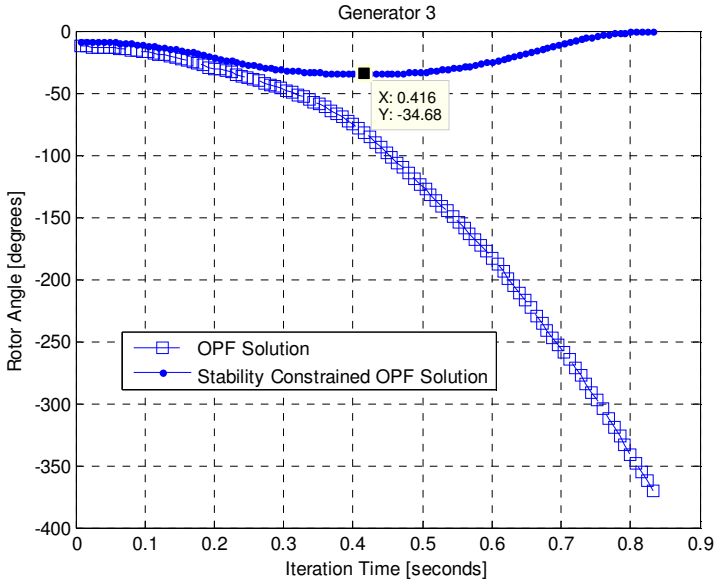

Fig. 4.55 Dynamic Response of the Generator 3 of the 3-machine 3-bus system at two operating points.

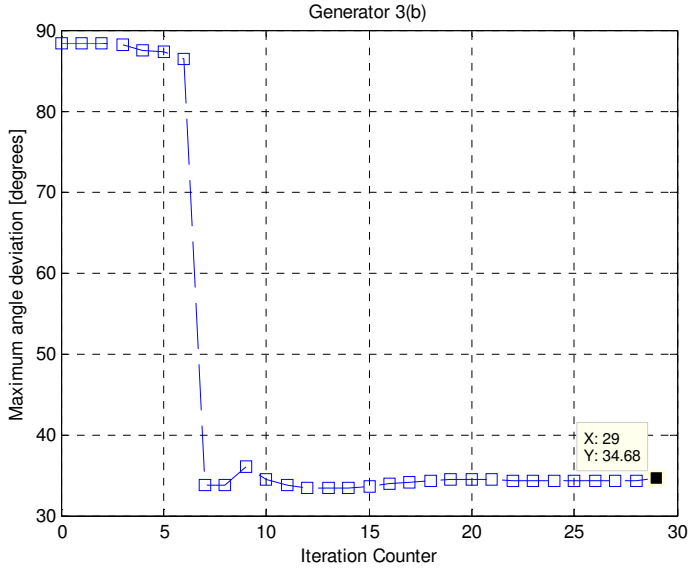

Fig. 4.56 Iteration Process of Stability Constrained OPF. Maximum angle of Generator 3

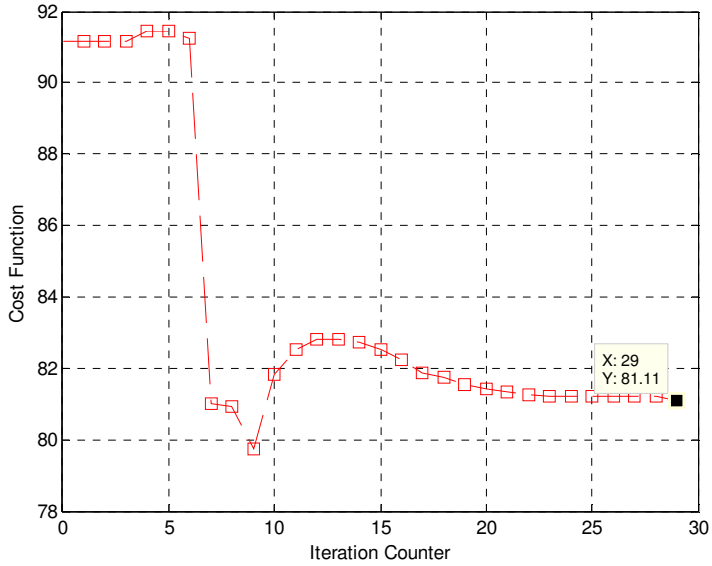

Fig. 4.57 Iteration Process of Stability Constrained OPF. Cost Function.

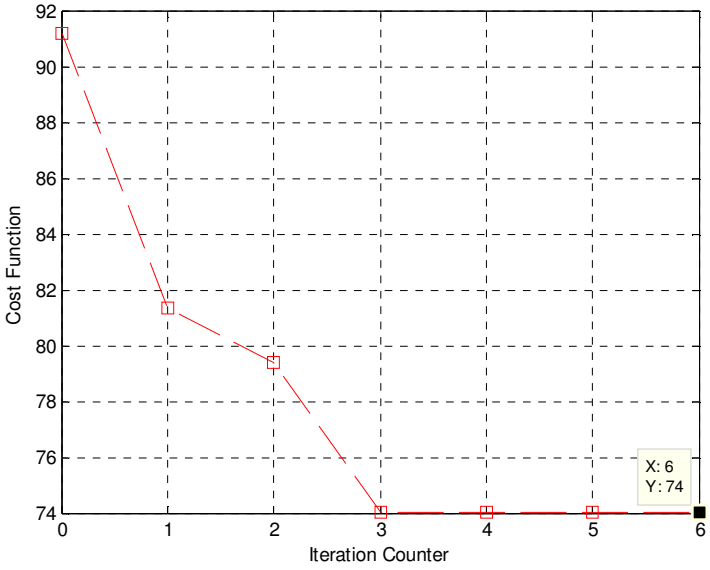

Fig. 4.58 Iteration Process of OPF solution. Cost Function.

4.6.4.2 Results for Scenario 2

In this section we present the results of the application of the Interior point method for the first stage of the Multi-step optimization approach for the scenario 2 described in section 4.6.1.

The Power Flow solution of scenario 2 presented in section 4.6.3 is used to resolve the equivalent algebraic equations of the dynamical swing equations by means of numerical integration for a fault-

on time of 232 ms. The results of this numerical integration are shown in Fig. 4.28, showing that the system is unstable for this contingency. Consequently, stability constraints are violated for the initial state of the system.

The power flow solution and the points obtained for the rotor angles using the trapezoidal integration method were used as starting points to resolve the Stability Constrained Optimal Power Flow (SCOPF) (4.22)-(4.31) and Optimal Power Flow (OPF) (4.8)-(4.18).

The initial interval time for the optimization problem is set to zero. We increment this interval of time to 0.64 s for the resolution of the SCOPF and OPF problem using Interior point method. The solution is updated until the KKT conditions are satisfied.

The results for the Stability Constrained OPF (4.22)-(4.31) solution are: $\theta_1 = 26.3^\circ$, $\theta_2 = 12.8^\circ$, $P_{g1} = 3{,}71$ p.u., $P_{g2} = 3{,}25$ p.u., $P_{g3} = 7.92$ p.u., $Q_{g1} = 0.9$ p.u., $Q_{g2} = 0.67$ p.u., $Q_{g3} = 2.65$ p.u., $\delta_1^0 = 43.2^\circ$, $\delta_2^0 = 21.8^\circ$, $\delta_3^0 = 6.5^\circ$, $E_{g1} = 1.12$ p.u., $E_{g2} = 1.04$ p.u., $E_{g3} = 1.04$ p.u.

We also resolve OPF problem (4.8) to (4.18) to compare these two solutions. Results for the OPF solution are: $\theta_1 = 43.9^\circ$, $\theta_2 = 22.5^\circ$, $P_{g1} = 4.96$ p.u., $P_{g2} = 4.96$ p.u., $P_{g3} = 4{,}97$ p.u., $Q_{g1} = 1.7$ p.u., $Q_{g2} = 1.4$ p.u., $Q_{g3} = 2.81$ p.u., $\delta_1^0 = 64.84^\circ$, $\delta_2^0 = 35.63^\circ$, $\delta_3^0 = 4.09^\circ$, $E_{g1} = 1{,}22$ p.u., $E_{g2} = 1{,}09$ p.u., $E_{g3} = 1{,}044$ p.u.

Fig. 4.59, Fig. 4.61 and Fig. 4.63 respectively display the rotor angle of Generator 1, Generator 2 and Generator 3 when the contingency is applied, in two operation points: Optimal Power Flow (OPF) solution and the Stability Constrained OPF (SCOPF) solution. It can be seen that the system does not survive after the contingency at operating point given by OPF solution, but it does at operating point given by SCOPF solution.

Fig. 4.60, Fig. 4.62 and Fig. 4.64 illustrate the Iteration Process of the Stability Constrained OPF (SCOPF) by showing the maximum rotor angle deviation of Generator 1, Generator 2 and Generator 3, respectively, with respect to the inertia center angle. Fig. 4.65 shows the evolution of the cost function in the Iteration Process of the SCOPF while Fig. 4.66 shows the evolution of the cost function for the Iteration Process of the OPF. Observe that the final cost of the OPF is lower than the final cost of the SCOPF. This was expected because the system is unstable to the contingency with the operating state produced by the OPF.

These results are obtained applying Interior point method. Convergence for times higher than 0.64s was not achieved.

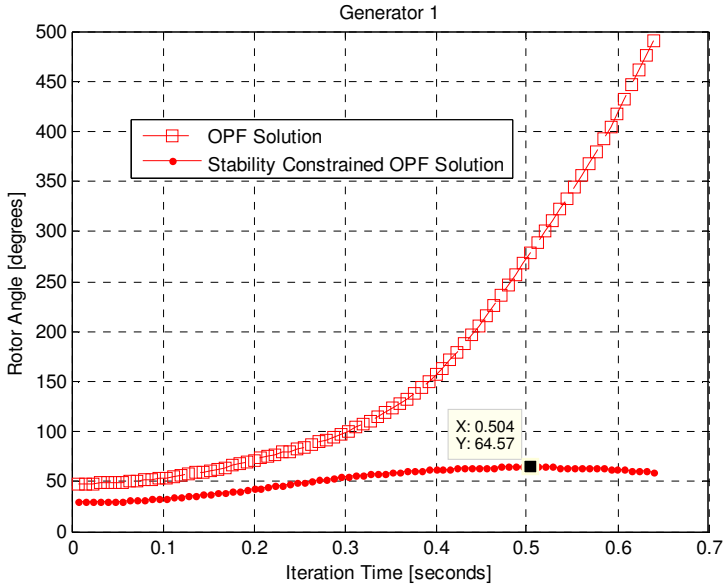

Fig. 4.59 Dynamic Response of the Generator 1 of the 3-machine 3-bus system at two operating points.

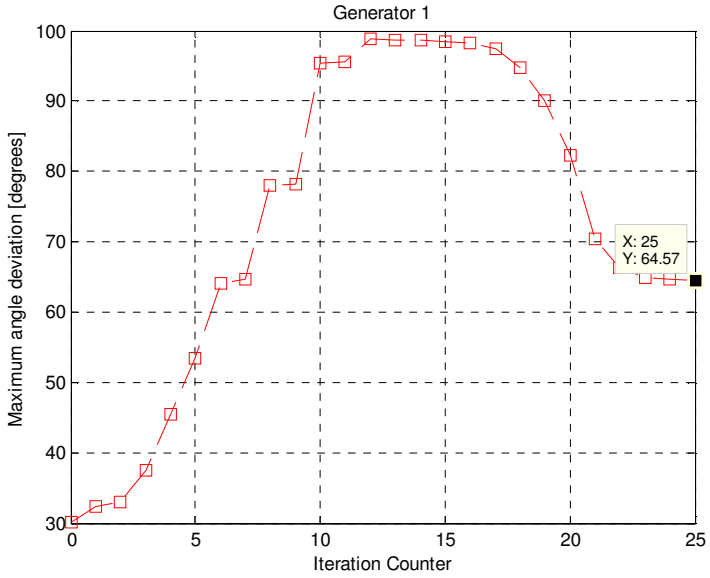

Fig. 4.60 Iteration Process of Stability Constrained OPF. Maximum angle of Generator 1

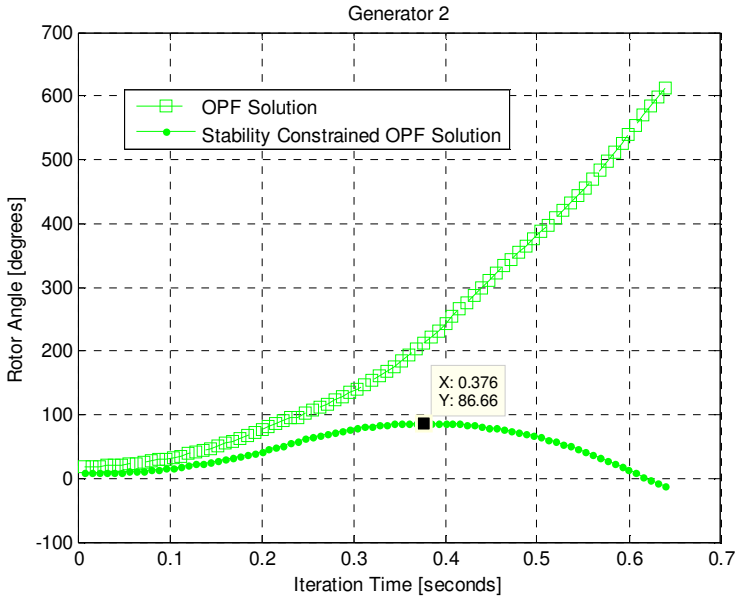

Fig. 4.61 Dynamic Response of the Generator 2 of the 3-machine 3-bus system at two operating points.

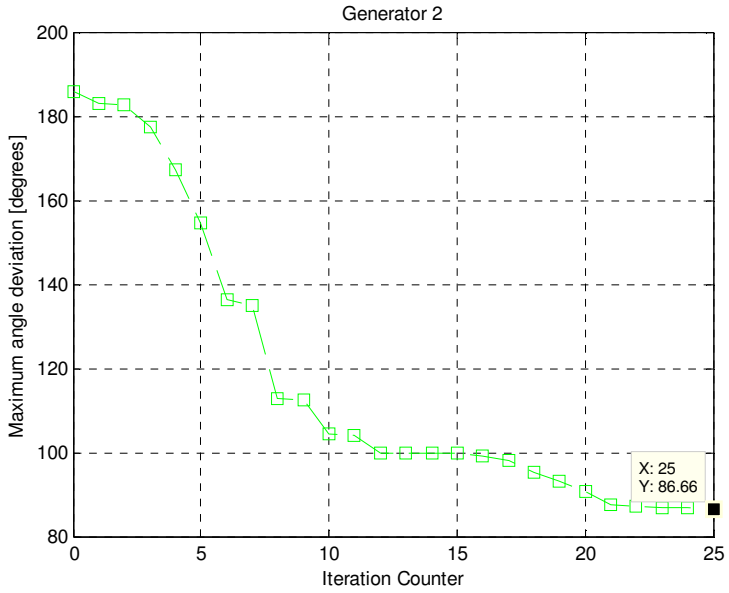

Fig. 4.62 Iteration Process of Stability Constrained OPF. Maximum angle of Generator 2

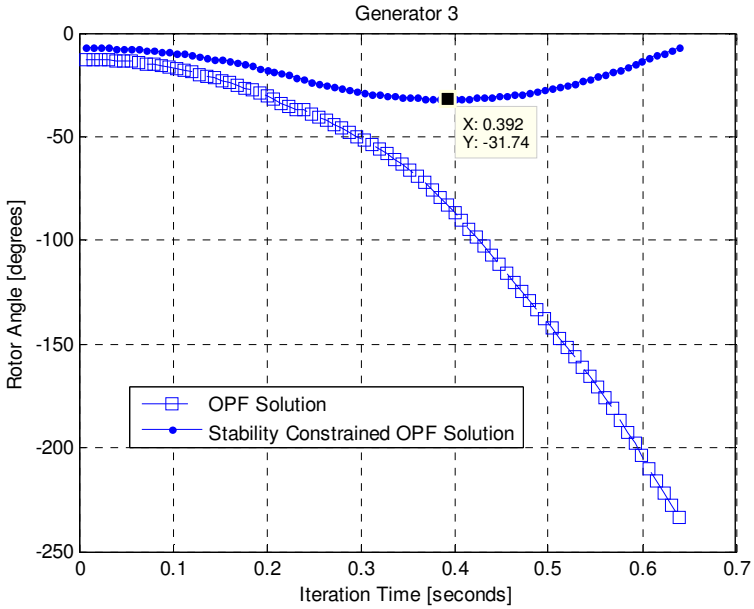

Fig. 4.63 Dynamic Response of the Generator 3 of the 3-machine 3-bus system at two operating points.

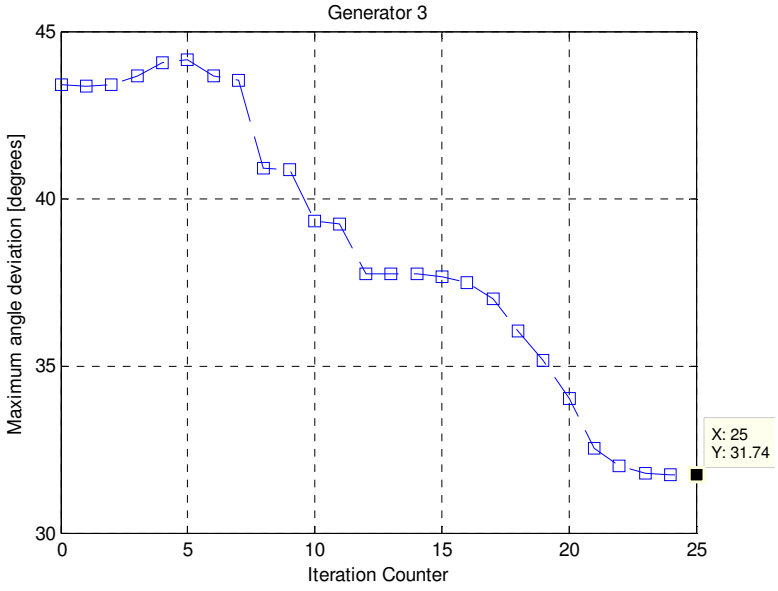

Fig. 4.64 Iteration Process of Stability Constrained OPF. Maximum angle of Generator 3

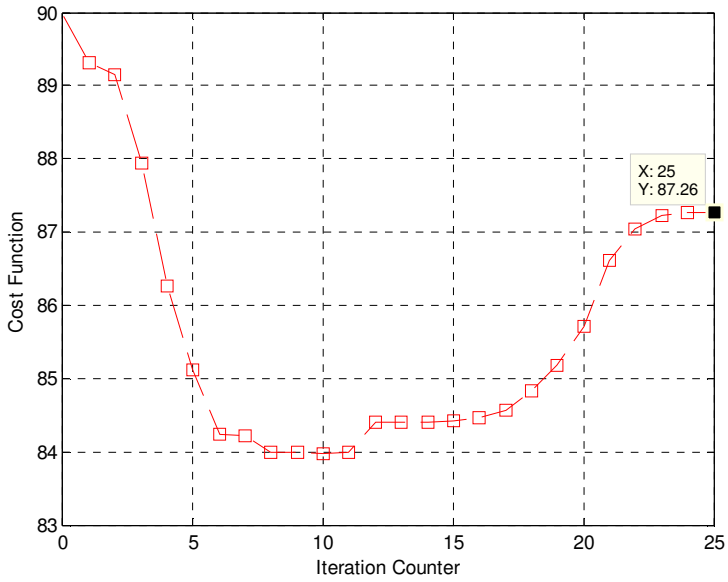

Fig. 4.65 Iteration Process of Stability Constrained OPF. Cost Function.

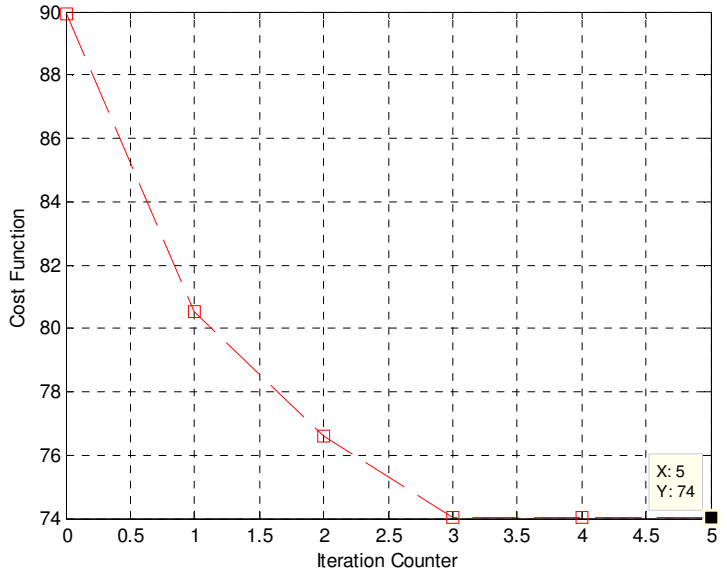

Fig. 4.66 Iteration Process of OPF solution. Cost Function.

Chapter 5

5. Comments and final conclusions, contributions and future research suggested

This chapter summarizes the main conclusions and some contributions of this dissertation. Finally, future research directions are suggested.

5.1 Comments and final conclusions

The issue of incorporating transient stability constraints in the OPF formulation is very challenging. In chapter 4, it was discussed how to incorporate transient stability constraints into the OPF problem; stating that the subject of checking these stability constraints is composed mainly of the following steps: the resolution of fault-on differential equations and determining the stability region boundary. These solutions cannot be expressed as an analytical form in a function of the control variables, leading to difficulties in the application of conventional algorithms for solving this Nonlinear Programming (NP) problem.

In this dissertation, stability constraints were approximated by means of a maximal angle deviation. One of the advantages of this representation of stability constraints is that these constraints can be written directly into the state variables of the problem, with the disadvantage that the verification of these stability constraints requires numerical computation, associated with high-cost computational procedures, such as numerical integration of a large set of differential-algebraic equations for the fault-on and post-fault system. Summarizing, the main difficulties for the solution of this NP problem are: handling differential equations that models the behavior of the system, and the difficulty of the conventional numerical algorithms to give optimal solutions in high non-linear and non-convex scenarios.

In this dissertation, the approach of Gan, Thomas and Zimmerman, 2000 was followed; this approach considers the center of angle restriction to approximate stability constraints. One important issue to consider for the development of this dissertation was the selection of the optimization algorithm. The majority of methods for solving quadratic programs can be categorized into either active-set methods or interior methods.

The use of interior point method (IPM) for the solution of this high-dimension SCOPF problem presented non-convergence problems. By means of the use of the IPM, it was achieved an optimal

solution for this high-dimension SCOPF problem (4.22)-(4.31), this was presented in section 4.6.4. But with the use of the active-set method, convergence process had a better performance. The use of Active-set method allowed optimal solutions for higher simulation times than using Interior point method; for both scenarios presented in section 4.6.1. Moreover, the number of iterations along the convergence process was lower with the use of the active-set method, for all simulations.

It is believed that the reasons for the non-convergence problems with the application of IPM in the SCOPF problem were: 1) IPM computes iterates that lie in the interior of the feasible region, in this context, it is important to have a good estimate for the initial feasible point, otherwise, this algorithm will spend unnecessary time in the searching for a feasible starting point; 2) Also, each iterate of interior-point methods is more expensive in comparison with active-set methods, because IPM must solve linear systems involving all the variables of the problem whereas active-set methods solve systems involving some subset of the variables.

Active-set methods works with one working set at each iterate until the optimal working set is found. This working set is updated and is composed; at each iterate, only of some subset of variables in the active constraints, reducing in this way, the number of variables and systems in comparison with interior-point method. For these reasons, Active-set method was considered adequate for the searching of solutions of this high-dimension SCOPF problem, giving optimal solutions for simulation times higher than 1 second.

A Multi-step optimization approach was proposed to enhance the capabilities of the active-set method with the target of developing a methodology that speeds up the computational calculation of this SCOPF problem.

Although the proposed high-dimension SCOPF problem is non-linear and non-convex and a global optimum cannot be guaranteed, this proposed procedure was successfully tested on a 3-machine system, having the generated powers as control variables. For these reasons, the proposed procedure has some potential to become a useful tool for helping system operators achieve secure operation status in power systems. Despite that, the computational burden is still high and future research is necessary to develop algorithms that are capable of analyzing power system of higher dimension and subject to several contingencies.

In section 5.3, future research is suggested, as a way to overcome the difficulties encountered by means of the use of the proposed methodology.

5.2 Contributions

The main contributions of this dissertation are summarized below:

A multi-stage optimization algorithm was proposed in this dissertation. The results of its application were promising, revealing this proposed procedure is efficient to mitigate computational issues that lead to the resolution of this high-dimension SCOPF problem.

The results of this dissertation were accepted and/or presented in two relevant conferences:

a) Moreno Alamo, Ana Cecilia; Costa Alberto, Luís Fernando. "A Multi-Step Optimization Approach for Power Flow with Transient Stability Constraints", accepted for a presentation and publication at the international conference "Powertech 2015 Conference", Eindhoven University of Technology, Eindhoven, The Netherlands, 29 June - 2 July 2015.

b) Moreno Alamo, Ana Cecilia; Costa Alberto, Luís Fernando. "Fluxo de potência ótimo com restrições de estabilidade transitória", accepted for a presentation and publication at the "XXIII SNPTEE - Seminário Nacional de Produção e Transmissão de Energia Elétrica", Foz do Iguaçu, Paraná, Brazil, 8-21 October, 2015.

5.3 Future research

Suggestions for future research are listed below.

1) Another way to attack the problem of transient stability could be using direct methods to formulate transient stability constraints. In this case, only the knowledge of fault-on trajectory would be enough to conclude about stability; which will reduce drastically the computational effort.

   As a first step, it is necessary to study how direct methods can be applied to formulate transient stability constraints. As we mentioned before, the representation of the dynamics of the system significantly increases the number of variables of the optimization problem. Therefore, computational costs significantly are increased by means of this approach**.** For this reason, the approach followed in this dissertation is not of practical use for high-dimension power system models, and direct methods appear as an alternative to make viable the incorporation of transient stability constraints into the OPF formulation.

2) We believe direct methods can accelerate the solution of the stability constrained optimal power flow. Moreover, they might eliminate the heuristic approach of selecting a threshold as an angle constraint. We believe the existence of two possible ways to achieve this:

a) Using an energy threshold instead of angle threshold.

b) Transform the energy threshold into an angle threshold.

3) Another possibility is studying the sensitivity of the stability margin, measured by means of an energy function, with respect to the control variables and resolve the optimization problem, iteratively.

In all cases, only the fault-on trajectory would be enough to conclude about stability; reducing drastically the computational effort as compared to the approach proposed in: Gan, Thomas and Zimmerman, (2000). The use of direct methods in the future may drastically reduce the computational effort as compared to the approach described in this dissertation.

References

ANDERSON P. M.; FOUAD A. A. “Power System Control and Stability”. The Iowa State University Press, Arnes, Iowa, 1977.

BALU, N.; BERTRAM, T.; BOSE A.; BRANDWAJN, V. On-line power system security analysis. IEEE Journals & Magazines. February 1992.

BIAN J.; RASTGOUFARD P. “Power system voltage stability and security assessment”. Electric Power Systems Research, Volume 30, Issue 3, Pages 197–201. September 1994.

BRETAS N.; ALBERTO L. F. C. Estabilidade transitória em sistemas eletroenergéticos. São Carlos, SP. 2000.

CAI, H.R.; CHUNG, C.Y.; WONG, K.P. “Application of Differential Evolution Algorithm for Transient Stability Constrained Optimal Power Flow”. IEE Proceedings. Volume: 23, 2008.

CAIN M.B.; O’NEILL R.P.; CASTILLO A. "History of Optimal Power Flow and Formulations" December 2012. Available: < http://www.ferc.gov/industries/electric/indus-act/market-planning/opf-papers/acopf-1-history-formulation-testing.pdf >. Acceded in 23th May 2015.

CHIANG H.-D., WU F. F.; VARAIYA P. P. "Foundations of direct methods for power system transient-stability analysis ", IEEE Transactions on Circuits and Systems, vol. CAS-34, pp.160 -173, 1987.

CHIANG H.-D., WU F. F.; VARAIYA P. P. "Foundations of the potential energy boundary surface method for power system transient-stability analysis ", IEEE Trans. Circuits Syst., vol. CAS-35, pp.712 -728, year 1988.

CHIANG H.-D; THORP, J.S. The closest unstable equilibrium point method for power system dynamic security assessment. IEEE Transactions on Circuits and Systems, (Volume: 36, Issue: 9); 1989.

CHIANG, H.-D.; WU F. F.; VARAIYA P. P. "A BCU method for direct analysis of power system transient-stability analysis", IEEE Trans. Power Syst., vol. 9, pp.1194 -2000, year 1994.

CHIANG H.-D.; CHU CH.; CAULEY G. "Direct stability analysis of electric power systems using energy functions: theory, applications, and perspective". Proceedings of the IEEE. Vol. 83, Issue: 11. Nov, 1995.

CHIANG, H.-D.; TADA Y.; Li H.; Takazawa T. “TEPCO-BCU for On-line Dynamic Security Assessments of 12,000-bus Power Systems”, X Symposium of Specialists in Electric Operational and Expansion Planning, X SEPOPE, Florianopolis(SC)- Brasil, May 21-25, 2006.

CHIANG, H.-D. Direct methods for Power System Stability Analysis: Fundamental theory, BCU Methodologies and Applications, John Wiley and IEEE Press, 2010.

CHENG D.; MA J. “Calculation of stability region”; Decision and Control, Proceedings, 42nd IEEE Conference, Vol.: 6, pp. 5615 – 5620, Dec. 2003.

CHOQUE E. Máster Thesis. "A importância da região de estabilidade no problema de análise de estabilidade de tensão em sistemas elétricos de potência". São Carlos, SP, 2011.

CLEMENTS K. A.; DAVIS P. W. ; FREY K. D. "An Interior Point Algorithm for Weighted Least Absolute Value Power System State Estimation", IEEE/PES, 1991.

COSTA G. R. M. da; COSTA C.E.U; SOUZA A. M. "Comparative studies of optimization methods for the optimal power flow problem". Electric Power Systems Research. v. 56, n. 3, Pages 249–254, December 2000.

DOMMEL H.W.; TINNEY W.F. “Optimal power flow solutions,” IEEE Transactions on Power Apparatus and Systems, PAS-87, pp. 1866–1876, October 1968.

FANG D.Z.; XIAODONG Y.; JINGQIANG S.; SHIQIANG Y.; YAO Z. “An Optimal Generation Rescheduling Approach for Transient Stability Enhancement”. IEEE TRANSACTIONS ON POWER SYSTEMS, Vol. 22, No. 1, Feb. 2007.

FLETCHER R. "Practical Methods of Optimization," John Wiley and Sons, 1987.

FOUAD A. A.; VITTAL. “Power System Transient Stability Analysis Using the Transient Energy Function Method”. Englewood Cliffs: Prentice-Hall, 1991.

FORSGREN A.; GILL P. E.; MURRAY W. "On the identification of local minimizers in inertia controlling methods for quadratic programming". SIAM J. Matrix Anal. Appl., 12:730-746, 1991.

GAN D.; THOMAS R. J.; ZIMMERMAN R. D. “Stability-Constrained Optimal Power Flow”, IEEE Trans. on Power Systems, vol. 15, no. 2, pp. 535–540, May 2000.

GILL P.E.; MURRAY W.; WRIGHT M.H. Practical Optimization, London, Academic Press, 1981.

GILL P.E.; MURRAY W.; SAUNDERS M.A.; WRIGHT M.H. "Procedures for Optimization Problems with a Mixture of Bounds and General Linear Constraints" ACM Trans. Math. Software, Vol. 10, pp 282–298, 1984.

GILL P.E.; MURRAY W.; WRIGHT M.H. Numerical Linear Algebra and Optimization, Vol. 1, Addison Wesley, 1991.

GRANVILLE S. “Optimal Reactive Dispatch by means of Interior Point Method,” IEEE Transactions on Power Systems, Volume: 9 Issue: 1. p. 136-146. Feb. 1994

HIRSCH, M. W.; SMALE S.; Differential Equations, Dynamical Systems, and Linear Algebra. New York: Academic Press, 1974.

HOCK W.; SCHITTKOWSKI K. "A Comparative Performance Evaluation of 27 Nonlinear Programming Codes," Computing, Vol. 30, p. 335, 1983.

KARMARKAR N. A polynomial-time algorithm for linear programming. Combinatorica 1984; 4: 373-95.

KUNDUR P. Power System Stability and Control. McGraw-Hill. New York, NY, 1994.

KUNDUR P.; PASERBA J.; AJJARAPU V.; ANDERSSON G.; BOSE A.; CANIZARES C.; HATZIARGYRIOU N.; HILL D.; STANKOVIC A.; TAYLOR C.; VAN CUTSEM T.; VITTAL V. IEEE/CIGRE joint task force on stability terms and definitions. “Definition and classification of power system stability”. IEEE transactions on power systems, VOL. 19, NO. 2, 1387-1401, MAY 2004.

LAYDEN D.; JEYASURYA B. “Integrating security constraints in optimal power flow studies,” in Proc. IEEE Power Eng. Soc. General Meeting, vol. 1, Jun. 2004.

LAGE G. “O fluxo de potência ótimo reativo com variáveis de controle discretas e restrições de atuação de dispositivos de controle de tensão”. Tese de Doutorado. Escola de Engenharia de São Carlos. Universidade de São Paulo. 2013.

MATHWORKS, Inc. Optimization Toolbox 4 Users's Guide. V 6.5. Available: <http://www.mathworks.com/access/helpdesk/help/pdf_doc/optim/optim_tb.pdf>., 2008.

NAZARETH. J. L. Differentiable Optimization and Equation Solving: A Treatise on Algorithmic Science and the Karmarkar Revolution. pp 167, 173. Springer, New York, 2003.

NGUYEN; PAI M. A. “Dynamic security-constrained rescheduling of power systems using trajectory sensitivities,” IEEE Trans. Power Syst., vol. 18, no. 2, pp. 848–854, May 2003.

NOCEDAL J.; WRIGHT S. Numerical Optimization. Springer, New York, 1999.

PAVELLA; ERNST; RUIZ-VEGA. Transient Stability of Power Systems. An Unified Approach to Assessment and Control, 2000.

POWELL M.J.D. "Variable Metric Methods for Constrained Optimization," Mathematical Programming: The State of the Art, Springer Verlag, pp 288–311, 1983.

RASHED; KELLY D. “Optimal Load Flow Solution Using Lagrangian Multipliers and the Hessian Matrix,” IEEE Transactions on Power Apparatus and Systems, vol. PAS-93, pp. 1292-1297, Feb. 1974.

SASSON A. M.; VILORIA F.; ABOYTES F. “Optimal Load Flow Solution Using the Hessian Matrix”. IEEE Transactions on Power Apparatus and Systems, (Volume: PAS-92), pp. 31–41, Jan. 1973.

SAUER P.W.; PAI M.A. “Power System Dynamics and Stability”. Upper Saddle River, NJ: Prentice-Hall, 1998.

SHEVADE S. Numerical Optimization. (Engineering Lectures On DVD). Department of Computer Science and Automation. Indian Institute of Science, Bangalore, 2012. Available: <http://nptel.ac.in/courses/106108056/>. Accessed in: 23th May, 2015.

SCHITTKOWSKI K. "NLQPL: a Fortran-subroutine Solving Constrained Nonlinear Programming Problems," Annals of Operations Research, Vol. 5, pp 485-500, 1985.

SHUBHANGA K. N; KULKARNI A. M.; “Stability-constrained generation rescheduling using energy margin sensitivities,” IEEE Trans. Power Systems., vol. 19, no. 3, pp. 1402–1413, August, 2004.

SOUSA V. A. "Resolução do problema de fluxo de potência ótimo reativo via método da função lagrangiana barreira modificada". Tese de Doutorado. Escola de Engenharia de São Carlos. Universidade de São Paulo. 2006.

SUAMPUN W. “Novel BCU-Based Methods For Enhancing Power System Transient Stability”, Ph.D. Dissertation of Electrical Engineering, Cornell University, New York, USA, Aug-2013.

SUN D. I; BRUCE A.; BREWER B.; ART H.; TINNEY W.F. “Optimal Power Flow by Newton Approach”, IEEE Transactions on Power Apparatus and Systems,vol.PAS-103, no. 10, pp. 2864-2879, Oct 1984.

THEODORO E. "Desenvolvimento de uma ferramenta computacional para análise de segurança dinâmica, no contexto da estabilidade transitória, de sistemas elétricos de potência via métodos

diretos". Tese de Mestrado. Escola de Engenharia de São Carlos. Universidade de São Paulo. 2010.

VARGAS L. S.; QUINTANA V. H.; VANELLI A. “A Tutorial Description of an Interior Point Method and its Applications to Security-Constrained Economic Dispatch”, IEEE Transactions on Power Systems, Vol. 8, No. 3, pp. 1315-1324., 1993.

VENKATARAMAN P., Applied Optimization with Matlab Programming, A Wiley-Interscience publication, John Wiley & Sons, New York, 2001.

WEHENKEL L.; PAVELLA M. “Preventive vs. emergency control of power systems” Power Systems Conference and Exposition, 2004.

WISCONSIN INSTITUTE FOR DISCOVERY, University of Winsconsin - Madinson. "Neos Optimization Guide: State-of-the-Art Solvers for Numerical Optimization", 2013. Available: <http://neos-guide.org/content/quadratic-programming-algorithms>. Accessed in: 23th May, 2015.

WONG E. Active-Set Methods for Quadratic Programming. PhD. Dissertation. University of California, San Diego. 2011.

XIA Y.; CHAN K.W.; LIU M. “Direct nonlinear primal–dual interior-point method for transient stability constrained optimal power flow” Generation, Transmission and Distribution, IEEE Proceedings. Volume: 152, 2005.

ZÁRATE-MIÑANO R. Optimal Power Flow with Stability Constraints. PhD. Dissertation. Universidad de Castilla, La Mancha. 2010.

ZÁRATE-MIÑANO R.; MILANO F.; CONEJO A. J. Securing Transient Stability Using Time-Domain Simulations within an Optimal Power Flow. 2010.

ZÁRATE-MIÑANO R. "Optimal Power Flow with Stability Constraints: Redispatching procedures to ensure power system security in the context of real-time operation". Lambert Academic Publishing. 2012.